Inhibitory studies of *Neisseria meningitidis* and *Campylobacter jejuni* *N*-acetylneuraminic acid synthase

A thesis submitted for the fulfilment of the requirements for the Degree of

Master of Science in Biochemistry

in the University of Canterbury

by

Ryu Wayne Toyama

Department of Chemistry
University of Canterbury

May 2014

Acknowledgements

Firstly, I would like to thank my supervisor, Professor Emily Parker for her supervision, guidance and wisdom. Without her encouragement the completion of this thesis would not have been possible.

I would like to especially thank my mentor Dmitri Joseph who helped me get up and going in the biochem lab and for clarifying the things that I did not know. I would also like to thank Sebastian Reichau, Gert-Jan Moggre, and Logan Heyes for helping me to get familiar with the organic synthesis Lab.

I would like to give an extra special thank you to Andrew Watson for providing me with the product analogue rNANA and to all of the technical staff in the UC Chemistry and Biology departments for their help.

I would like to thank everyone in the Parker group for all of their advice, encouragement, humour (or trickery…), and kindness. A special thanks to Michael "1.0" Hunter, Penel Cross, Ali Nazmi, Nicky Blackmore, Francis Huisman, Sarah Wilson-Coutts, Gerd Mittelstaedt, and Tammie Cookson for sharing all of their knowledge and experience with me. I would also like to thank Tyler Clarke, Mohamad Othman, Michael "2.0" Weusten, Tom Cotton, Davie Lim, Vicky Zhang, Emma Livingstone, and Yifei Fan for all of their friendship, and support.

Lastly, a super special thanks to my mum and little brother for all of their encouragement, support (and hassling) when things got rough.

To all those I have mentioned, I am certain that my experiences and memories with all of you will give me strength when I need it the most.

Abstract

N-Acetylneuraminic acid synthase (NANAS) is an enzyme responsible for the biosynthesis of *N*-acetylneuraminic acid (NANA). NANA is the most common form of a group of nine carbon sugar molecules called the sialic acids. NANA production is common in mammalian cells for vital physiological processes. A few species of microorganisms, including pathogenic bacteria such as *Neisseria meningitidis* and *Campylobacter jejuni*, are known to synthesise NANA by their bacterial NANAS. These pathogenic bacteria synthesise NANA for molecular mimicry, allowing them to evade the host immune system.

This thesis examines the NANAS enzymes from *N. meningitidis* and *C. jejuni*. Inhibitory studies with these enzymes were explored by performing enzyme kinetics with substrate analogues and a product analogue which structurally mimic the natural substrates or product of NANAS. Inhibition constants were determined for a variety of analogues to give insight in to how the enzyme accommodates its substrates within the active site of NANAS. This study may be a useful step in the development of alternative antibiotics for bacterial meningitis and other diseases in the future.

NANAS catalyses a condensation reaction between phosphoenolpyruvate (PEP) and *N*-acetyl mannosamine (ManNAc). Both PEP and ManNAc analogues were explored as inhibitors of the enzymes. Results from this study show that increasing steric bulk of the substituents at C3 of PEP unexpectedly delivers more potent inhibition of the enzyme. This finding suggests that a slightly modified binding position of the PEP analogue within the PEP binding site of the enzyme may be responsible for the inhibition. A reduced acyclic analogue of ManNAc was found to be an effective inhibitor of the enzymes. This finding indicates how important the acyclic form of ManNAc is in the reaction mechanism catalysed by this enzyme.

Table of content

Chapter 1 Background information

Chapter 2 Preparation of the enzyme NANAS and kinetic assays with PEP analogues

Chapter 3 Kinetic assays with ManNAc analogues and a NANA analogue

Chapter 4 Summary of thesis and future directions

Chapter 5 Materials and methods

List of Figures

List of tables

List of abbreviations

2DG	2-Deoxy-D-glucose
A5P	Arabinose 5-phosphate
Ala	Alanine
Arg	Arginine
Asn	Asparagine
Asp	Asparagine
Br-PEP	3-Bromo-PEP
BTP	Bis-tris-propane
***Cje*NANAS**	*Campylobacter jejuni* NANAS
Cl-PEP	3-Chloro-PEP
DAH7P	3-Deoxy-D-*arabino*-heptulosonate 7-phosphate
DAH7PS	3-Deoxy-D-*arabino*-heptulosonate 7-phosphate synthase
E4P	D-Erythrose 4-phosphate
F-PEP	3-Fluoro-PEP
GalNAc	*N*-Acetyl-D-galactosamine
Gln	Glutamine
GluNAc	*N*-Acetyl-D-glucosamine
Gly	Glycine
His	Histadine
IMAC	Immobilised metal affinity chromatography
IPTG	Isopropyl β-D-1-thiogalactopyranoside
KDN	2-Keto-3-deoxy-glycero-galacto-nonulosonic acid
KDO8P	3-Deoxy-D-*manno*-octulosonate 8-phosphate

KDO8PS	3-Deoxy-D-*manno*-octulosonate 8-phosphate synthase
LB	Lysogeny-broth solution
LegS	*N,N*-Diacetyllegionaminic acid synthase
Lys	Lysine
Lys	Lysine
ManCl	D-Mannosamine Hydrochloride
ManNAc	*N*-Acetyl mannosamine
ManNAc-6-P	*N*-Acetyl mannosamine 9-phosphate
Me-PEP	3-Methyl-PEP
NANA	*N*-Acetylneuraminic acid
NANA-9-P	*N*-Acetylneuraminic acid 9-phosphate
NANA-9-PS	*N*-Acetylneuraminic acid 9-phosphate synthase
NANAS	*N*-Acetylneuraminic acid synthase
***Nme*NANAS**	*Neisseria meningitidis* NANAS
PDB	Protein data bank
PEP	Phosphoenolpyruvate
Phe	Phenylalanine
PseS	Pseudaminic acid synthase
PTS	Phosphotransferase system
rManNAc	*N*-Acetylmannosaminitol
rNANA	Reduced NANA
***Sag*NANAS**	*Streptococcus agalactaie* NANAS
SEC	Size exclusion chromatography
SEP	Sulfoenolpyruvate
Ser	Serine
TEV	Tobacco etch virus protease

| **Thr** | Threonine |
| **Tyr** | Tyrosine |

Chapter 1
Background information

1.1 Introduction

Sialic acids are a group of nine carbon α-ketoacid molecules of which *N*-acetylneuraminic acid (NANA) is the most common. Sialic acids play many important physiological roles in mammalian systems.[1,2] The aim of this research is to study the inhibition of the enzyme responsible for the synthesis of NANA, bacterial *N*-acetylneuraminic acid synthase (NANAS) from both *Neisseria meningitidis* (*Nme*NANAS) and *Campylobacter jejuni* (*Cje*NANAS). NANAS catalyses the reaction between phosphoenol pyruvate (PEP) and *N*-acetylmannosamine (ManNAc) to form NANA and inorganic phosphate (Pi) (**Figure 1.1**).[3]
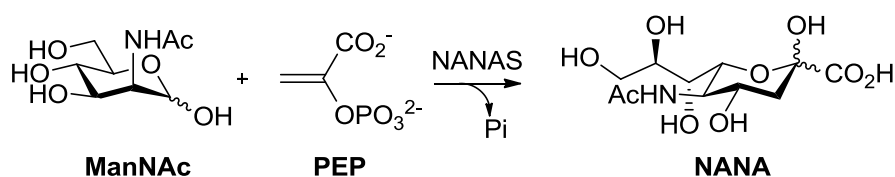
Figure 1.1 Biosynthesis of NANA.

NANA is synthesised using slightly different biosynthetic routes in mammals and bacteria. Mammalian biosynthesis of NANA requires two extra enzymatic steps which involve the phosphorylation of ManNAc into *N*-acetyl mannosamine 9-phosphate (ManNAc-6-P) followed by the dephosphorylation of the synthesised product (**Figure 1.2**).
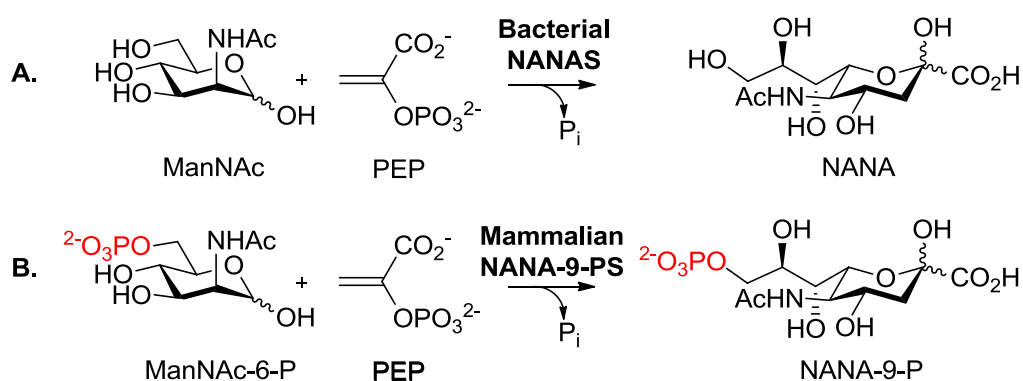
Figure 1.2 Difference between bacterial and mammalian NANAS biosynthesis. (A) Shows bacterial biosynthesis of NANA. (B) Shows the mammalian biosynthesis of N-acetylneuraminic acid 9-phosphate (NANA-9-P) by the catalytic reaction of mammalian N-acetylneuraminic acid 9-phosphate synthase (NANA-9-PS).

This difference between mammalian and bacterial metabolism makes NANAS a possible target for antibacterial drug discovery. By elucidating and developing potent inhibitors for this enzyme, new and possibly more effective antibiotics against pathogenic bacteria may be discovered. This is of specific importance given the emergence of multi-drug resistant meningitis strains, and other pathogenic organisms.[4]

1.2 The sialic acid synthase family

Sialic acid synthases are a group of enzymes which produce sialic acids. There are different sialic acid synthases, each responsible for the biosynthesis of different sialic acids. For example, pseudaminic acid synthase (PseS) and *N,N*-diacetyllegionaminic acid synthase (LegS) catalyse the condensation of PEP with 2,4-diacetamido-2,4,6-trideoxy-β-L-altropyranose and 2,4-diacetamido-2,4,6-trideoxy-D-mannopyranose respectively (**Figure 1.3**).[5,6]
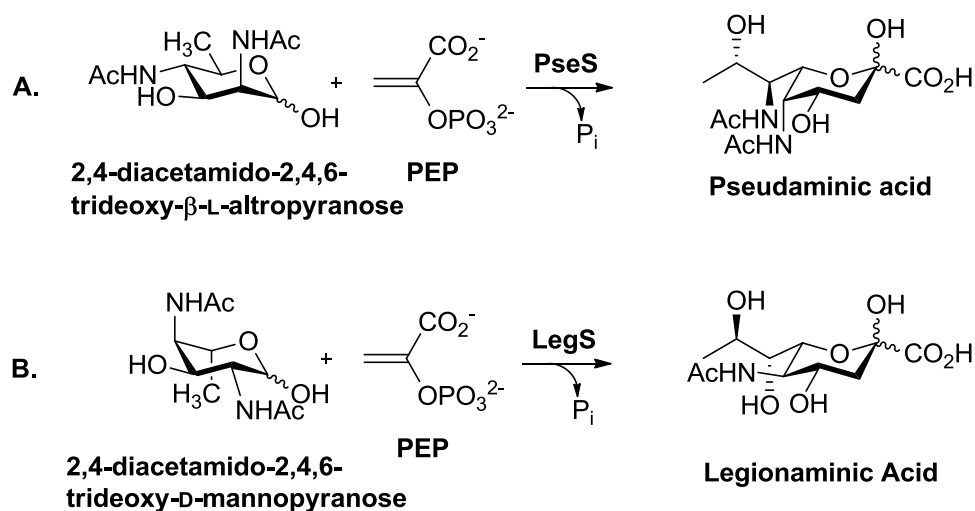
Figure 1.3 Catalytic reaction of pseudaminic acid synthase (PseS) and legionaminic acid synthase (LegS) (A) Shows the reaction catalysed by PseS, producing psedaminic acid and (B) details the reaction catalysed by LegS which produces legionaminic acid.

1.3 Sialic acids and N-acetylneuraminic acid (NANA)

1.3.1 Characteristics of sialic acids

Sialic acids are a group of diverse sugar molecules which have an α-keto acid functional group on a nine carbon backbone.[1] The diversity is due to the fact that these molecules have large variety of modifications,[1,7] ranging from the esterification of the hydroxyl groups at C7,C8 and C9 positions with acetic acid, to the addition of another functional group such as a lactoyl group at C9 and a methyl, or sulphate group at the C8 position (**Figure 1.4**).[8]

3
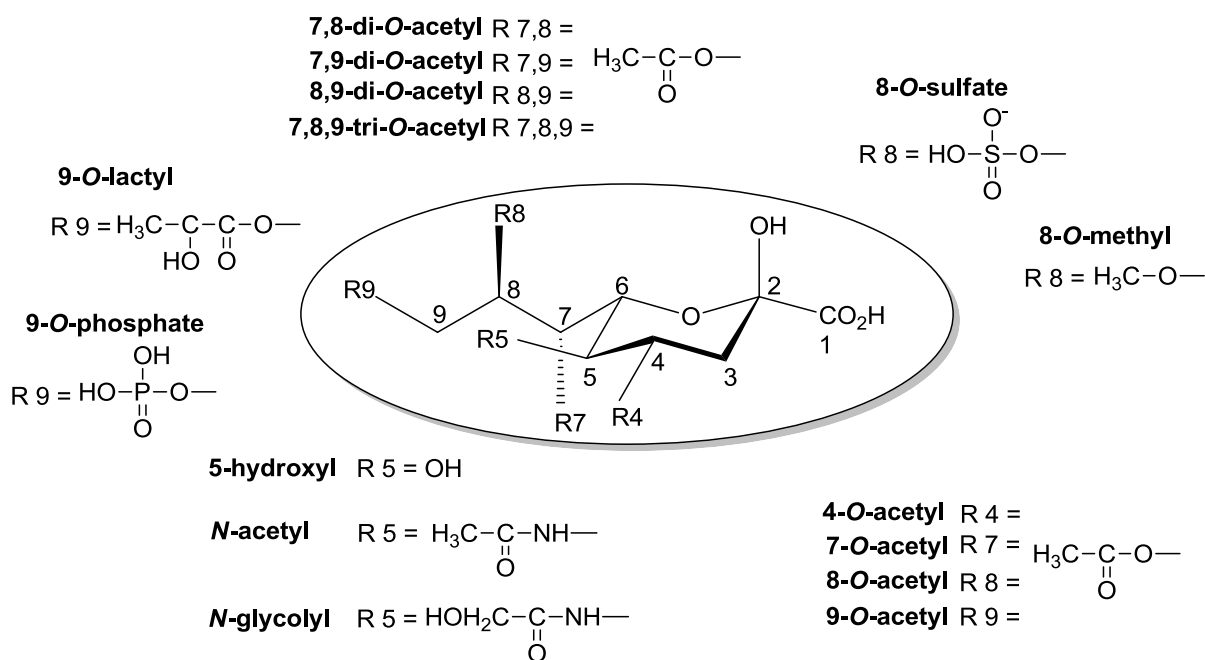
Figure 1.4 Sialic acid diversity.[1]

The enzyme of interest for this study produces the specific sialic acid NANA. This type of sialic acid is the most common type in mammals, including humans, and NANA has an *N*-acetyl functional group at the C5 position.[1,2] NANA is so common that the term sialic acid is often used synonymously with NANA.

Other significant forms of sialic acid include; neuraminic acid, *N*-glycolylneuraminic acid and 2-keto-3-deoxy-glycero-galacto-nonulosonic acid (KDN) (**Figure 1.5**) which are all closely related to NANA.[2,9] Neuraminic acid is an unmodified form of sialic acid that lacks the C5 acetyl group; this form of sialic acid rarely exists in nature.[8] *N*-Glycolylneuraminic acids have an *N*-glycolyl functional group instead of the *N*-acetyl functional group, which is formed from an oxidation of the acetyl group in the cytosol of the cell during biosynthesis.[9] This form of sialic acid is also common in mammals except for humans due to an irreversible mutation to the human gene responsible for the *N*-glycolylneuraminic acid synthesis.[10] KDN is considered unusual because of its deaminated form.[11]
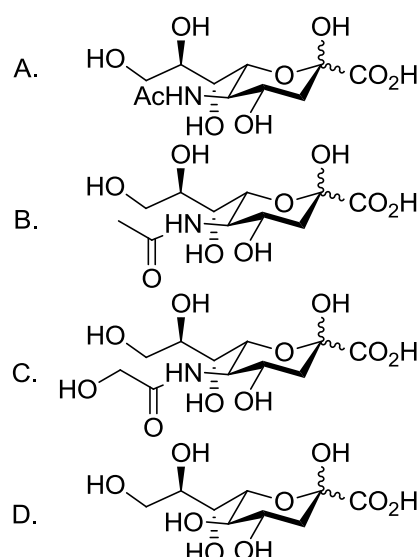
Figure 1.5 Examples of sialic acid structures: A) Neuraminic acid; B) N-acetylneuraminc acid; C) *N*-glycolneraminic acid; D) 2-keto-3-deoxy-glycero-galacto-nonulosonic acid (KDN).

1.3.2 Physiological roles in mammals

In biological systems, sialic acids are expressed on the very outer periphery of glycoproteins or glycolipids which act as "surface markers" as they are known to interact with various cells and physiological agents.[8,12] The diverse nature of sialic acids gives an overwhelming variety to the characteristics of glycoproteins and glycolipids, particularly glycans, thereby sialic acids play a crucial role in intercellular processes such as cell recognition, physiological development, and cell adhesion.[13] This makes sialic acids essential for normal physiological processes in multicellular organism including mammals.[14]

Sialic acids participate in various recognition processes by expressing themselves as "patterns", allowing the immune system to distinguish between their host and foreign or invading structures.[15]

For physiological development and cell adhesion, sialic acids have roles in the brain, or more specifically, on the outer surface of the neural cell adhesion molecules, which is another type of protein responsible for the adhesion of adjacent neurons.[16] Sialic acids can be expressed as repetitive chains of polysialic acids, which have an overall negative charge that prevents the cross linking of neural cell adhesion molecules by electronegative repulsion. The presence of polysialic acids in the intercellular spaces of neurons (on the cell adhesion

molecules) prevents other neurons from collapsing together allowing the neurons to have just enough space to function properly.[17]

Sialic acids have structural and protective roles in mucins (proteins which makes up the mucus), providing the repulsive electronegative forces acting between their negative charges. This allows the trapping of water molecules on the surface of mucins *via* hydrogen bonds, giving mucus its slimy and protective properties.[8]

Since sialic acids play vital roles in metabolism, there are diseases associated with sialic acid expression. For example, tumour cells over express sialic acids in a form of glycoconjugates or polysialic acids on the cell surface.[18,19] The overall negative charge of sialic acid glycocojugates and polysialic acids on the tumour cell surface gives an electronegative repulsion between other cells, causing cancerous cells to lose cell adhesion to the tumour mass, aiding their pathology by proliferation across the body.[18,20] Conversely, the disruption of sialic acid biosynthesis caused by irreversible mutations can result in severe form of proteinuria (excessive urinary protein excretion) or neuromuscular disorders.[21,22]

1.3.3 The role of NANA in bacteria

There are at least two ways by which bacteria utilise NANA. Firstly, some bacteria use NANA as an alternative source of energy, in a catabolic pathway that ultimately produces fructose. Secondly, and most interestingly, some bacteria use NANA for the purpose of camouflage.[23,24]

Despite their diverse nature, the biosynthesis of sialic acids is not ubiquitous.[7] While the expression of sialic acids is common in mammalian cells, only certain species of microorganisms can synthesise and express NANA on their cell surface.[25] Such microorganisms include *Neisseria meningitidis* and *Campylobacter jejuni* as these bacteria utilise NANA for a clever survival strategy in a form of molecular mimicry.[23] *N. meningitidis* is often associated with meningitis[26] and other diseases such as meningococcemia,[27] a type of blood poisoning. *C. jejuni* is responsible for gastroenteritis, often associated with food-borne illness, and in the worst cases *C. jejuni* can cause paralysis in the form of Guillain-Barre syndrome.[28] These pathogenic bacteria coat themselves with sialic acids, so that the host immune system cannot readily tell the difference between the bacteria and their own cells to avoid being attacked by the immune system.[29]

1.4 The enzyme, NANAS

1.4.1 General enzyme structure

The structure of NANAS isolated from *Nme*NANAS has been previously determined.[3,9] The structure of *Nme*NANAS is a domain swapped homodimer (**Figure 1.6**)[9], consisting of two identical monomeric units. Each subunit comprises two distinct domains joined together by an extended linker region.[9]
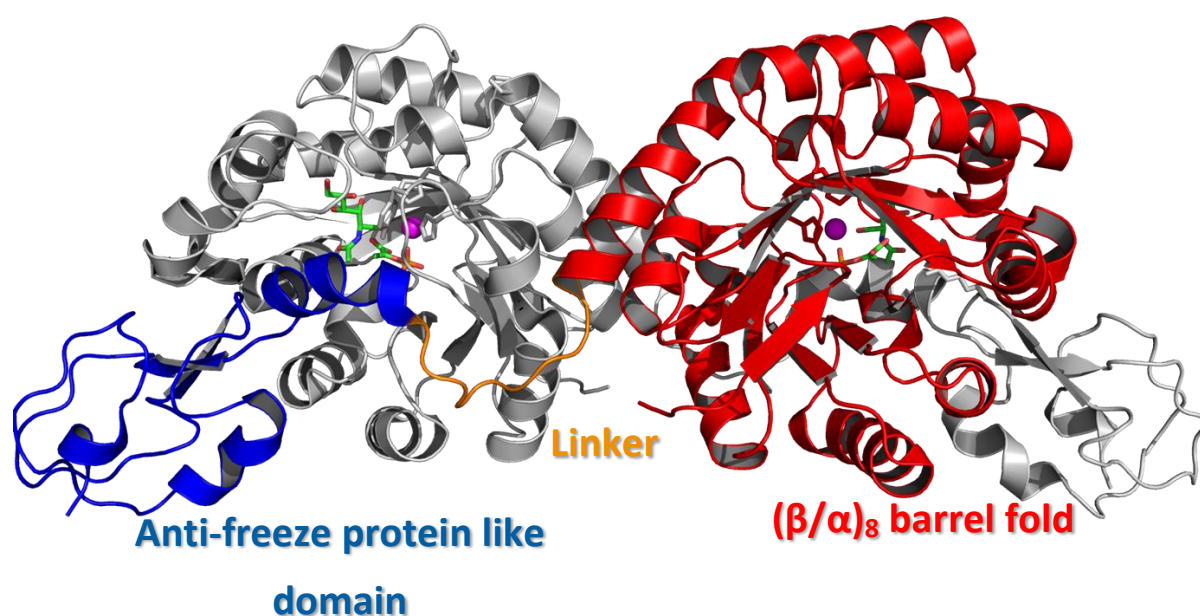
Figure 1.6 Quaternary structure (a domain swapped homodimer) is made up of two identical monomers/subunits. One monomer is shown in colour and the other identical monomer in grey. The monomeric unit consists of a TIM barrel fold (red) and an anti-freeze protein like domain (blue) connected by a linker region (orange) (PDB code 1XUZ).

The N-terminal region of the subunit is a TIM $(\beta/\alpha)_8$ barrel which has eight β strands forming a β-barrel enclosed by eight α helices.[9] The C-terminal region has a novel structure similar to that of functional type III antifreeze protein.[3] The interaction of the two subunits, includes the close packing between two ends of the C-terminus from the opposing TIM barrel, the packing of the extended linker region between one monomer with an opposing TIM barrel from the second monomer, and then the interaction between the N-terminal region antifreeze-like domain from one monomer with the opposing TIM barrel of the second monomer.[3]

1.4.2 Active site and key amino acid residues

The active site of the enzyme (**Figure 1.7**) is located at the C–terminal end of the TIM barrel domain.[3] The antifreeze domain contributes three residues into the catalytic site of the opposing monomer barrel. These three amino acid residues, Thr-285, Phe-288, and Arg-314, are involved in substrate binding.[3] Arg-314 is highly conserved suggesting it is likely that Arg-314 serves a specific role in the functionality of the enzyme. X-ray crystallography of *Nme*NANAS with PEP and *N*-acetylmannosaminitol (an unreactive, reduced form of ManNAc) bound, shows hydrogen bonding between Arg-314 and the carbonyl oxygen of *N*-acetylmannosamine. With this evidence it is proposed that the residue Arg-314 forms a hydrogen bond with the acetyl oxygen of the substrate ManNAc.[30] A previous study involving the substitutions of Arg-314 into either Lys or Ala suggested that Arg-314 is not necessary for binding, but rather for steering the ManNAc into a reactive position.[30]

The Arg-314-Lys variant had diminished catalytic activity, whereas the Ala substitution was non-functional. According to modelling studies, both variants accommodate the substrate ManNAc in the active site. The study proposed that the guanidinium functionality of Arg-314 is not essential for the ability to bind ManNAc but is required for orientating ManNAc into a correct position within the active site, in order to react with PEP.[30]
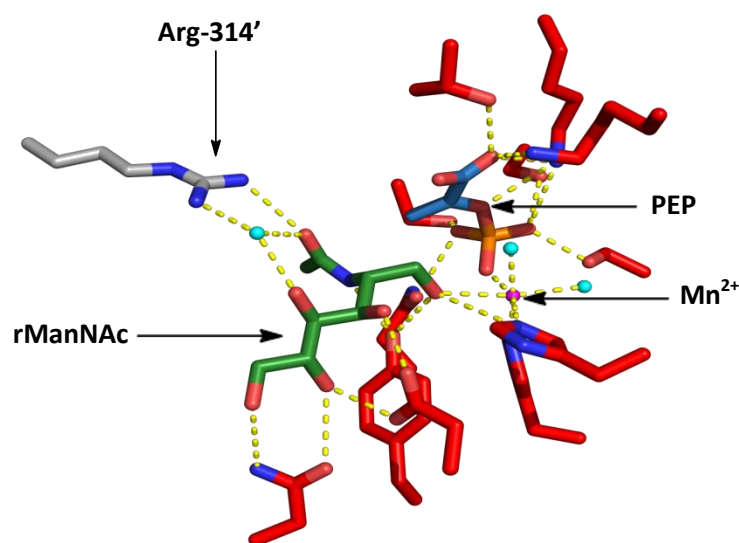
Figure 1.7 The active site of *Nme*NANAS. Arg-314' contributed by the other monomer is coloured as grey, Mn^{2+} as a pink sphere, PEP as blue with phosphate group shown as orange, and *N*-acetylmannosaminitol as green (rManNAc). The residues coloured red represent the amino acid residues from the TIM barrel fold. The cyan spheres represent water molecules. (PDB code 1XUZ).

1.5 Biosynthesis of NANA

1.5.1 Metabolic pathway for NANA synthesis

The bacterial pathway for NANA biosynthesis is distinct from that of mammals (**Figure 1.8**). In bacterial systems, NANA is synthesised by the enzyme NANAS, utilising the substrate PEP and ManNAc formed from another separate enzyme, UDP-*N*-acetylglucosamine epimerase.[2] Conversely, animals produce NANA by first phosphorylating ManNAc using ATP, in a reaction catalysed by ManNAc kinase to form *N*-acetylmannosamine 6-phosphate (ManNAc-6-P) and ADP.[2,13] ManNAc-6-P then undergoes a condensation reaction with PEP, catalysed by the mammalian enzyme *N*-acetylneuraminic-9-phosphate synthase (NANA-9-PS), to form *N*-acetylneuraminic acid 9-phosphate (NANA-9-P).[2] This phosphorylated version of NANA then undergoes dephosphorylation by the action of the enzyme NANA-9-P phosphatase to form NANA.[2] Finally NANA, formed in both mammalian and bacterial pathways, is activated by the action of the enzyme CMP-NANA synthetase, utilising cytosine triphosphate (CTP).[2]

This enzyme produces CMP-NANA (the activated form of NANA)[2] which is used to assimilate NANA into functional glycoproteins and glycolipids *via* endoplasmic reticulum–golgi apparatus pathways.[15,25]
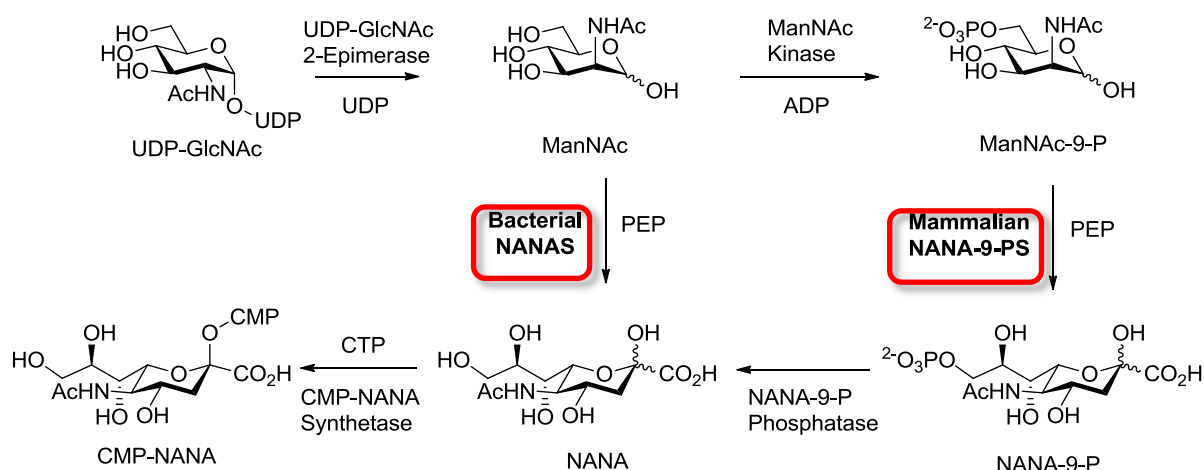
Figure 1.8 The bacterial and mammalian pathway for NANA synthesis.

The use of CTP to activate NANA is considered biologically unusual, since most other monosaccharides   are activated in the form of uridine or guanine (UDP or GDP) in vertebrates.[7] Sialic acid or NANA is also known to be an alternative source of energy *via* catabolic processes in some species of bacteria.[23,31]

These two different enzymatic pathways between mammals and bacteria allow the development of selective inhibitory compounds against bacterial NANAS. Inhibitors can be derived from PEP and ManNAc analogues as these substrate analogues can mimic the natural substrates of the enzyme. The results of inhibition studies may aid in the further design of specific drugs.

1.5.2 Reaction mechanism of *Nme*NANAS

NANAS catalyses the condensation reaction between the substrates, PEP and ManNAc, whereas the mammalian enzyme utilises ManNAc-6-P (mannosamine-6-phosphate). NANAS is a divalent metal ion dependent enzyme, and Mn^{2+}-bound enzyme displays the highest

catalytic activity. Two possible mechanisms for the catalytic action of the enzyme were proposed since there are two potential ways PEP can react with the aldehyde functional group of ManNAc.[9]

The first possible mechanism would occur *via* the cleavage of the O-P bond of PEP (**Figure 1.9**). This mechanism begins with the nucleophilic attack by a water molecule on the phosphorus, releasing phosphate and a pyruvate in a form of an enolate. This enolate subsequently attacks the carbonyl functional group of ManNAc, finally producing the product NANA in a linear form.
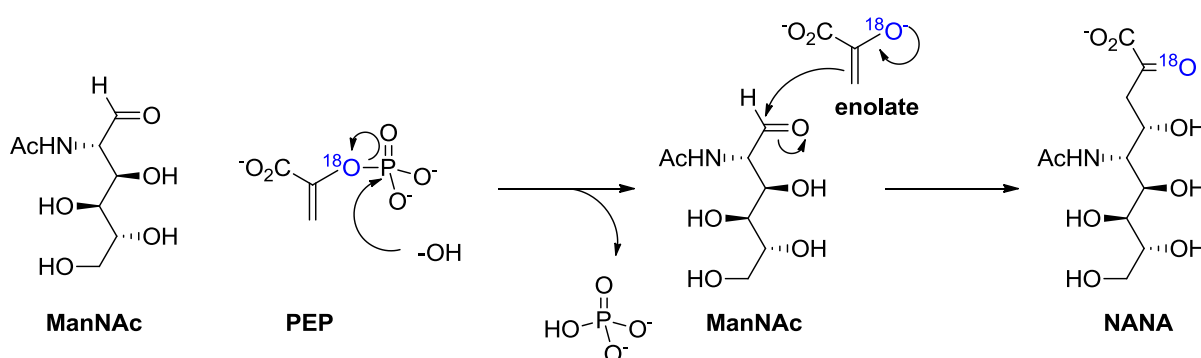
Figure 1.9 Possible reaction mechanism of NANAS *via* P-O cleavage.

The second possible mechanism begins with the carbonyl carbon of ManNAc undergoing nucleophilic attack by the C3 carbon of the PEP molecule forming an oxocarbenium ion intermediate (**Figure 1.10**).[9]
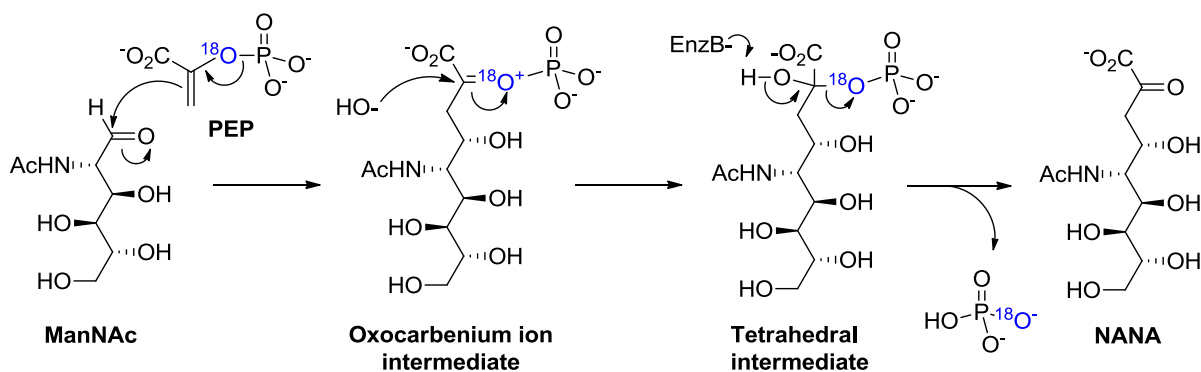
Figure 1.10 Possible reaction mechanism of NANAS *via* C-O bond cleavage.

11

The intermediate is then readily attacked by a water molecule to produce a tetrahedral intermediate.[3,9] The tetrahedral intermediate will then subsequently lose the phosphate group, which means that this reaction mechanism operates *via* cleavage of a C-O bond of PEP.[3] This mechanism also results in the formation of NANA as the ring opened form.

Isotopic labelling of oxygen was used to determine which of the two proposed mechanisms for the reaction catalysed by NANA was likely to be operating.[9] [18]O was incorporated into the phosphate group of the substrate, PEP. The use of this labelled PEP determined which mechanism occurred by examination of the products. If the reaction occurred *via* the P-O bond cleavage of PEP (the first mechanism), the [18]O label will be incorporated into the product, NANA. If the reaction proceeds *via* the C-O bond cleavage of PEP (the second mechanism) then the [18]O label will remain in the inorganic bi-product of phosphate. ^{31}P NMR spectroscopy was used to observe the reaction between [18]O incorporated PEP and ManNAc with *Nme*NANAS.[2,9] The upfield shift of resonance arising from the phosphorus bonded to the [18]O showed that the oxygen isotope was incorporated into the inorganic phosphate and not into the product NANA which is consistent with C-O bond cleavage (**Figure 1.11**).[2,9] This type of reaction is considered unusual because few other PEP utilising enzymes are known to proceed by C-O bond cleavage. Such enzymes that share this mechanism may be related by evolution and will be discussed in detail below.
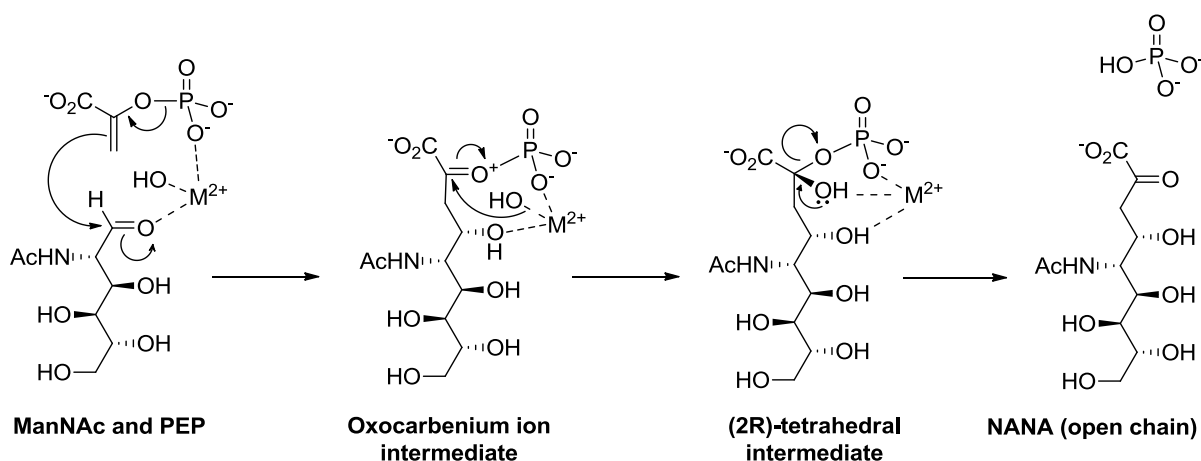
Figure 1.11 Proposed reaction mechanism of NANA synthesis.

The stereospecificity of the reaction has also been studied in other experiments using ^{1}H NMR spectroscopic analysis with *Cje*NANAS.[29] When the enzyme catalysed the reaction

with *Z*-[3-²H]-PEP, the enzyme produced (3*S*)-3-deutero-NANA (²H on the equatorial position), whereas *E*-[3-²H]-PEP produces (3*R*)-3-deutero-NANA (²H on the axial position) (**Figure 1.12**).[29] When *E*-[3-F]-PEP was used during a ¹⁹F NMR spectroscopic analysis, the enzyme did not accept this compound as an alternative substrate. *Z*-[3-F]-PEP on the other hand was accepted and formed (3*S*)-3-fluoro-NANA. These observations show that only the *si* face of the substrate PEP reacts with the *si* face of the carbonyl group of ManNAc.[29]
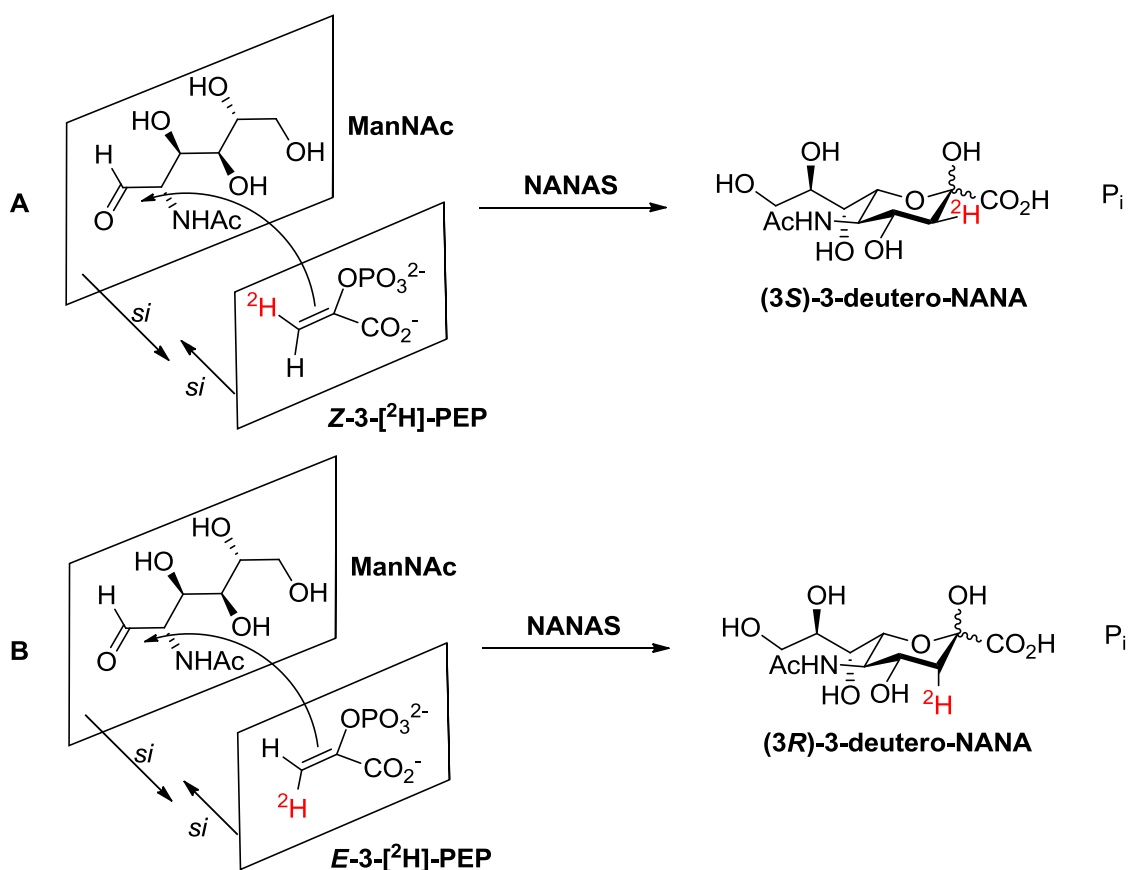
Figure 1.12 The investigation of the stereochemistry of NANAS reaction, (A) shows the NANAS catalysed reaction with Z-[3-2H]PEP which forms (3S)-3-deutero-NeuNAc. (B) Shows the reaction with E-[3-²H]PEP which gives (3*R*)-3-deutero-NeuNAc. Deuterium, ²H, is coloured red.

1.5.3 Metal dependency

All NANAS require a divalent metal ion to function.[9] Within the active site there are two key amino acid residues, His-215 and His-236 which coordinate to the divalent metal ion (**Figure 1.13**).[3] The divalent metal ion also coordinates with two water molecules, the carbonyl oxygen of the substrate ManNAc and the oxygen from the phosphate group of PEP giving an octahedral coordination geometry.[3]
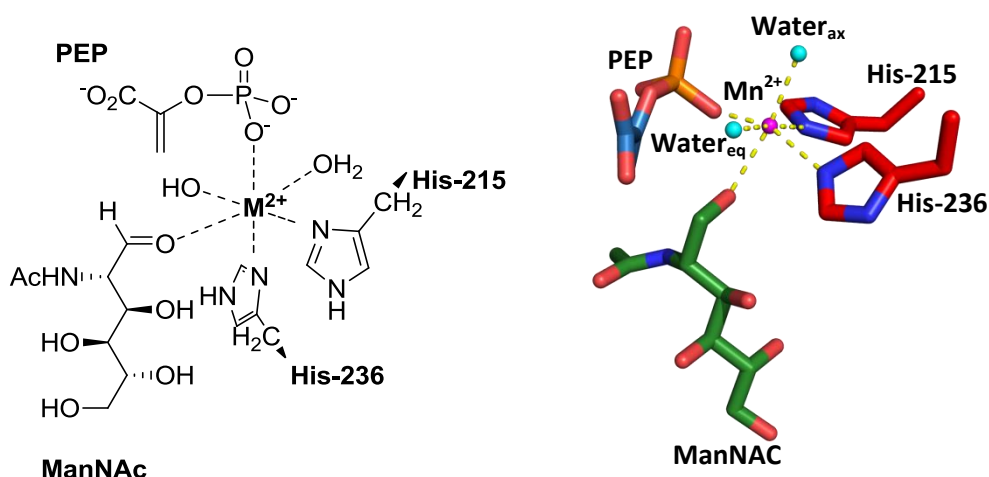
Figure 1.13 Divalent metal coordination within the active site of NANAS.

The Mn^{2+} ion gives the highest catalytic activity for *Nme*NANAS.[3,9] Other divalent metal ions are also known to activate the NANAS such as Co^{2+} and Mg^{2+} ions, where Mn^{2+} closelyfollowed by Co^{2+} both provide the highest catalytic activity for *Nme*NANAS and *Cje*NANAS.[9,29] In contrast the human NANAPS showed the highest catalytic activity for Mg^{2+}.[32]

The divalent metal ion coordinates to the carbonyl oxygen of the substrate ManNAc which activates the carbonyl group making ManNAc more susceptible to nucleophilic attack.[3,9]

1.5.4 Intermediates of NANAS reaction

Two intermediates are predicted to be part of the reaction: oxocarbenium intermediate and the tetrahedral intermediate, formed by the attack of water on the oxocarbenium ion (**Figure 1.14**).
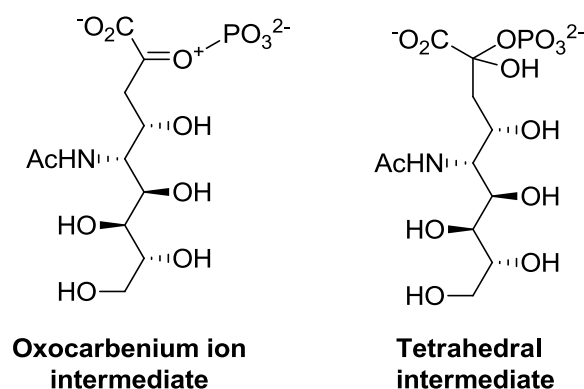
Figure 1.14 The intermediates of NANAS catalytic reaction.

The design of inhibitors, based on the structural mimicry of these intermediates has been carried out in past studies. Analogues of the high energy intermediates may be a useful strategy for disrupting the catalytic function of NANAS.

1.5.4.1 Inhibition of NANAS with a tetrahedral intermediate mimic.

An analogue which structurally mimics the tetrahedral intermediate was synthesised and tested on *Nme*NANAS reporting a potent inhibition constant of 3.1 ± 0.1 μM (**Figure 1.15**).[3]
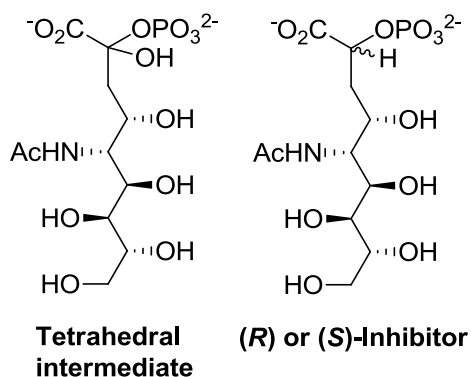
Figure 1.15 Tetrahedral intermediate mimicking inhibitor.

The hydroxyl group bonded to the C2 position were replaced in the inhibitor by a hydrogen atom.

In this study, NANAS was tested with two diastereoisomers of the inhibitor, which bears either (2*R*) or a (2*S*)-configuration at the tetrahedral centre. Inhibition studies using these

stereoisomers demonstrated that the (2*R*)-configuration exhibited a stronger inhibition constant than the compound with the (2*S*)-configuration. An X-ray crystallographic structure of *Nme*NANAS-inhibitor complex, showed the (2*R*) stereoisomer of the tetrahedral intermediate analogue bound in the active site. This suggests that the tetrahedral intermediate also bears the (2*R*)-configuration, formed from the water molecule attacking the *si* face of the oxocarbenium intermediate, during NANA biosynthesis.[3]

An oxocarbenium intermediate-mimicking analogue was tested on an enzyme which is related to NANAS. The study which uses this analogue will be explained in later sections of this chapter in detail.

1.6 Related Enzymes

Since NANAS catalyses a reaction *via* the unusual C-O bond cleavage of PEP, it is thought that other PEP utilising enzymes which cleave this C-O bond may be evolutionarily related.[2] There are only a few known enzymes which catalyse a similar reaction, but one particular category of enzyme are of interest (which includes NANAS), is the PEP aldolases. Such enzymes include 3-deoxy-D-*arabino*-heptulosonate 7-phosphate synthase (DAH7PS) and 3-deoxy-D-*manno*-octulosonate 8-phosphate synthase (KDO8PS) which both catalyse the addition of PEP to an aldehyde in an aldol condensation-like reaction, similar the mechanism used by NANAS.[33,34] Despite low sequence identity, NANAS, DAH7PS, and KDO8PS share structural similarities as these enzymes all share a TIM (βα)$_8$ barrel fold.[35,36]

The reaction mechanism occurring *via* C-O bond cleavage has been studied in both DAH7PS and KDO8PS. Both enzymes have also have been the subject of extensive inhibition studies with a variety of substrate analogues.[36-38]

1.6.1 Introduction to DAH7PS

DAH7PS catalyses the formation of 3-deoxy-D-*arabino*-heptulosonate 7-phosphate (DAH7P) from the substrates PEP and D-erythrose 4-phosphate (E4P), with the release of inorganic phosphate (**Figure 1.16**).[39,40]
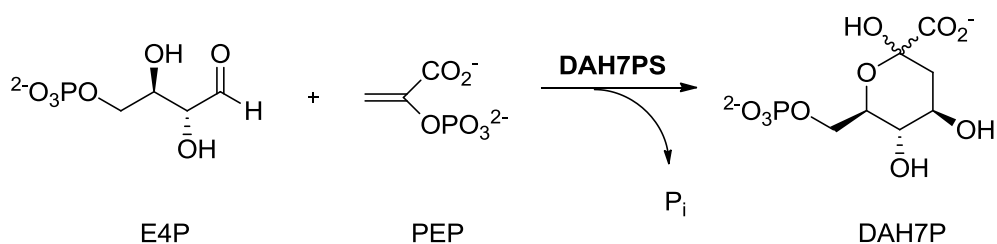
Figure 1.16 Reaction catalysed by DAH7PS.

DAH7PS is an important enzyme involved in the first step of the shikimate pathway, the metabolic pathway ultimately responsible for the biosynthesis of aromatic compounds.[41] The pathway not only synthesises the aromatic amino acids, phenylalanine, tyrosine and tryptophan, but also a number of other important aromatic compounds such as siderophores and quinone.[42] The shikimate pathway operates in plants, fungi and bacteria but is absent in mammals, which allows the development of herbicides, fungicides and antibiotics which target this pathway however do not affect mammals.[41,42]

The enzymatic mechanism of DAH7PS is similar to that of the related enzyme NANAS (**Figure 1.17**). DAH7PS catalyses the reaction between PEP and E4P by reacting PEP with the aldehyde of E4P in an aldol-addition like fashion. The enzymatic reaction proceeds *via* cleavage of the C-O bond.[43]
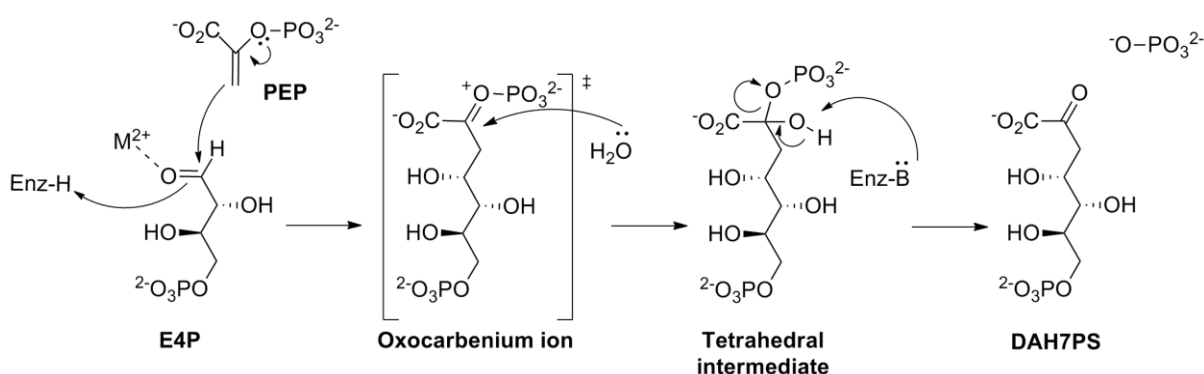
Figure 1.17 Proposed mechanism for DAH7PS.

One significant difference between the reaction mechanism of DAH7PS and NANAS is the stereospecificity of the reaction (**Figure 1.18**). For DAH7PS, PEP attacks the *re* face of the aldehyde.[44] This leads to altered styereochemistry at C4 of the product. In addition, it also has been proposed that the water attacks the oxocarbenium ion intermediate from the *re* face. This would result in a tetrahedral intermediate with the opposite configuration at C2 to that in the NANAS reaction.[35]
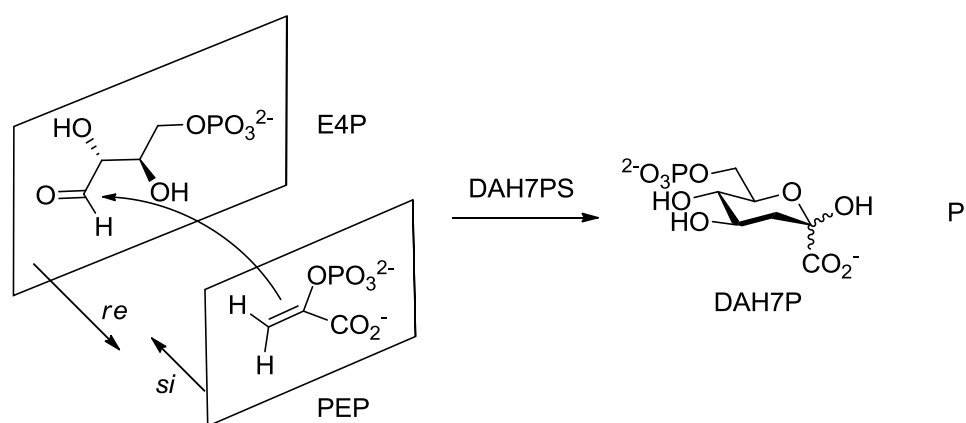
Figure 1.18 The *si* face of PEP attacks the *re* face of aldehyde during the reaction catalysed by the enzyme, DAH7PS.

1.6.1.2 Inhibition of DAH7PS with oxocarbenium mimic.

Past studies used analogues which mimic the structure of the oxocarbenium intermediate for the reaction catalysed by DAH7PS and showed great success in exhibiting potent inhibition.[42]

The oxocarbenium ion intermediate possesses a partial double bond between the C2 position of PEP structure and the bridging phosphate (**Figure 1.19**). This characteristic was taken advantage of by designing analogues which mimic the planar structure of the oxocarbenium ion intermediate.
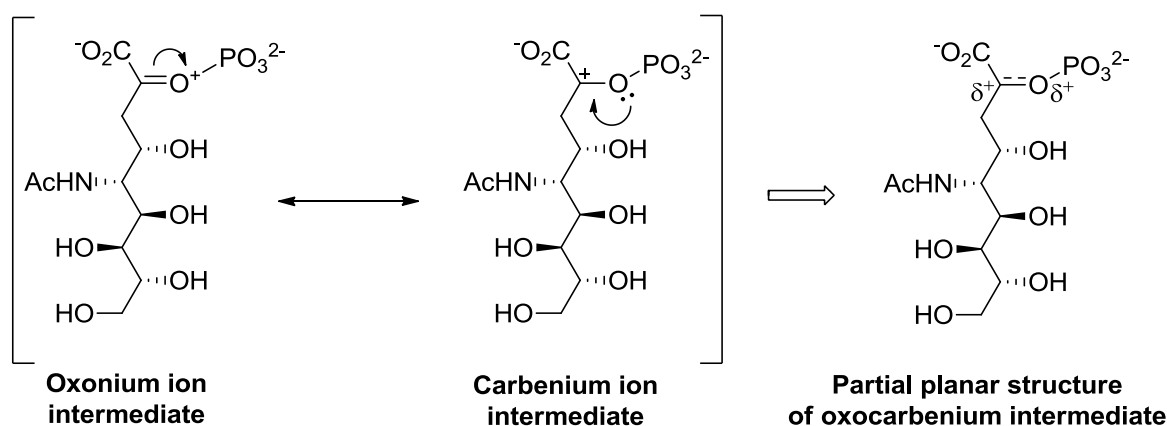
Figure 1.19 Resonance of the oxocarbenium ion.

The intermediate mimicking analogue tested against DAH7PS is vinyl phosphonate (**Figure 1.20**). This analogue has a planar double bond at C2, mimicking the planar geometry of the oxocarbenium intermediate.

Vinylphosphonate has a phosphate group replaced by a methyl phosphono group, effectively replacing an oxygen atom bonded to C2 with a methylene group. The strong C-P bond prevents any catalytic reaction in the active site. The inhibition constant for vinyl phosphonate against DAH7PS was determined to be 4.7 ± 0.7 µM.

Oxocarbenium ion intermediate   **Vinyl phosphonate**
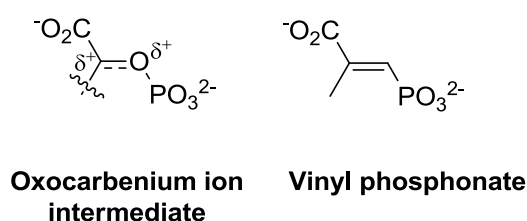
Figure 1.20 Vinyl phosphonate and the oxocarbenium intermediate.

1.6.2 Introduction to KDO8PS

KDO8PS utilises the substrate PEP and arabinose 5-phosphate (A5P) to synthesise 3-deoxy-D-*manno*-octulosonate 8-phosphate (KDO8P) with the release of phosphate (**Figure 1.21**).[45]
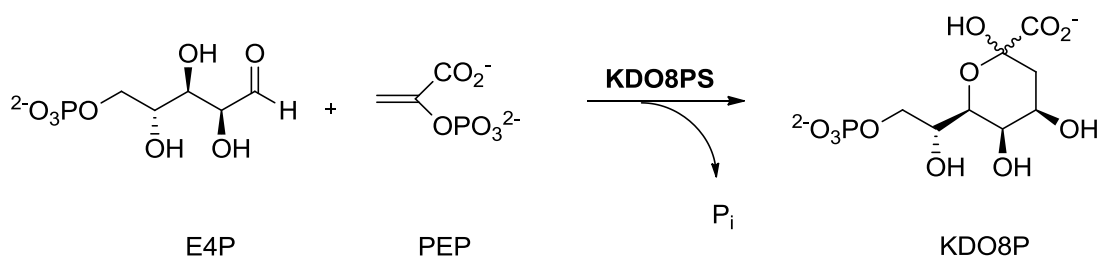
Figure 1.21 Reaction catalysed by KDO8PS.

KDO8PS is a key enzyme involved in the biosynthetic pathway of lipopolysaccharide synthesis in Gram-negative bacteria.[46] Lipopolysaccharides are used by bacteria to create a strong outer layer to their cell which gives the bacteria cell structural integrity.

As with DAH7PS, the enzymatic mechanism of KDO8PS is similar to that of the related enzyme NANAS (**Figure 1.22**). KDO8PS catalyses the reaction between PEP and E4P by reacting PEP with the aldehyde of A5P in an aldol reaction. As for NANAS, the enzymatic reaction also proceeds *via* the cleavage of the C-O bond.
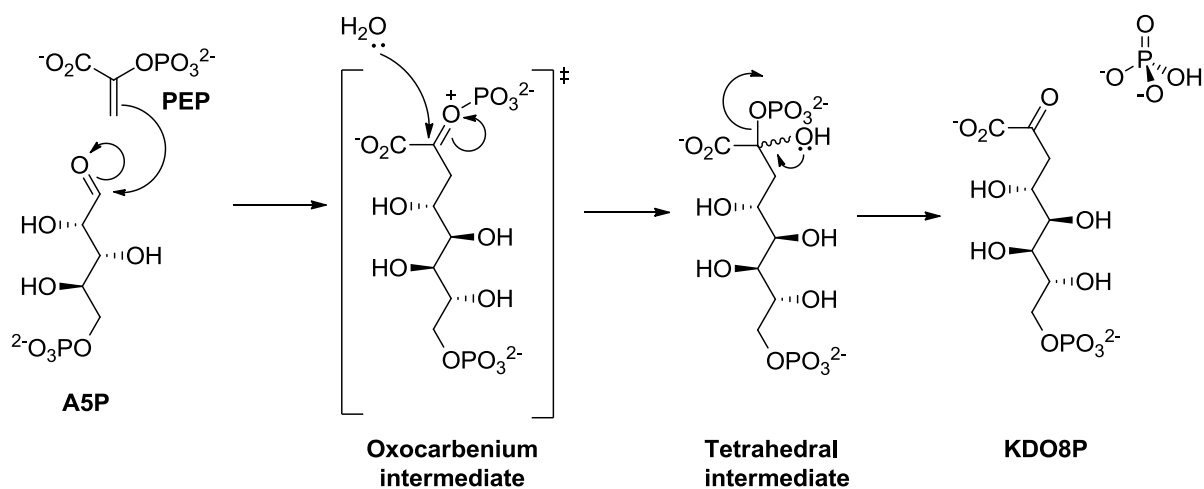
Figure 1.22 Proposed reaction mechanism of KDO8PS.

As for DAH7PS, PEP attacks the *re* face of the aldehyde (**Figure 1.23**).[47]
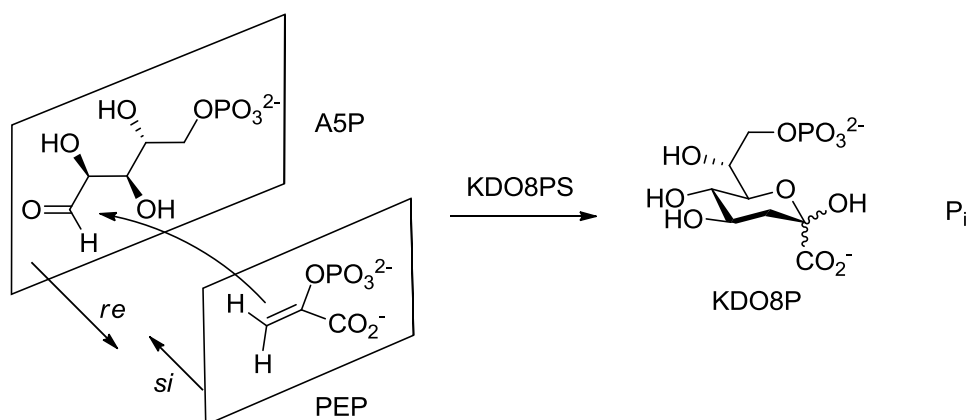
Figure 1.23 The *si* face of PEP attacks the *re* face of aldehyde during the reaction catalysed by the enzyme, KDO8PS.

1.7 Aims of this thesis

The aim of this research was to investigate and compare the inhibition of NANAS enzymes from two different species, *N. meningitidis* and *C. jejuni*, with inhibitors derived from substrate analogues.

In order to achieve this, kinetic assays were performed on *Nme*NANAS or *Cje*NANAS with their natural substrates (PEP and ManNAc) in presence of a variety of analogues.

Chapter two describes the studies with analogues of PEP. Chapter three outlines the studies with a ManNAc and a NANA analogue.

Chapter 2
Preparation of the enzyme NANAS and kinetic assays with PEP analogues

2.1 Introduction

The goal of this research was to test various substrate and product analogues on wild-type *Nme*NANAS and *Cje*NANAS. In order to undertake this work both *Nme*NANAS and *Cje*NANAS had to be obtained by protein expression and purification. For both enzymes, the genes encoding the proteins had been cloned and inserted into an expression plasmid prior to the commencement of this work.[30]

This chapter describes a series of experiments in which a range of PEP analogues were tested as alternative substrates and inhibitors for NANAS.

2.2 Preparation of the enzyme, *Nme*NANAS and *Cje*NANAS

2.2.1 Wild-type *Nme*NANAS and *Cje*NANAS expression in general

The pDEST™17 vectors bearing either the *NeuB* or *Cj1141* genes (encoding wild-type *Nme*NANAS or *Cje*NANAS respectively) were transformed into *E. coli* BL21 (DE3) pBB540 for expression and purification. The vector pDEST™17 also encodes an N-terminal His-tag to allow for purification of the protein by immobilised metal affinity chromatography (IMAC). A tobacco etch virus protease (TEV) cleavage sequence was also incorporated between the *Nme*NANAS or *Cje*NANAS gene and the His-tag sequence to allow for tag removal after purification. Protein expression was induced through the addition of isopropyl β-D-1-thiogalactopyranoside (IPTG), which binds to the *lac operon* site incorporated into the vector.

2.2.2 Growing cells producing NANAS

The cell lines bearing the plasmids for the expression of the two NANAS enzymes were grown and harvested by centrifugation.

The general protocol that was used for obtaining purified enzymes is shown in **Figure 2.1**.
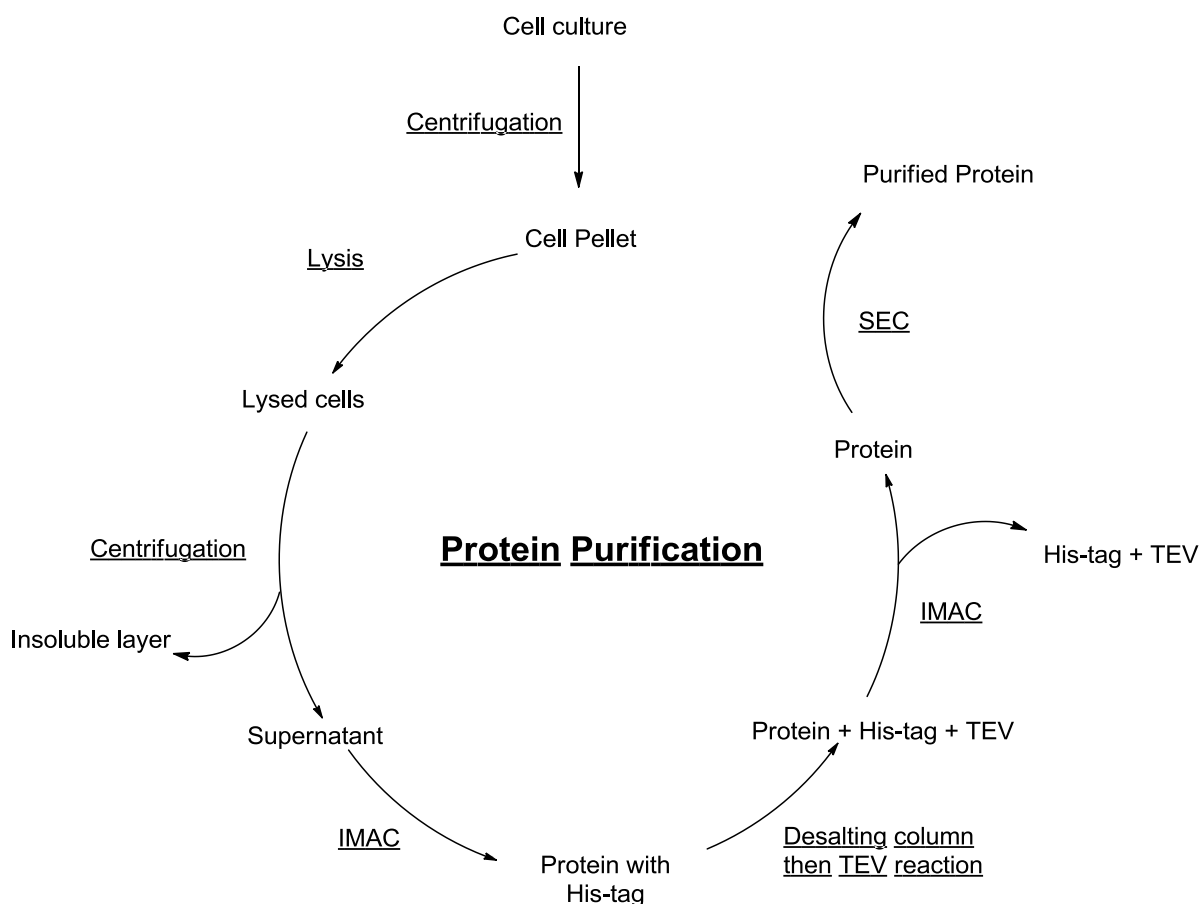
Figure 2.1 Flow diagram of protein purification in general.

2.2.3 Obtaining supernatant by cell lysis and centrifugation

Cells were lysed by sonication following their re-suspension in buffer solution. The resulting lysate was clarified by centrifugation allowing removal of the cell debris. Both *Nme*NANAS and *Cje*NANAS are soluble so large proportions of the over-expressed protein were observed in the supernatant after centrifugation in both cases.

2.2.4 Immobilised metal affinity chromatography (IMAC)

The NANAS enzymes were isolated from the supernatant using IMAC. The IMAC column used for this procedure was charged with Co^{2+} ions to allow binding of the His-tag incorporated at the N-terminal of both NANAS enzymes. This enabled the NANAS enzymes to be selectively separated from other background *E. coli* proteins. The proteins bound to the IMAC column were eluted using buffer containing high concentrations of imidazole. The

fractions containing NANAS were pooled together and subsequently run through a desalting column.

2.2.5 Desalting column and TEV cleavage

Following IMAC, each protein was desalted to remove the imidazole. The fractions that eluted from the desalting column were pooled together and treated with TEV protease. The TEV reaction was carried out overnight at 4°C as NANAS is known to be temperature sensitive. TEV recognises the protein cleavage sequence (**Figure 2.2)** engineered between the His-tag and NANAS sequences.

Site of cleavage

SYYHHHHHHSGGQFYLNESGSGM
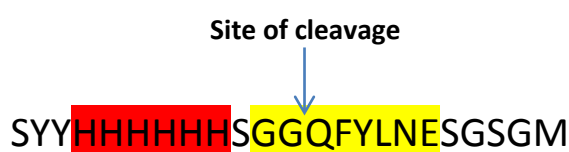
Figure 2.2 The His-tag sequence located at the N-terminus of the protein sequence from the vector, pDEST™17. In red is the polyhistidine tag which coordinates to a metal ion, and in yellow is the protein sequence recognised by TEV protease. The His-tag is cleaved by TEV protease between glycine and glutamine residues.

The TEV protease was expressed with its own noncleavable His-tag. The protein with the His-tag cleaved was therefore separated from both the TEV protease and the cleaved His-tags using a second IMAC step. Any other impurities that may have been eluted from the first IMAC step will be removed in this second IMAC procedure along with TEV and cleaved His-tag. Finally, the fractions containing NANAS were purified by size exclusion chromatography (SEC).

2.2.6 Size-exclusion chromatography

The pooled fractions of His-tag cleaved NANAS were eluted through a SEC column in order to purify the protein further. The eluted protein was collected as fractions, pooled together and concentrated. The purified *Nme*NANAS or *Cje*NANAS were flash frozen in the SEC buffer and stored at -80 °C until required for experimentation.

The procedure of protein purification and the purity of the final products were checked using gel electrophoresis. The molecular weight of *Nme*NANAS and *Cje*NANAS is 38.34 kDa and 38.48 kDa respectively shown in **Figures 2.3 and 2.4** respectively.
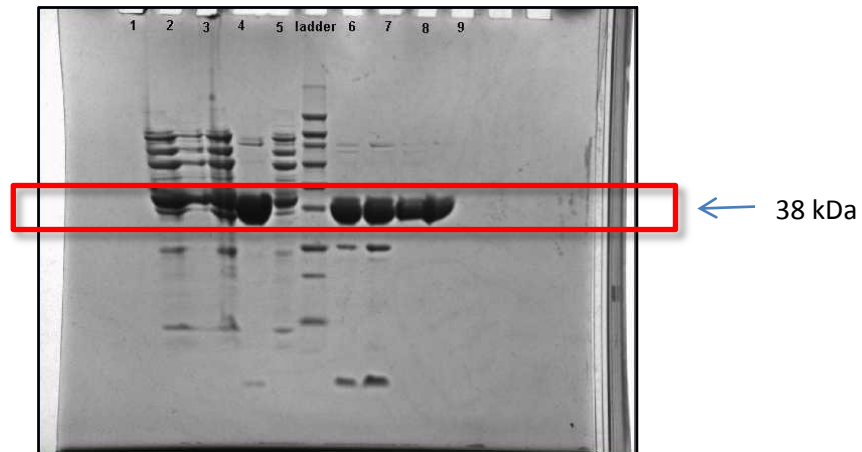
Figure 2.3 SDS-PAGE gel showing purification steps of *Nme*NANAS (1 whole lysed cells, 2 supernatant, 3 insoluble protein, 4 IMAC bound protein, 5 IMAC flowthrough, 6 Desalt and TEV protease, 7 IMAC bound, 8 IMAC flow through, 9 SEC).
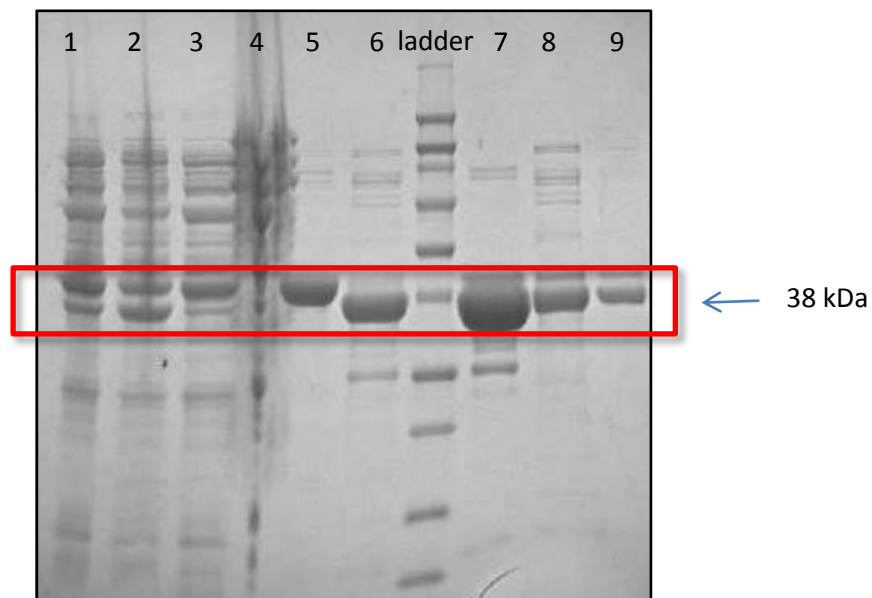
Figure 2.4 SDS-PAGE gel showing purification steps of *Cje*NANAS (1 whole lysed cells, 2 supernatant, 3 IMAC bound protein 4 insoluble protein, 4 IMAC bound protein, 5 IMAC flowthrough, 6 Desalt and TEV protease, 7 IMAC bound, 8 IMAC flow through, 9 SEC).

As shown in lane seven of both gels (**Figures 2.3 and 2.4**), a large proportion of NANAS was lost in the flowthrough due to the incomplete TEV cleavage of His-tags. The cleavage of His-tags may have not gone to completion due to the low temperature at which the TEV reactions were carried out or not left for sufficient time at this temperature.

There are some impurities in lane nine of the gel shown in **Figure 2.4** for the purification of *Cje*NANAS. The impurity corresponds to *Cje*NANAS with the His-tag still attached. Some of this protein which was not removed in the second IMAC, may have co-purified with the cleaved NANAS by intermolecular interactions or homodimer formation.

According to the gel analysis, the impurity is relatively small when compared with the band corresponding to the protein of interest. The presence of the contaminant tagged protein does not change the catalytic reaction rate of the untagged NANAS, meaning that the effect of the impurity upon kinetic analysis of the purified enzyme is likely to be negligible.[48]

2.3 PEP the natural substrate of NANAS

PEP is a common anionic compound which has great significance in biochemical processes. This molecule is a small, three carbon compound which has three key functional groups (**Figure 2.5**); the carboxylic acid group, the phosphate group, and the double bond between C2 and C3.
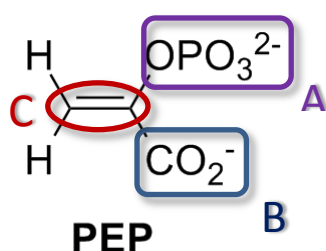
Figure 2.5 The three functional groups of PEP; A, phosphate group, B, carboxylic acid, and C, carbon-carbon double bond.

The key feature of PEP is that it is an enol, and thus nucleophilic at C3. However, the double bond is also conjugated to the carboxylic functionality, potentially making the compound electrophilic at C3 (**Figure 2.6**).
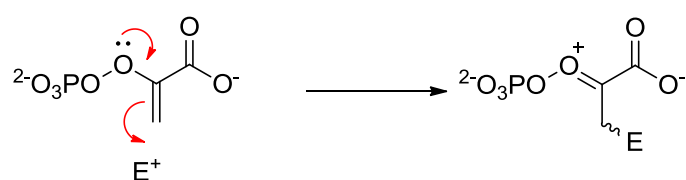
Nucleophilic property of PEP
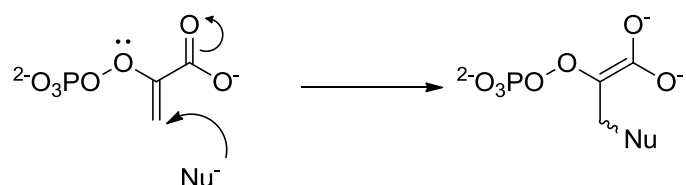
Electrophilic property of PEP

Figure 2.6 The enol characteristic of PEP.

PEP is synthesised during glycolysis in the reaction catalysed by enolase (**Figure 2.7**). Glycolysis is the catabolic pathway for the breakdown of glucose that ultimately forms pyruvate. This metabolic pathway is made up of 10 separate enzymatic reactions. One of these enzymatic reactions is the conversion of 2-phospho-D-glycerate into PEP by the action of enolase.
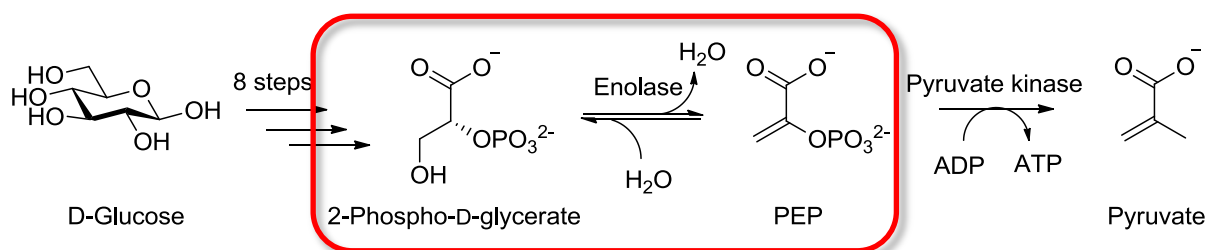
Figure 2.7 Glycolysis and enzymatic reaction of enolase.

PEP is a particularly important metabolite as it is an essential component in a wide variety of biological pathways, serving as a central precursor to many metabolic processes (**Figure 2.8**). Such metabolic processes include the Kreb's cycle, the shikimate pathway, and gluconeogenesis. PEP also serves as an alternative source of energy for bacteria, and it is utilised in the phosphotransferase system.
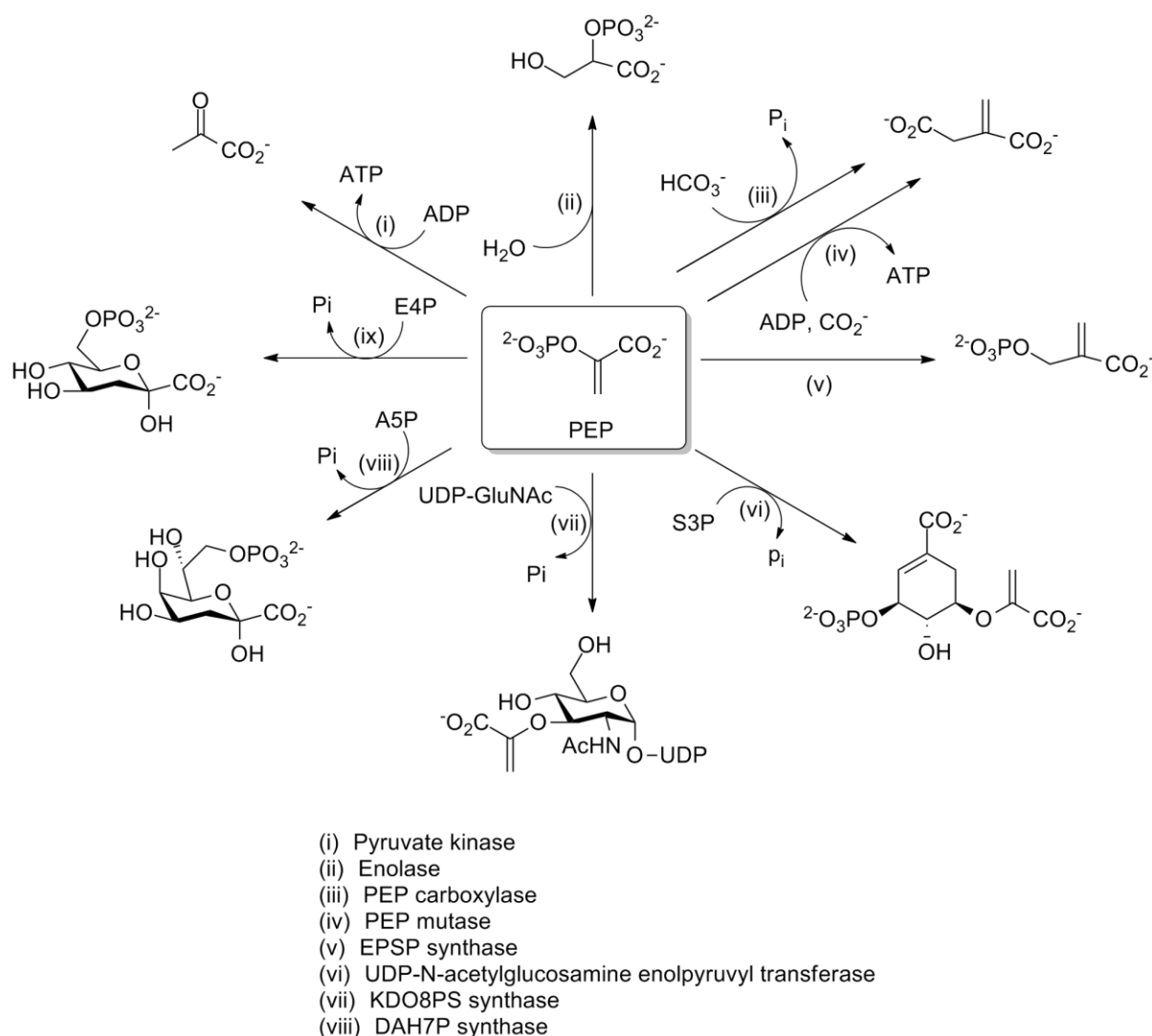
Figure 2.8 Examples of catalytic reactions and their enzymes, involving PEP.

(i) Pyruvate kinase
(ii) Enolase
(iii) PEP carboxylase
(iv) PEP mutase
(v) EPSP synthase
(vi) UDP-N-acetylglucosamine enolpyruvyl transferase
(vii) KDO8PS synthase
(viii) DAH7P synthase

PEP is a highly efficient reactant and intermolecular bond formation is energetically favourable due to the high phosphate group transfer potential (ΔG = -14.8 kcal mol^{-1}).[49] The $\Delta G°´$ of the hydrolysis of PEP is approximately -62 kJ mol^{-1}, whereas that of a typical phosphate ester of an ordinary alcohol is approximately -13 kJ mol^{-1}. This high phosphate transfer potential of PEP is due to the fact that the phosphate group traps the PEP structure in an energetically unstable enol form.[49,50] Only after the phosphate transfer, the product pyruvate is formed which is relatively more stable than PEP, allowing PEP to have favourable transfer of the phosphate group. PEP undergoes a range of reactions by either cleaving the C-O bond to form a reactive pyruvyl group or the O-P bond to form a reactive phosphoryl group.[49]

There are four different modes of reaction by which PEP can act as a substrate (**Figure 2.9**):

A. An addition reaction to the double bond.

B. The addition of an electrophile from the C3 position of PEP leading to the cleavage of the P-O bond, transferring the phosphate group to the nucleophile.

C. The addition of C3 position of PEP, as a nucleophile, to an electrophile. This is followed by the cleavage of the C-O bond and releasing the phosphate as an inorganic group.

D. The addition followed by the elimination to generate a compound with an enolpyruvyl functional group, transferring phosphate to another molecule. This results in the cleavage of the C-O bond as well.
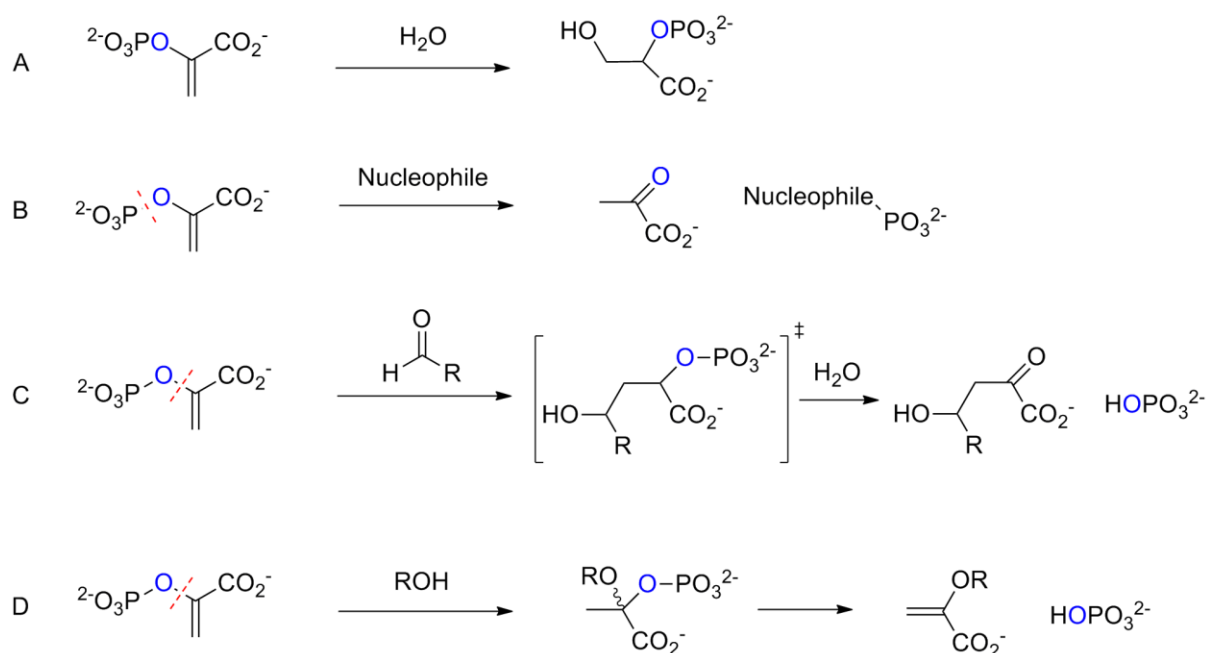
Figure 2.9 Examples of the four different types of enzymatic reactions with PEP.

The enzyme of interest in these studies, NANAS, catalyses the reaction with PEP in a form of "mode C" with C3 of PEP acting as a nucleophile on an aldehydic co-substrate and the reaction occuring *via* C-O cleavage of the C-O-P bond of PEP.[2,9] The reaction results in a new C-C bond at the C3 position of PEP and the release of phosphate. The related enzymes, DAH7PS and KDO8PS also follow the same general mechanism of reaction with PEP, with
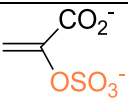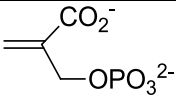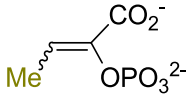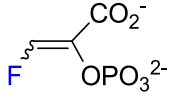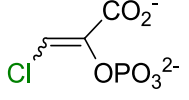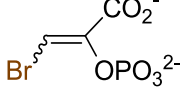
the exception of different stereochemistry. DAH7PS and KDO8PS catalyse the addition of PEP to the *re* rather than *si* face of their aldehydic substrates.[44,47,51]

2.4 PEP analogues used in this study

In previous studies, PEP analogues have been used to explore and understand the reaction mechanisms of PEP-utilising enzymes. [42,52-56] As NANAS is also a PEP-utilising enzyme, a range of PEP analogues were used to observe how the compounds interact with NANAS and disrupt catalysis. The analogues shown in **Table 2.1** were tested as potential substrates or inhibitors against NANAS. The PEP analogues used in this study include sulfoenolpyruvate (SEP), allylic phosphonate, 3-methyl-PEP (Me-PEP), 3-fluoro-PEP (F-PEP), 3-chloro-PEP (Cl-PEP), and 3-bromo-PEP (Br-PEP). The PEP-utilising enzymes investigated in the past using these analogues, include enzyme I of the phosphotransferase system (PTS), pyruvate kinase, PEP carboxylase and PEP enolase.[37,52,57]

Table 2.1 Summary of PEP analogues tested on *Nme*NANAS and *Cje*NANAS.

Analogues	structure
Sulfoenolpyruvate (SEP)	CO_2^- OSO_3^-
Allylic phosphonate	CO_2^- OPO_3^{2-}
3-Methyl-PEP (Me-PEP)	CO_2^- Me OPO_3^{2-}
3-Fluoro-PEP (F-PEP)	CO_2^- F OPO_3^{2-}
3-Chloro-PEP (Cl-PEP)	CO_2^- Cl OPO_3^{2-}
3-Bromo-PEP (Br-PEP)	CO_2^- Br OPO_3^{2-}

The PEP analogues were tested on *Nme*NANAS and *Cje*NANAS to determine if the active site and the catalytic function of the enzyme could accommodate the modification of PEP

functionalities. SEP and the allylic phosphonate were tested to determine whether the enzyme could tolerate the substitution of the phosphate group of PEP. The 3–substituted PEP analogues were tested on the NANAS to determine whether the enzymes could tolerate PEP analogues with a range of different substituents at the C3 position.

The PEP analogues used in this study were synthesised by Hemi Cumming and Scott Walker.[42,51]

2.4.1 SEP

SEP is a PEP analogue in which the phosphate group is replaced by a sulfate group, effectively replacing the phosphorus atom within PEP with a sulphur atom (**Figure 2.10**).
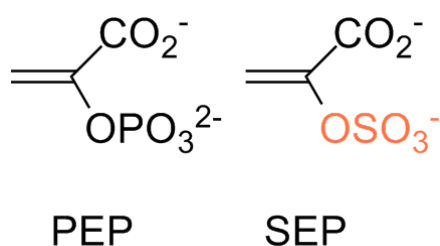
Figure 2.10 PEP analogue, SEP

The sulfate group of SEP is expected to mimic the phosphate group of PEP because past investigations have found evidence of sulfate ions occupying the phosphate binding sites of DAH7PS, as observed by X-ray crystallography.[53,54,57] In previous studies, SEP was tested with pyruvate kinase. It was found that the sulfuryl group of SEP was transferred to ADP, further suggesting that the SEP may mimic the structural features of PEP.[52] The sulfate group of SEP has structural similarities with the phosphate group from PEP as both groups have similar steric size, and the same molecular tetrahedral geometry. However, possible intolerance of the enzyme for the substitution of the phosphate group needs to be considered. One significant difference between the sulfate and the phosphate groups is the charge. SEP, which has a sulfate group substituted for the phosphate, has only one negative charge while the phosphate group is likely to have two negative charges at physiological pH (in addition to the negative charge on the carboxylic functionality). The use of SEP, bearing a

monoanionic functionality, may probe the importance of the dianionic phosphate group of PEP.

2.4.2 Allylic phosphonate

The allylic phosphonate is another PEP analogue which has an altered phosphate group. This analogue has a methyl phosphono group instead of a phosphate group, effectively replacing the bridging oxygen atom between C2 and the phosphorus atom with a methylene carbon (**Figure 2.11**).
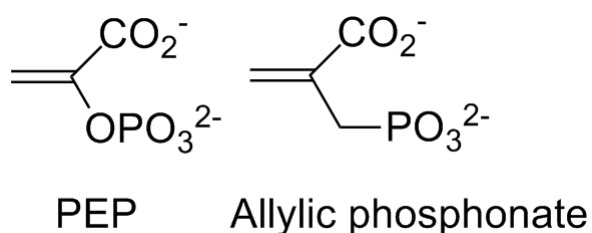
Figure 2.11 PEP analogue, allylic phosphonate

A phosphate group is an excellent leaving group but a phosphonate group is a poor leaving group due to the strong C-P bond. This analogue was chosen for investigation, as the allylic phosphonate had previously been observed to cause moderate inhibition of DAH7PS.[37]

However, the phosphonate functionality has significantly higher pK_a values than the phosphate group which means that the phosphonate group of this analogue, is expected to be protonated at physiological pH. Therefore it is likely that allylic phosphonate is monoanionic, once again probing the importance of a dianionic phosphate group of PEP.

2.4.3 3-Substituted PEP Analogues

2.4.3.1 3-Halo-PEP

Several C3-substituted PEP analogues were also investigated in this study. For the 3-halo-PEP compounds one of the vinyl hydrogens is replaced by an electronegative halogen. Such analogues include F-PEP, Cl-PEP, and Br-PEP (**Figure 2.12**).
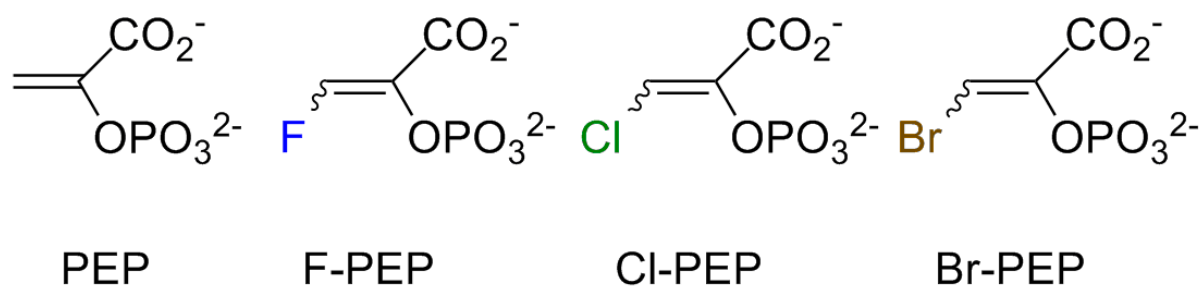
Figure 2.12 The 3-halo-PEP series (*Z*)-isomers

These analogues were tested on a variety of PEP utilising enzymes exhibiting inhibition in past studies.[52,56] In these studies the majority of PEP utilising enzymes were inhibited with the 3-substituted PEP analogues suggesting that the vinylic hydrogens bonded to the C3 position of PEP are not important for the enzymes ability to utilise PEP, in catalysis.[52] The inhibition did however vary from weak to strong depending on the enzyme. For example, (*Z*)-isomers of F-PEP and Cl-PEP weakly inhibited enzyme I of PTS, exhibiting an inhibition constant of 0.4 mM for both inhibitors. For pyruvate kinase the (*Z*)-isomers of F-PEP and Cl-PEP both displayed significant inhibition, with inhibition constants of 57 nM and 39 nM for F-PEP and Cl-PEP respectively. (*E*)-Cl-PEP was also tested but this analogue was reported to inhibit pyruvate kinase 2400-fold less strongly than its (*Z*)-isomer. The results of this study highlight the observation that most PEP utilising enzymes appear to favour the (*Z*)-isomer of these 3-substituted analogues.[52]

The highly electron withdrawing nature of the halogen substituents decreases the electron density in the double bond and therefore reduces the nucleophilicity of C3 of PEP, meaning that the 3-halo-PEP might be expected to be less reactive as substrates for NANAS. Whilst fluorine is more electronegative than both chlorine and bromine, fluorine is the smallest substituent. The 3-halo-PEP series therefore tests both electronic and steric effects at C3 position.

(*Z*) and (*E*)-isomers of these 3-substituted PEP analogues are possible. In this study, the analogues were predominantly (*Z*)-isomer with an approximate (*Z*):(*E*) ratio of 10:1, 4:1, and 10:1 for F-PEP, Cl-PEP, and Br-PEP respectively.

Firstly, these analogues were tested to determine whether they were able to act as alternative substrates for the NANAS enzymes, and to determine whether the active sites and the catalytic functions of the enzymes can tolerate such substitutions at the C3 position of PEP. The analogues were further tested as inhibitors of NANAS. F-PEP is a known substrate for *Nme*NANAS as described in chapter one.[29] This analogue was also tested in this study for comparison with the other analogues.

2.4.3.2 3-Methyl-PEP (Me-PEP)

Another C3-substituted PEP analogue used in this study was the 3-methyl-PEP (Me-PEP). This analogue has a methyl group at the C3 position of PEP (**Figure 2.13**).

$$CO_2^- \quad CO_2^-$$
$$OPO_3^{2-} \quad Me \quad OPO_3^{2-}$$

PEP   Me-PEP
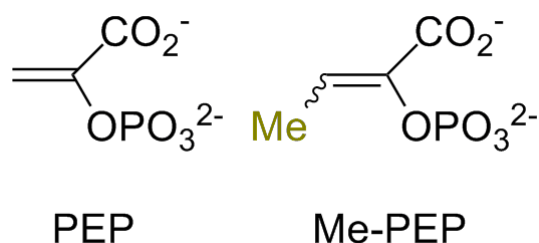
Figure 2.13 PEP analogue Me-PEP (*Z*)-isomer

The methyl substituent has a similar size to the bromo substituent of the Br-PEP, but the electron donating nature of the methyl group is significantly different to the other 3-substituted PEP analogues. This analogue is also in a mixture of a (*Z*) and (*E*)-stereo-isomers but this analogue is predominantly in the form of the (*Z*)-isomer, with an approximate (*Z*):(*E*) ratio of 4:1.

Me-PEP was tested as an alternative substrate for NANAS to determine whether the active site and the catalytic function of the enzyme could accommodate the methyl substitution at the C3 position of PEP. It was also tested as an inhibitor of NANAS.

The aforementioned PEP analogues were tested and their interactions with the enzyme were compared between two different types of NANAS; *Nme*NANAS and *Cje*NANAS.

2.5 Kinetic results

Kinetic assays were performed on *Nme*NANAS and *Cje*NANAS as described in the materials and methods section. The initial reaction rate between PEP and ManNAc, catalysed by the enzyme, was measured *via* monitoring the loss of PEP over time. A series of measured initial rates of reaction were used to calculate kinetic constants including the Michaelis-Menten constant (K_M) and inhibition constant (K_i), in order to characterise the effect of analogues on NANAS catalysis.

2.5.1 Michaelis-Menten constant, K_M, of PEP with NANAS

Before investigating the effects of the PEP analogues on *Nme*NANAS and *Cje*NANAS, the kinetic constants for the natural substrate of the enzyme, PEP, were determined.

The K_M for PEP was obtained for both *Nme*NANAS and *Cje*NANAS. The kinetic data for the initial rate of reaction catalysed by NANAS at a constant concentration of ManNAc and increasing concentrations of PEP is represented as a Michaelis-Menten plot. The Michaelis-Menten plot was used to derive kinetic parameters using non-linear fitting (**Figure 2.14**).
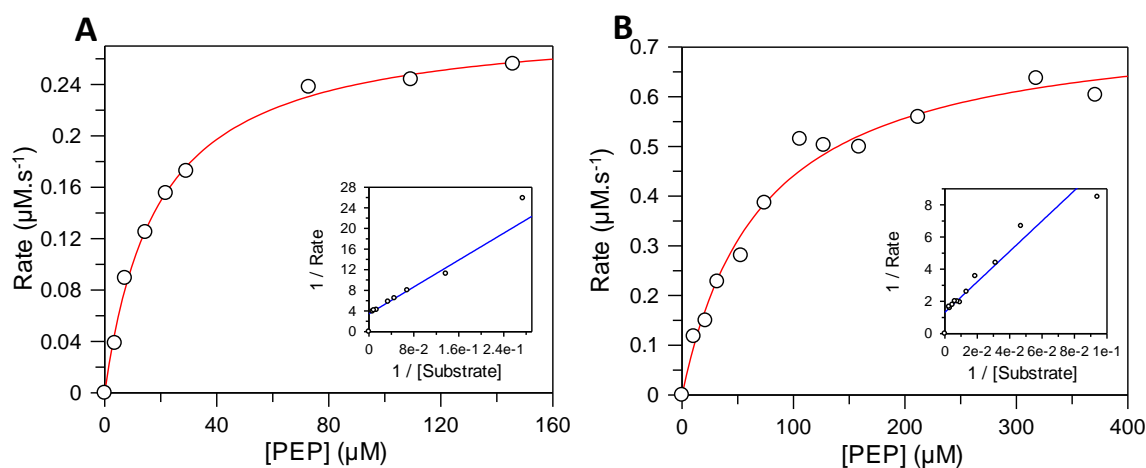
Figure 2.14 Michaelis-Menten plots for PEP utilisation by (A) *Nme*NANAS and (B) *Cje*NANAS. Kinetic assays were performed using variable concentrations of PEP, a constant concentration of 11.3 mM ManNAc and were initiated with approximately 15 µg of the enzyme. The assay was completed at 25 °C in Bis-tris-propane (BTP) buffer (50 mM) at pH 8.

The K_M values of PEP for NmeNANAS and CjeNANAS were determined as 20 ± 1 μM and 70 ± 10 μM respectively, whereas the k_{cat} values were determined to be 1.13 s^{-1} and 1.9 s^{-1} respectively. This shows that both enzymes have a high affinity for PEP and require relatively small concentrations of the substrate PEP to achieve saturation (**Table 2.2**).

Table 2.2 Table of Kinetic constants determined for NANAS with PEP.

Enzyme	PEP K_M (μM)	k_{cat} (s^{-1})	k_{cat} / K_M PEP (s^{-1}/ μM)
NmeNANAS	20 ± 1	1.13 ± 0.06	0.057 ± 0.006
NmeNANAS past study 1[9]	250	0.9	0.0036
NmeNANAS past study 2[30]	28 ± 3	3.1 ± 0.1	0.111 ± 0.003
CjeNANAS	70 ± 10	1.9 ± 0.3	0.027 ± 0.008
CjeNANAS past study 1[48]	33 ± 1	1.7 ± 0.1	0.052 ± 0.005
CjeNANAS past study 2[29]	7300	1194	0.16

The K_M values obtained from the prepared enzymes were significantly smaller than the literature values for NmeNANAS and CjeNANAS which were 0.25 mM and 7.3 mM respectively.[9,29] The literature kinetic constants obtained for NmeNANAS were determined by using a continuous coupled assay with NANA lyase, in a Tris acetic acid buffer (pH 8.3) at 37 °C, while increasing the concentration of PEP and keeping the concentration of ManNAc constant.[9] The literature value for the kinetic constant obtained for CjeNANAS were determined by the use of a stopped thiobarbiturate assay, measuring the rate of formation of NANA in a bicine buffer (pH 8) at 37 °C.[29] Significant differences between the experimental values and the literature values are likely due to the different methods used, and the difference in the temperature at which the kinetic assays were performed. Literature values from past investigations using a similar method as this study obtained K_M values for PEP for NmeNANAS and CjeNANAS of 28 μM and 33 μM respectively, which is in good agreement with the experimental values obtained in these studies.[30] This literature K_M (PEP) value for NmeNANAS was obtained by monitoring PEP consumption at 232 nm (ε = 2.8 x 10^3 M^{-1}cm^{-1}) as a function of time. The assay was completed in BTP buffer (pH 7.5) at 25 °C, with variable concentrations of PEP and a fixed concentration of ManNAc.[30,48]

2.5.2 Testing PEP analogues for alternative substrate or inhibition

Each of the PEP analogues were tested with *Nme*NANAS and *Cje*NANAS to determine if they act as alternative substrates for the enzyme, and to examine if they were capable to inhibiting the enzyme. If so, the inhibition constant, K_i, was obtained for each inhibitor.

To test PEP analogues as potential alternative substrates for NANAS, enzyme activity was observed in the presence of the PEP analogue and ManNAc, but in the absence of PEP. High concentrations of enzymes were used to observe if any reaction was occurring between the PEP analogues and ManNAc. The exact wavelength at which each PEP analogue absorbs maximally is uncertain, however all PEP analogues share the same conjugated structure as PEP. Assuming PEP and the analogues absorb at similar wavelength, the wavelength of 232 nm was used to measure the concentration-dependent absorbance of all PEP analogues. Any consumption of the alternative PEP analogue in the NANAS catalysed reaction would be expected to be observed by a decrease absorbance at 232 nm. The rate of reaction was measured in absorbance units per minute (Abs min^{-1}).

Due to the relatively high concentration of enzymes and substrates, cuvettes with a 0.2 cm pathlength were used to maintain an absorbance below 1 absorbance unit during all kinetic assays of enzymes with PEP analogues. If the absorbance is too high, the measurement of absorbance becomes less accurate as Beer's law is no longer obeyed.

2.5.2.1 Testing the PEP analogues with the modifications to the phosphate group

SEP and allylic phosphonate were investigated to see if they function as alternative substrates for either *Nme*NANAS or *Cje*NANAS.

SEP

SEP was tested against *Nme*NANAS or *Cje*NANAS in the presence of ManNAc, and absence of PEP. High concentrations of enzymes (10-20 times those used in the standard assay with PEP) were used in these assays in order to detect relatively low reaction rates. The change in absorbance at 232 nm was monitored, however no decrease in the absorbance was observed for either enzyme, suggesting that SEP is not an alternative substrate for either *Nme*NANAS or *Cje*NANAS.

Allylic phosphonate

The phosphonate was tested as an alternative substrate for *Nme*NANAS and *Cje*NANAS in a similar fashion. The change in absorbance at 232 nm was monitored, however no decrease in the absorbance was observed for either enzyme, suggesting that the allylic phosphonate is not an alternative substrate for either *Nme*NANAS or *Cje*NANAS. This result was expected as it was considered unlikely that this analogue would be able to undergo the catalytic cycle due to the presence of the non-cleavable C-P bond.

2.5.2.2 Testing the 3-substituted PEP analogues

The 3-substitituted PEP analogues Cl-PEP, Br-PEP, and Me-PEP were investigated as possible alternative substrates for *Nme*NANAS and *Cje*NANAS.

F-PEP

F-PEP, is one of the 3-substituted PEP analogues used to obtain an inhibition constant for this study. F-PEP is a known alternative substrate for NANAS and has been used previously to determine the stereospecificity of the NANAS catalysed reaction as mentioned in chapter 1. A previous study which elucidated the stereospecificity of the NANAS catalysed reaction, reports that only the *si* face of PEP attacks the *si* face of the carbonyl group of ManNAc.[29] Using a reaction mixture containing F-PEP and ManNAc, *Nme*NANAS or *Cje*NANAS was used to initiate the reaction. Approximately 10 to 20 times more enzyme (approximately 100 – 200 µg) was used to initiate the reaction than was used for the standard kinetic assays with PEP. A slow loss of absorbance with time was observed for *Nme*NANAS at a rate of 0.007 Abs min^{-1}. This is approximately four fold slower than the rate of reaction with the same concentration of natural substrates initiated with much lower concentration of *Nme*NANAS (approximately 10 µg). Conversely, addition of *Cje*NANAS resulted in a relatively fast loss of absorbance over time with a rate of 0.020 Abs min^{-1} was observed. This rate is only one and a half fold slower than the reaction rate with the same concentration of natural substrates initiated with one tenth the amount of *Cje*NANAS. When the amount of enzyme used for initiation was doubled, the rate of reaction (for both *Nme*NANAS and *Cje*NANAS) increased proportionally, to 0.012 Abs min^{-1} and 0.038 Abs min^{-1} respectively, indicating that the observed absorbance losses was indeed due to the enzyme-catalysed reaction.

The observed absorbance loss at 232 nm using F-PEP with both *Nme*NANAS and *Cje*NANAS supports the previous finding that F-PEP is an alternative substrate for NANAS. The proportionate increase of reaction rate upon the increase of enzyme concentration provides strong evidence that F-PEP is an alternative substrate for NANAS and undergoes reaction with ManNAc.

Cl-PEP

*Nme*NANAS or *Cje*NANAS were used to initiate the reaction between Cl-PEP and ManNAc by adding approximately 10 to 20-fold more enzyme (approximately 100 – 200 μg) than used in the standard assays with PEP. Both NANASs were added to a cuvette containing a set concentration of Cl-PEP and ManNAc.

A slow loss of absorbance at 232 nm was observed for both *Nme*NANAS and *Cje*NANAS with measured rates of 0.01 Abs min^{-1}, and 0.0019 Abs min^{-1} respectively. The rate of reaction of *Nme*NANAS with Cl-PEP is three orders of magnitude slower than the reaction with the natural substrates at similar concentrations, and initiated with 10 μg of *Nme*NANAS. Conversely the rate of reaction for *Cje*NANAS with Cl-PEP is 16-fold slower than the reaction rate of with natural substrates at similar concentrations initiated with 10 μg of *Cje*NANAS.

The kinetic assays were repeated using the same concentrations of Cl-PEP and ManNAc in the absence of PEP, but was initiated with twice the concentration of either the *Nme*NANAS or *Cje*NANAS enzymes. The rates of reaction did not increase proportionally to the increase of *Nme*NANAS with the rate only increasing to 0.013 Abs min^{-1} when 200 μg of enzymes was added. On the other hand, when the amount of *Cje*NANAS was doubled, the reaction rate also approximately doubled, to 0.0026 Abs min^{-1} which may suggest that Cl-PEP is a potential alternative substrate for *Cje*NANAS.

Br-PEP

Either *Nme*NANAS or *Cje*NANAS was used to initiate the reaction between Br-PEP and ManNAc, again at approximately 10 to 20 times higher enzyme concentration (approximately 100 – 200 μg) than used for the standard assay.

Loss of absorbance was observed as a function of time for both *Nme*NANAS and *Cje*NANAS, with rates of at 0.016 Abs min^{-1} and 0.00012 Abs min^{-1} respectively. The rate of reaction catalysed by *Nme*NANAS with Br-PEP is two-fold slower than the reaction rate of *Nme*NANAS with the same concentration of natural substrates, initiated with 10 μg enzyme. The rate of reaction catalysed by *Cje*NANAS is approximately 200 fold slower with Br-PEP, than the reaction rate of *Cje*NANAS with the same concentrations of its natural substrates and 10 μg enzyme.

The kinetic assay was repeated using the same concentrations of Br-PEP and ManNAc but was initiated with twice the concentration of either *Nme*NANAS or *Cje*NANAS enzymes. The reaction rates did not increase proportionally with the increase of *Nme*NANAS. Conversely, when the concentration of *Cje*NANAS was doubled, the rate of reaction nearly doubled to 0.0016 Abs min^{-1}. This may suggest that Br-PEP is an alternative substrate for *Cje*NANAS but not *Nme*NANAS.

Me-PEP

Me-PEP was tested as an alternative substrate of *Nme*NANAS and *Cje*NANAS. 100 μg and 80 μg of *Nme*NANAS and *Cje*NANAS respectively were used to initiate a reaction between set concentrations of Me-PEP and ManNAc.

A change in the measured absorbance over time was observed indicating catalysis in the presence of the enzyme. A slow reaction rate was observed between Me-PEP and ManNAc with *Nme*NANAS and *Cje*NANAS as 0.0015 Abs min^{-1} and 0.0017 Abs min^{-1} respectively. The rate of reaction catalysed by *Nme*NANAS and *Cje*NANAS with Me-PEP is approximately 20-fold slower than the rate of reaction of *Nme*NANAS and *Cje*NANAS with similar concentration of their natural substrates, and initiated with 10 μg of enzyme.

The kinetic assay was repeated using the same concentrations of Me-PEP and ManNAc but was initiated with twice the concentration of either *Nme*NANAS or *Cje*NANAS. The rates of reaction did not did not increase proportionally to the increase of both *Nme*NANAS and *Cje*NANAS indicating that Me-PEP is not a viable alternate substrate for either enzyme.

2.5.3 Inhibition of NANAS with PEP analogues

The inhibition constants for each inhibitor tested against both orthologues of NANAS were determined. Generally, significantly lower K_i values were obtained with *Cje*NANAS in comparison to *Nme*NANAS. Each K_i was determined from nonlinear fitting the inhibition data, and the data is also displayed as a Lineweaver-Burke plot.

Although some of the tested PEP analogues were determined to be alternative substrates for NANAS (**section 2.5.2**), their rates of reaction were very slow in comparison to the reaction with natural substrate PEP, and their reactions were only observable in the presence of very high concentrations of enzyme. Therefore, any effect the alternative substrates (reacting with ManNAc) may have upon the determination of K_i for each PEP analogue should be negligible.

2.5.3.1 Inhibition by PEP analogues with the modifications to the phosphate group

2.5.3.1.1 Inhibition of *Nme*NANAS or *Cje*NANAS with SEP

SEP was assumed to be a possible inhibitor due to its structural similarities with PEP, however no significant inhibition was detected for both homologues of NANAS in the presence of 1 mM or 4 mM SEP.

2.5.3.1.2 Inhibition of NmeNANAS or CjeNANAS with the allylic phosphonate

Allylic phosphonate was tested for inhibition of *Nme*NANAS and *Cje*NANAS. No inhibition was observed upon addition of 0.8 mM and 1.0 mM allylic phosphonate respectively.

2.5.3.2 Inhibition of NANAS with the 3-substituted PEP analogues

2.5.3.2.1 Inhibition of *Nme*NANAS with Me-PEP

The inhibition assay of *Nme*NANAS with Me-PEP was used to obtain a K_i of 0.8 mM ± 0.1 mM, this being the poorest inhibition of *Nme*NANAS observed for any of the PEP analogues (**Figure 2.15**). The obtained K_i of Me-PEP is approximately 40 times greater than the measured K_M of PEP. Me-PEP showed competitive inhibition with respect to PEP.
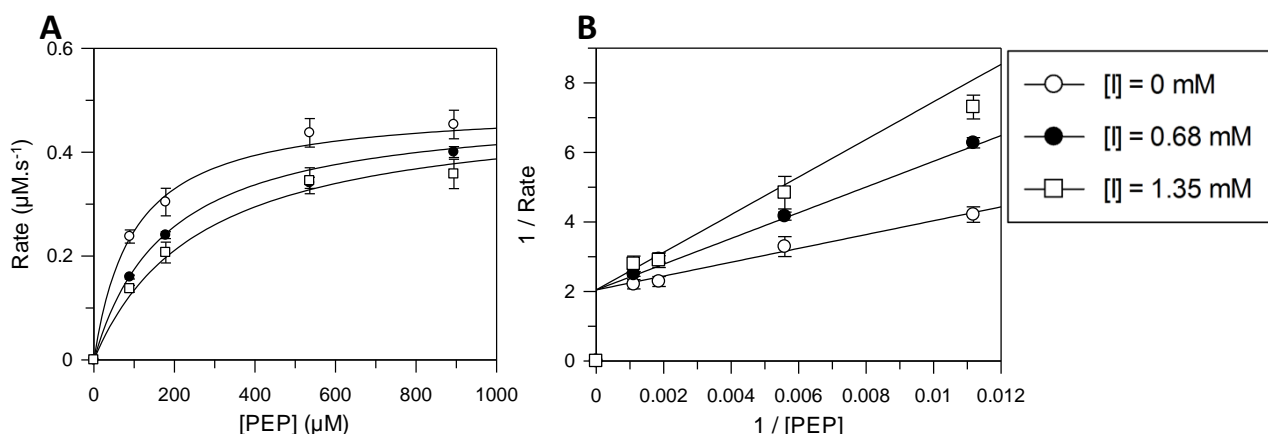
Figure 2.15 (A) Raw data and (B) Lineweaver-Burke plot of *Nme*NANAS inhibition with Me-PEP. Kinetic assays were performed using varied concentrations of PEP, 10.9 mM ManNAc and were initiated with approximately 10 μg of the enzyme. The kinetic assay was repeated with the additional presence of 0.68 mM and 1.35 mM Me-PEP. The assay was completed at 25 °C in BTP buffer (50 mM) at pH 8.

2.5.3.2.2 Inhibition of *Cje*NANAS with Me-PEP

The inhibition assay of *Cje*NANAS with Me-PEP was used to obtain a K_i of 23 ± 2 μM for Me-PEP, exhibiting competitive inhibition with respect to PEP (**Figure 2.16**). This value is approximately three times lower than the measured K_M of PEP for *Cje*NANAS. This indicates that the inhibition of *Cje*NANAS with Me-PEP is surprisingly potent. As described below, this compound is still one of the poorest inhibitors of *Cje*NANAS; however, the K_i of Me-PEP for *Cje*NANAS is significantly lower than that of *Nme*NANAS with Me-PEP, demonstrating that Me-PEP is a far more efficient inhibitor of *Cje*NANAS than *Nme*NANAS.
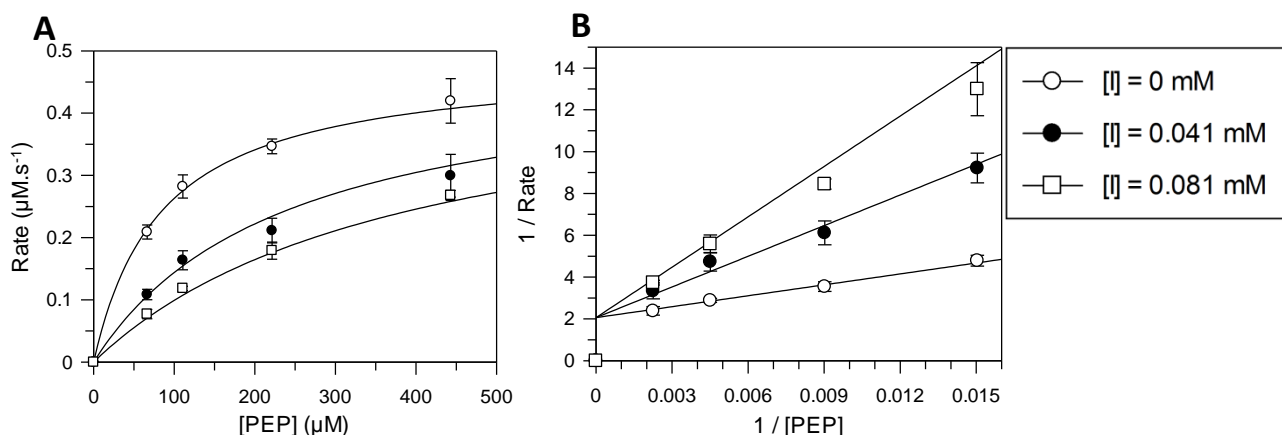
Figure 2.16 (A) Raw data and (B) Lineweaver-Burke plot of *Cje*NANAS Inhibition with Me-PEP. Kinetic assays were performed using varied concentrations of PEP, a constant concentration of 10.1 mM ManNAc and were initiated with approximately 15 µg of enzyme. The kinetic assay was repeated with the additional presence of 0.041 mM and 0.081 mM Me-PEP. The assay was completed at 25 °C in BTP buffer (50 mM) at pH 8.

2.5.3.2.3 Inhibition of *Nme*NANAS with F-PEP

The inhibition assay of *Nme*NANAS with F-PEP was used to obtain a K_i of 0.19 ± 0.02 mM, exhibiting competitive inhibition with respect to PEP (**Figure 2.17**). This value is approximately 9.5 times greater than the measured K_M of PEP for *Nme*NANAS. F-PEP is a stronger inhibitor than Me-PEP for *Nme*NANAS.
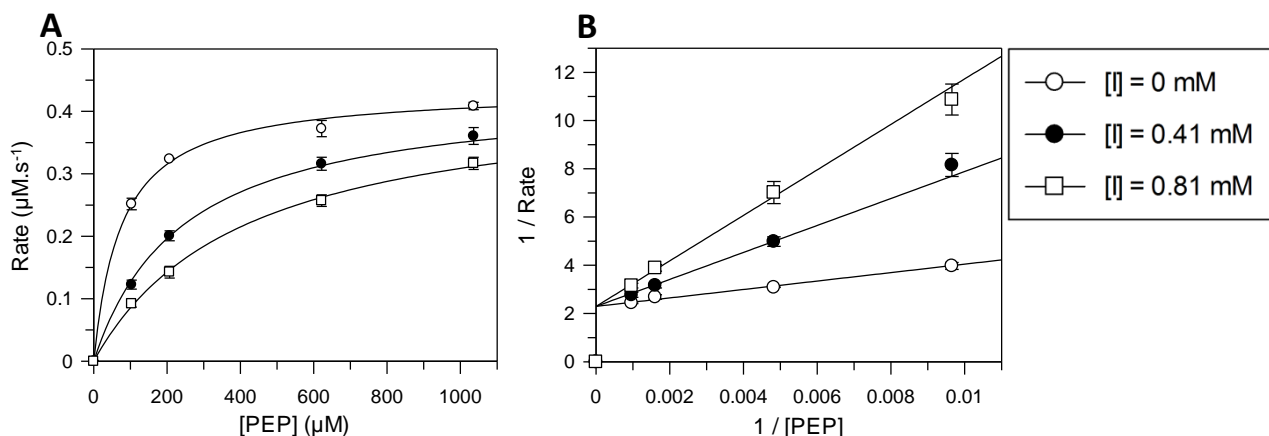
Figure 2.17 (A) Raw data and (B) Lineweaver-Burke plot of *Nme*NANAS Inhibition with F-PEP. Kinetic assays were performed using varied concentrations of PEP, a constant concentration of 10.8 mM ManNAc and were initiated with approximately 10 µg of enzyme. The kinetic assay was repeated with the additional presence of 0.41 mM and 0.82 mM F-PEP. The assay was completed at 25 °C in BTP buffer (50 mM) at pH 8.

2.5.3.2.4 Inhibition of *Cje*NANAS with F-PEP

The inhibition assay of *Cje*NANAS with F-PEP was used to obtain a K_i of 24 ± 2 µM, exhibiting competitive inhibition with respect to PEP (**Figure 2.18**). This value is about three-fold lower than the measured K_M of PEP for *Cje*NANAS. This suggests that F-PEP is a strong inhibitor for *Cje*NANAS. The relative potency of F-PEP as an inhibitor compared to the K_M of PEP for *Cje*NANAS, seems to be similar to that of Me-PEP with *Cje*NANAS.
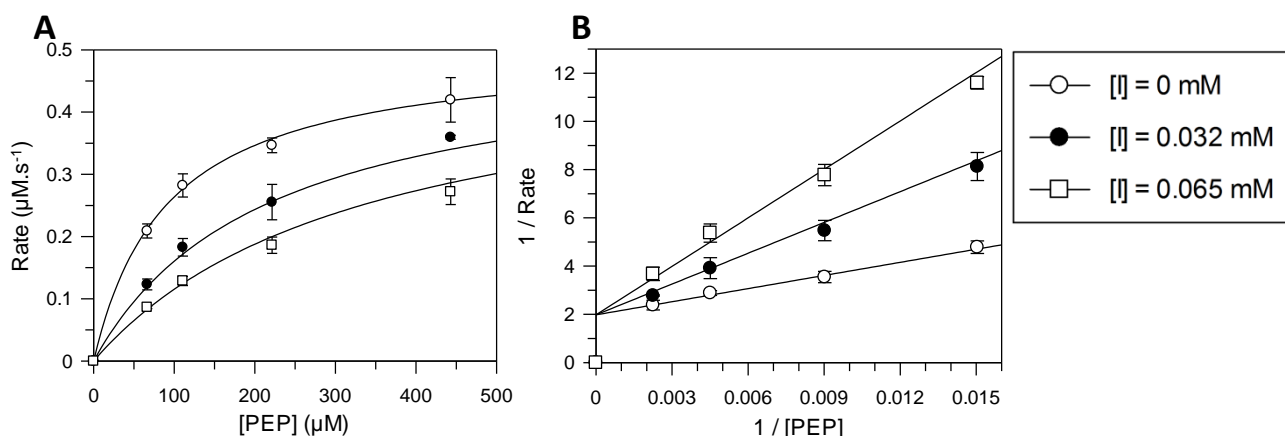
Figure 2.18 (A) Raw data and (B) Lineweaver-Burke plot of *Cje*NANAS Inhibition with F-PEP. Kinetic assays were performed using varied concentrations of PEP, a constant concentration of 10.05 mM ManNAc and were initiated with approximately 15 µg of the enzyme. The kinetic assay was repeated with the additional presence of 0.032 mM and 0.065 mM F-PEP. The assay was completed at 25 °C in BTP buffer (50 mM) at pH 8.

2.5.3.2.5 Inhibition of *Nme*NANAS with Cl-PEP

The inhibition assay of *Nme*NANAS with Cl-PEP was used to obtain a K_i of 0.10 ± 0.01 mM, this value is about five times greater than the measured K_M of PEP for *Nme*NANAS (**Figure 2.19**). Cl-PEP exhibits competitive inhibition with respect to PEP. Cl-PEP is a more potent inhibitor than F-PEP for *Nme*NANAS.
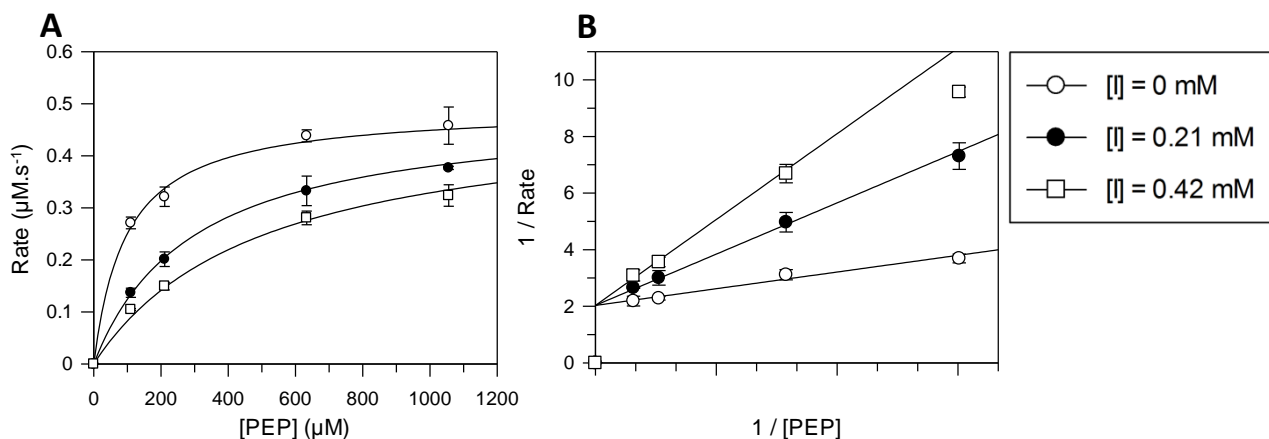
Figure 2.19 (A) Raw data and (B) Lineweaver-Burke plot of *Nme*NANAS Inhibition with Cl-PEP. Kinetic assays were performed using varied concentrations of PEP, a constant concentration of 10.9 mM ManNAc and were initiated with approximately 10 μg of the enzyme. The kinetic assay was repeated with the additional presence of 0.21 mM and 0.42 mM Cl-PEP. The assay was completed at 25 °C in BTP buffer (50 mM) at pH 8.

2.5.3.2.6 Inhibition of *Cje*NANAS with Cl-PEP

The inhibition assay of *Cje*NANAS with Cl-PEP was used to obtain a K_i of 3.3 ± 0.4 μM, exhibiting competitive inhibition (**Figure 2.20**). This value is about 20-fold smaller than the measured K_M of PEP for *Cje*NANAS. This is a very strong inhibitor and it is the PEP analogue which displays the most potent inhibition of *Cje*NANAS.
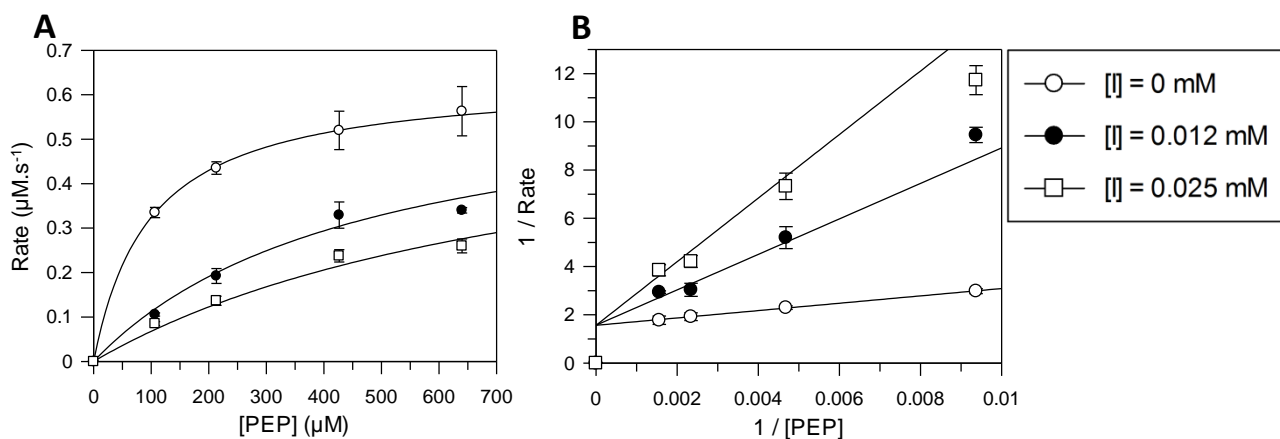
Figure 2.20 (A) Raw data and (B) Lineweaver-Burke plot of *Cje*NANAS Inhibition with Cl-PEP. Kinetic assays were performed using varied concentrations of PEP, a constant concentration of 11.15 mM ManNAc and were initiated with approximately 10 μg of the enzyme. The kinetic assay was repeated with the additional presence of 0.012 mM and 0.025 mM Cl-PEP. The assay was completed at 25 °C in BTP buffer (50 mM) at pH 8.

2.5.3.2.7 Inhibition of *Nme*NANAS with Br-PEP

The inhibition assay of *Nme*NANAS with Br-PEP was used to obtain a K_i of 0.096 ± 0.007 mM, exhibiting competitive inhibition with respect to PEP (**Figure 2.21**). This value is about 4.8 times greater than the measured K_M of PEP for *Nme*NANAS. Br-PEP is a strong inhibitor which has the lowest K_i of the PEP analogues tested against *Nme*NANAS. The potency of F-PEP as an inhibitor seems to be similar to that of Me-PEP with *Cje*NANAS.
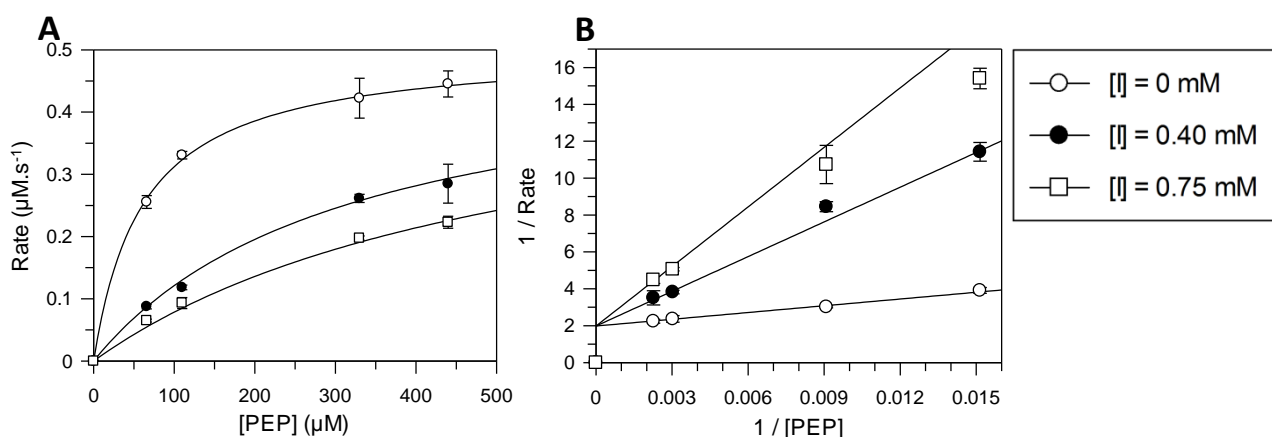
Figure 2.21 (A) Raw data and (B) Lineweaver-Burke plot of *Nme*NANAS Inhibition with Br-PEP. Kinetic assays were performed using varied concentrations of PEP, a constant concentration of 20.2 mM ManNAc and were initiated with approximately 10 µg of the enzyme. The kinetic assay was repeated with the additional presence of 0.40 mM and 0.75 mM Br-PEP. The assay was completed at 25 °C in BTP buffer (50 mM) at pH 8.

2.5.3.2.8 Inhibition of *Cje*NANAS with Br-PEP

The inhibition assay of *Cje*NANAS with Br-PEP was used to obtain a K_i of 3.6 ± 0.4 µM, exhibiting competitive inhibition with respect to PEP (**Figure 2.22**). This value is approximately 19 times lower than the measured K_M of PEP for *Cje*NANAS. Br-PEP is a strong inhibitor of *Cje*NANAS but the obtained K_i is only slightly higher than that of Cl-PEP compared to the K_M of PEP for *Cje*NANAS.
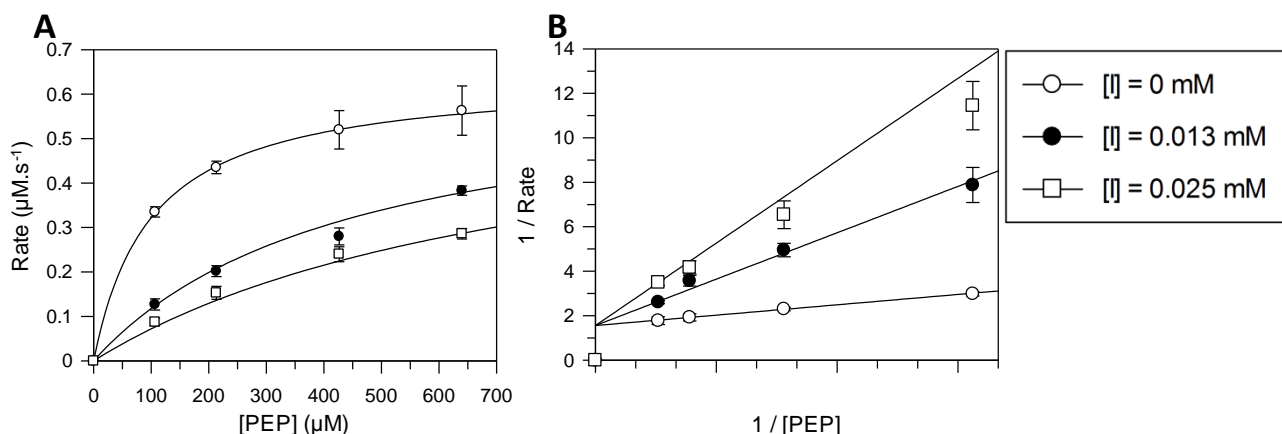
Figure 2.22 (A) Raw data and (B) Lineweaver-Burke plot of *Cje*NANAS Inhibition with Br-PEP. Kinetic assays were performed using varied concentrations of PEP, a constant concentration of 11.2 mM ManNAc and were initiated with approximately 10 µg of the enzyme. The kinetic assay was repeated with the additional presence of 0.013 mM and 0.025 mM Br-PEP. The assay was completed at 25 °C in BTP buffer (50 mM) at pH 8.

2.5.4 Summary of the kinetic analysis with PEP analogues

The kinetic constants that were determined for *Nme*NANAS and *Cje*NANAS with each of the PEP analogues are summarised in **Table 2.3**.

The only PEP analogue which exhibited activity as an alternative substrate for *Nme*NANAS was F-PEP, whereas F-PEP, Cl-PEP and Br-PEP all demonstrated loss of absorbance at 232 nm for *Cje*NANAS, in line with their possible utilisation as alternative substrates of this enzyme. In all cases the reactions were very slow and observable only if more than ten times the amount of enzyme (approximately 100 µg – 200 µg) was used to initiate the reaction than was normally employed for assays with PEP. Therefore without full characterisation of the substituted NANA products, their role as substrates cannot be confirmed. It is noted that F-PEP has already been characterised as a substrate for *Nme*NANAS.[29] In future studies, the full kinetic constants may be investigated for F-PEP against *Nme*NANAS using the continuous assay system used in these studies. In addition, it should be possible to confirm that F-PEP is a substrate of *Cje*NANAS *via* product identification between F-PEP and NANAS reaction.
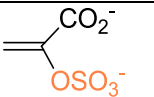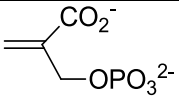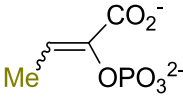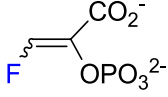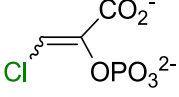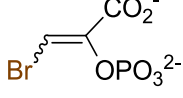
K_i values were determined for the PEP analogues against both NANAS enzymes, except for SEP and the allylic phosphonate analogue which did not exhibit inhibition. All inhibitors of NANAS were found to exhibit competitive inhibition with respect to PEP. The obtained K_i

values for *Nme*NANAS were typically larger than those obtained for *Cje*NANAS in comparison to their respective K_M (PEP) values.

For the PEP analogues tested against *Nme*NANAS, Me-PEP exhibited the poorest inhibition. The strongest inhibition of *Nme*NANAS was obtained by Br-PEP followed by Cl-PEP and F-PEP.

For *Cje*NANAS, the poorest inhibitors were Me-PEP and F-PEP. The strongest inhibition was observed by Cl-PEP and Br-PEP. Given the relatively large size of both the bromo and chloro substituents this result was unexpected.

Table 2.3 Summary of NANAS inhibition with PEP analogues

Name	Structure	*Nme*NANAS K_i	*Cje*NANAS K_i	Alternative substrate for *Nme*NANAS	Alternative substrate for *Cje*NANAS
SEP	CO_2^- / OSO_3^-	NA	NA	No	No
Allylic phosphonate	CO_2^- / OPO_3^{2-}	NA	NA	No	No
Me-PEP	CO_2^- / Me / OPO_3^{2-}	0.8 ± 0.1 mM	23 ± 2 µM	No	No
F-PEP	CO_2^- / F / OPO_3^{2-}	0.19 ± 0.02 mM	24 ± 2 µM	Yes	Yes
Cl-PEP	CO_2^- / Cl / OPO_3^{2-}	0.10 ± 0.01 mM	3.3 ± 0.4 µM	No	Yes
Br-PEP	CO_2^- / Br / OPO_3^{2-}	0.096 ± 0.007 mM	3.6 ± 0.4 µM	No	Yes

Chapter 3
Kinetic assays with ManNAc analogues and a NANA analogue

3.1 Introduction

The previous chapter was concerned with the range of substrate analogues that are similar in structure to PEP, the natural substrate for *Nme*NANAS and *Cje*NANAS. The other natural substrate utilised by *Nme*NANAS and *Cje*NANAS is ManNAc, which reacts with PEP to produce NANA.

Since the goal of this research was to test various substrate and product analogues on wild-type *Nme*NANAS and *Cje*NANAS, this chapter describes a series of experiments in which a range of ManNAc analogues and a NANA analogue were tested as alternative substrates and inhibitors of NANAS.

3.2 ManNAc the natural substrate

ManNAc is the natural substrate for the enzymatic synthesis of NANA by NANAS. This compound is a monosaccharide, comprising a six carbon chain and an aldehyde functional group. Hydroxyl groups are found at positions C3, C4, C5 and C6 and an *N*-acetyl group is located at the C2 position (**Figure 3.1**).
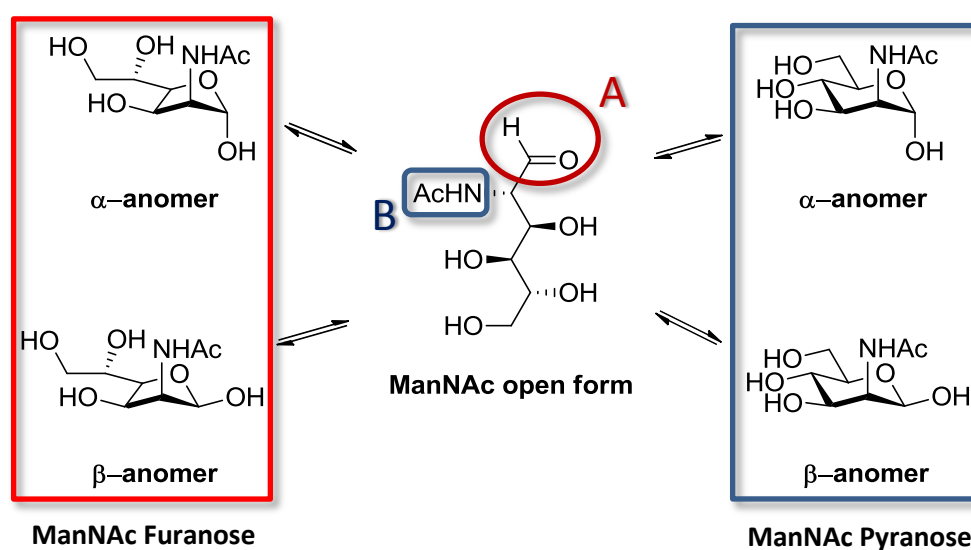
Figure 3.1 The key functional groups of ManNAc; (A) aldehyde group, and (B) *N*-acetyl group. ManNAc is capable of cyclisation, forming either a pyranose or a furanose ring.

Whilst ManNAc can exist as a linear compound, the presence of the aldehyde group allows ManNAc to undergo cyclisation to both hemiacetal pyranose and furanose forms (**Figure 3.1**). The position of the equilibrium favours the formation of the α-anomer of the pyranose form over the β-anomer of pyranose and both furanose forms.[58] The percentage of the equilibrium position of the structurally related molecule mannose is 67%, 33%, 0%, and 0% for α-pyranose, β-pyranose, α-furanose, and β-furanose respectively.[58] It is assumed that the cyclic structure of ManNAc is more prevalent due to the thermodynamic favourability and stability of the six-membered pyranose, however it is the open form of ManNAc that binds to the active site of NANAS and undergoes reaction with PEP. Although the mutarotation of ManNAc is a "facile" process, the sugar substrate predominantly exists in a closed ring form. The reaction must proceed using the open ring form of ManNAc thus it is likely that the NANAS catalyses the ring opening of ManNAc prior to reaction.[59]

According to the proposed reaction mechanism of NANAS the open chain form of ManNAc binds to the active site, so that the aldehyde functionality at position C1 is exposed for catalysis.[3,9] Crystallographic analysis of *Nme*NANAS in complex with PEP, Mn^{2+}, and rManNAc supports the proposed reaction mechanism, which shows the metal ion coordinating the hydroxyl group at the C1 position of rManNAc. For ManNAc the metal ion would activate the aldehyde functionality to nucleophilic attack on its carbonyl carbon.[3,9]

As explained in Chapter 1, the *N*-acetyl group of ManNAc is a key functionality which is used by the enzyme to orientate ManNAc in the active site. The aldehyde group gives ManNAc its reactive functionality with PEP. In these studies, ManNAc analogues with modifications of the *N*-acetyl group and the aldehyde group were investigated to determine the effects of such modifications on the catalytic properties of NANAS.

ManNAc is synthesised in biological systems by the enzyme UDP-*N*-acetylglucosamine epimerase. This enzyme converts UDP-*N*-acetylglucosamine (UDP-GlcNAc) into ManNAc (**Figure 3.2**).[2]
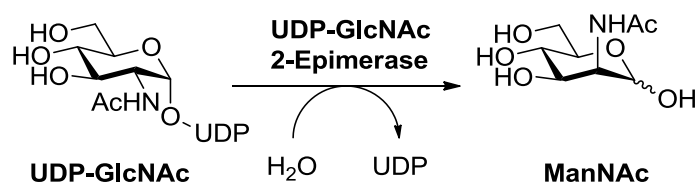
Figure 3.2 Biosynthesis of ManNAc.

Not only is ManNAc a precursor for sialic acid biosynthesis but may also play other important physiological roles. For example, ManNAc has been shown that ManNAc improves object recognition and hippocampal cell proliferation in mice, suggesting that ManNAc may be related to cognitive development and age-related dementia in mammals.[60] Currently there are clinical studies and trials investigating the therapeutic potential of ManNAc for the treatment of patients with severe neurodegenerative disorders caused by the defective gene which encodes UDP-GlcNAc.[21,61]

In bacteria, ManNAc is incorporated into common antigens and is also an alternative source of energy *via* catabolism, since ManNAc is a good source of carbon and nitrogen.[23,62]

3.3 ManNAc analogues used in this study

A variety of ManNAc analogues were tested against both *Nme*NANAS and *Cje*NANAS (**table 3.1**). The analogues were chosen based on their structural similarity to the natural substrate ManNAc, with the idea that the analogues might be able to access the ManNAc binding site of the enzyme. The ManNAc analogues displayed in **Table 3.1** were tested as potential substrates or inhibitors against both NANAS enzyme. The ManNAc analogues used for this study include *N*-acetylmannosaminitol (rManNAc), *N*-acetyl-D-glucosamine (GluNAc), *N*-acetyl-D-galactosamine (GalNAc), D-Mannosamine Hydrochloride (ManCl), and 2-deoxy-D-glucose (2DG).

Table 3.1 Summary of ManNAc analogues tested against *Nme*NANAS and *Cje*NANAS. The displayed ManNAc analogues which are capable of cyclisation are depicted as pyranose forms because they are the most thermodynamically stable.

Analogues	structure
N-Acetylmannosaminitol (rManNAc)	
N-Acetyl-D-glucosamine (GluNAc)	
N-Acetyl-D-galactosamine (GalNAc)	
D-Mannosamine Hydrochloride (ManCl)	
2-Deoxy-D-glucose (2DG)	

The ManNAc analogues were tested as potential substrates for *Nme*NANAS and *Cje*NANAS to determine if the active site and the catalytic function of the enzymes could accommodate the substitution or alteration of the stereochemistry of the ManNAc functionalities. rManNAc was used to determine whether the enzyme active site could accomodate the reduced aldehyde group. GluNAc and GalNAc were tested with NANAS to determine whether the enzymes could utilise analogues with alternative stereochemistry. ManCl was tested to determine whether NANAS could tolerate the substitution of the *N*-acetyl group whilst 2DG was tested to determine whether NANAS could utilise a sugar substrate lacking the *N*-acetyl group entirely.

In a past study, GluNAc and GalNAc were tested on NANAS from *Streptococcus agalactaie* (*Sag*NANAS) as part of an investigation into the substrate specificity of *Sag*NANAS.[63] GluNAc and GalNAc responded positively with *Sag*NANAS suggesting the importance of the *N*-acetyl group at the C2 position for catalytic activity.[63]

3.3.1 Aldehyde altered ManNAc analogue

3.3.1.1 rManNAc

This ManNAc derived analogue has the functional group reduced to a primary alcohol (**Figure 3.3**). The reduction of the carbonyl group also prevents this analogue from forming a cyclic structure. Since this analogue no longer carries the reactive carbonyl of the aldehyde functional group, this compound is no longer susceptible to a nucleophilic attack by PEP, therefore preventing the reaction within the enzyme. rManNAc was tested on *Nme*NANAS and *Cje*NANAS because it had been previously used as a substitute for ManNAc in the X-ray crystal structure of ligand bound *Nme*NANAS (PDB code 1XUZ).[3,9] rManNAc was tested to determine whether the removal of an aldehyde group would affect the kinetic properties with NANAS and to determine the level of inhibition afforded by this compound.
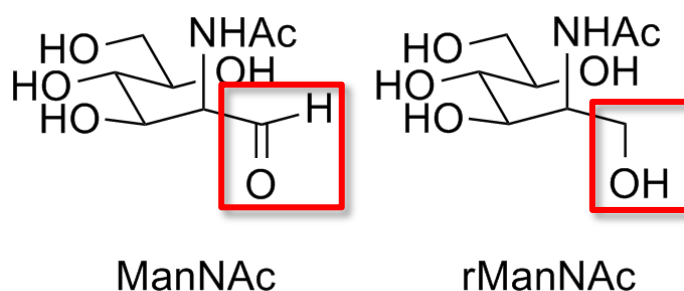
Figure 3.3 ManNAc and analogue *N*-acetylmanosaminitol

3.3.2 N-Acetyl altered ManNAc analogue

Previous studies have shown that cells readily take up and metabolise *N*-acetyl modified ManNAc analogues to synthesise their respective modified sialic acids, suggesting that NANAS may be able to accommodate ManNAc analogues with their *N*-acetyl functional group altered.[64,65] ManNAc analogues mentioned earlier in this chapter (GluNAc, GalNAc, ManCl, and 2DG), which have modified *N*-acetyl groups, were tested as alternative sugar substrates for *Nme*NANAS and *Cje*NANAS.

3.3.2.1 GluNAc and GalNAc

GluNAc and GalNAc are ManNAc analogues which were used to investigate the importance of the conformational position of the *N*-acetyl group for catalysis by NANAS (**Figure 3.4**).
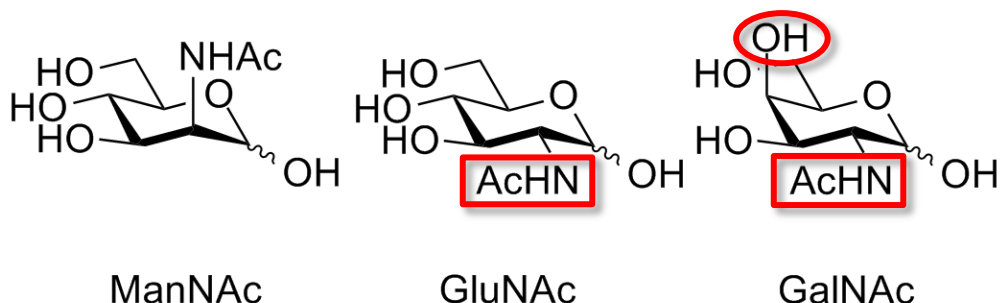
Figure 3.4 Pyranose forms of ManNAc and analogues *N*-acetylglucosamine (GluNAc) and *N*-acetylgalactosamine (GalNAc).

The configuration of the *N*-acetyl functional group at C2 for GluNAc is different to that of ManNAc. The C2 *N*-acetyl group of ManNAc is in (*R*)-configuration whereas GluNAc has an (*S*)-configuration. GluNAc in the lowest energy conformer of its pyranose form, has an *N*-acetyl functional group on an equatorial position. GalNAc on the other hand, is an isomer of GluNAc with the hydroxyl group at the C4 position in an axial position, and an (*S*)-configuration in the lowest energy conformer.

Due to their structural similarity with ManNAc, GluNAc and GalNAc may competitively inhibit NANAS. However, the analogues may bind poorly with the ManNAc binding site given that the configuration of the *N*-acetyl functional group, which is a key component for substrate recognition, has been altered.

3.3.2.2 ManCl

ManCl is an analogue of the natural sugar substrate, ManNAc (**Figure 3.5**). This ManNAc analogue lacks the acetyl group present on the C2 amino group of ManNAc. ManCl was tested to probe the importance of the *N*-acetyl functionality of ManNAc for substrate recognition and catalysis of NANAS.
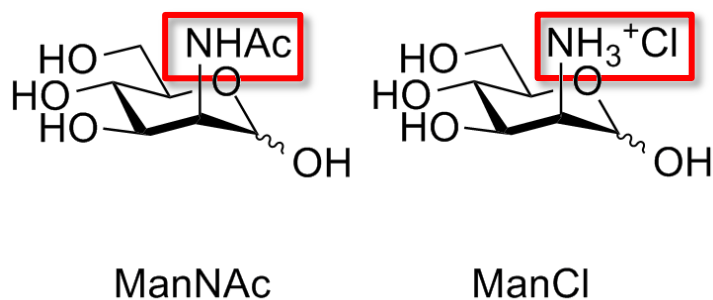
Figure 3.5 ManNAc and analogue ManCl

3.3.2.3 2DG

2DG is a ManNAc analogue which was used to investigate how the lack of an *N*-acetyl functional group might affect NANAS activity (**Figure 3.6**). The difference between this analogue and the natural substrate is that the *N*-acetyl group and the amine functionality at the C2 position have been completely removed.
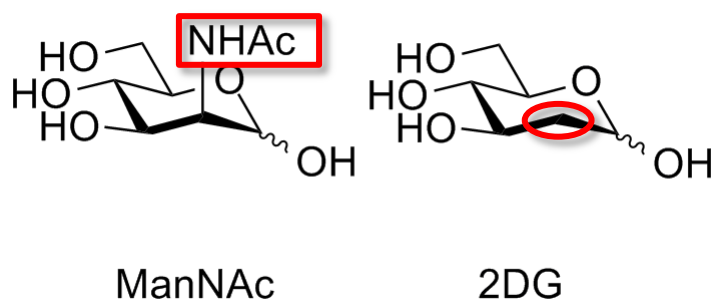
Figure 3.6 ManNAc and analogue 2DG

As mentioned in the first chapter, the *N*-acetyl group of ManNAc is not required for the binding of the substrate into the active site but for driving ManNAc into a favourable orientation within the active site for catalysis.[30] 2DG mimics the structure of ManNAc, but the lack of an *N*-acetyl group may alter 2DG's ability to act as an alternative substrate.

3.4 Kinetic assay results

Kinetic assays were performed on *Nme*NANAS and *Cje*NANAS as described in the materials and method section. The initial reaction rate between PEP and ManNAc, catalysed by the enzyme, was measured as the loss of PEP over time. A series of measured initial rates of reaction were used to calculated kinetic constants including the Michaelis-Menten constant

(K_M) and inhibition constant (K_i) in order to characterise the effect of ManNAc analogues on the two wild-type NANAS enzymes.

3.4.1 Michaelis-Menten constant (KM) of ManNAc with NANAS

Resulting to the studies described in the previous chapter, before investigating any kinetic effects from the use of ManNAc analogues on *Nme*NANAS and *Cje*NANAS, the kinetic constants for the natural substrate, ManNAc, were determined.

The apparent K_M values for ManNAc were obtained for both *Nme*NANAS and *Cje*NANAS. The kinetic data for the initial rate of reaction catalysed by NANAS at a constant concentration of PEP and increasing concentrations of ManNAc are represented as a Michaelis-Menten plot which was used to derive kinetic parameters using non-linear fitting (**Figure 3.7**).
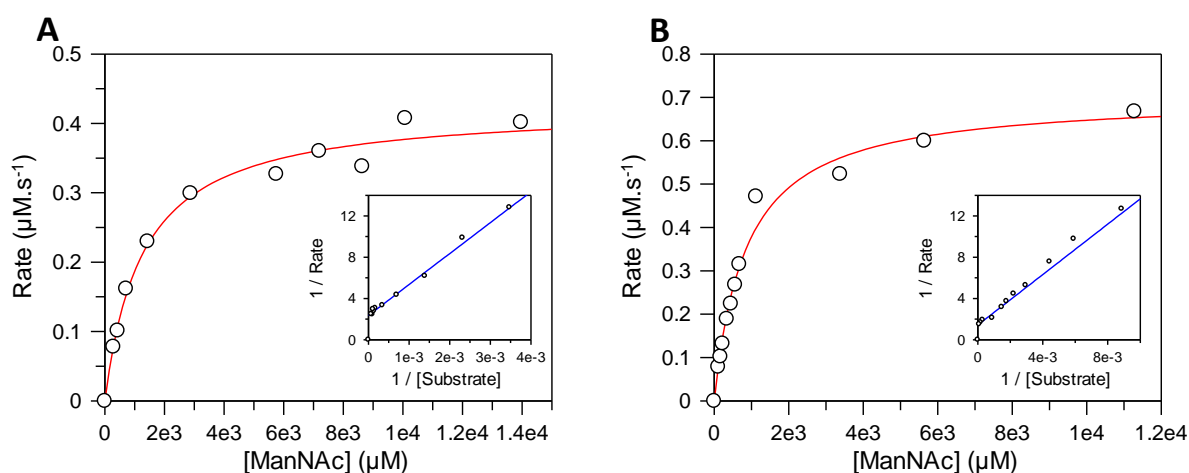
Figure 3.7 Michaelis-Menten plots for ManNAc utilisation by (A) *Nme*NANAS and (B) CjeNANAS. Kinetic assays were performed using increasing concentrations of ManNAc, constant concentration of 0.32 mM PEP, and were initiated with approximately 15 µg of the enzyme. The assay was completed at 25 °C in BTP buffer (50 mM) at pH 8.

The K_M values of ManNAc for *Nme*NANAS and *Cje*NANAS were determined as 1300 ± 100 µM and 860 ± 90 µM respectively, while the k_{cat} values were determined to be 1.13 s^{-1} and 1.9 s^{-1} respectively. The K_M values obtained for both orthologues of NANAS indicate that both enzymes have a relatively low affinity for ManNAc and require high substrate concentrations to achieve saturation (**Table 3.2**).

Table 3.2 Table of Kinetic constants for NANAS with ManNAc

Enzyme	ManNAc K_M (µM)	k_{cat} (s^{-1})	k_{cat} / K_M ManNAc (s^{-1} µM^{-1})
*Nme*NANAS	1300 ± 100	1.13 ± 0.06	0.057 ± 0.06
*Nme*NANAS past study 1[30]	2900 ± 200	3.1 ± 0.1	11 x 10^{-4} ± 1 x 10^{-4}
*Nme*NANAS past study 2[9]	9400	0.9	9.57 x 10^{-5}
*Cje*NANAS	860 ± 90	1.9 ± 0.3	0.027 ± 0.008
*Cje*NANAS past study 1[48]	4900 ± 200	1.7 ± 0.1	3.5 x 10^{-4} ± 3 x 10^{-5}
*Cje*NANAS past study 2[29]	17600	1194	0.068

The K_M values obtained for the prepared enzymes were significantly smaller than the literature values reported for *Nme*NANAS (9.4 mM)[9] and *Cje*NANAS (17.6 mM)[29]. The kinetic constants reported in the literature obtained for *Nme*NANAS were determined by using a continuous coupled assay with NANA lyase, in a Tris acetate buffer (pH 8.3) at 37 °C. The literature values for the kinetic constants obtained for *Cje*NANAS were determined by the use of a thiobarbiturate assay, measuring the rate of formation of NANA in bicine buffer (pH 8) at 37 °C.[29] Significant differences between the experimental values and the literature values are likely due to the variation in methodologies of the kinetic assays used and the different temperatures at which the kinetic assays were performed. Literature values from previous investigations using a similar kinetic method as this study obtained a K_M value for ManNAc of 2.9 mM and 4.9 mM for *Nme*NANAS and *Cje*NANAS respectively, which is closer in magnitude to the experimental value than the aforementioned reported value but still approximately three fold larger for *Nme*NANAS and six fold larger for *Cje*NANAS.[30,48] This difference may be due to the difference in assay pH or other experimental variations.

3.4.2 Testing ManNAc analogues as alternative substrates or inhibitors

Kinetic assays were performed using *Nme*NANAS and *Cje*NANAS with ManNAc analogues as described in the previous section. The ManNAc analogues were tested on the enzymes to determine whether the analogues could act as viable alternative substrates of the enzyme and/or if they were able to inhibit enzyme activity. If so, the inhibition constants were obtained for each compound using kinetic analysis.

To verify whether or not a ManNAc analogue was an alternative substrate, the activity of the enzyme was determined in the presence of the ManNAc analogue and PEP but in the

absence of ManNAc. As with the kinetic procedures described in Chapter two, high concentrations of enzymes were required (more than ten times the amount of enzyme used in standard assays with natural substrate ManNAc), to observe the rate of catalytic reaction between the ManNAc analogues and PEP.

Any utilisation of ManNAc analogues in the enzyme catalysed reaction would result in a decrease of PEP concentration in the reaction mixture, which would be observed by a concentration-dependent loss of absorbance at 232 nm. The rate of reaction was measured as absorbance per minute (Abs min^{-1}).

3.4.2.1 The analogue rManNAc is not an alternative substrate

The reduced form of ManNAc (rMAnNAc) is not an alternative substrate for either *Nme*NANAS or *Cje*NANAS. This is likely due to the absence of the reactive carbonyl functionality of the aldehyde group in rManNAc. Nucleophilic attack by PEP cannot occur with rManNAc, preventing catalysis. Therefore rManNAc was not investigated to determine whether the analogue could act as an alternative substrate.

3.4.2.2 Analysis of other ManNAc analogues

Several ManNAc analogues were investigated as potential alternative substrates for *Nme*NANAS and *Cje*NANAS.

Each ManNAc analogue, was tested as an alternative substrate by initiating the enzymatic reaction with high concentration of either *Nme*NANAS or *Cje*NANAS (approximately 50 µg). Enzyme was added to a reaction mixture containing PEP and the ManNAc analogue at fixed concentrations, in the absence of ManNAc. None of the tested analogues showed activity with either enzyme with the exception of 2DG which had slow reaction rate of only 0.0041 Abs min^{-1}. When the enzyme concentration was doubled for the same conditions, a rate of 0.0057 Abs min^{-1} was observed. The proportional increase of reaction rate with respect to the increase of enzyme concentration suggests that 2DG may be an alternative substrate for NANAS. To conclusively prove that this was a substrate for the enzyme, the alternative NANA product would need to be isolated and characterised completely. Due to the extremely low reaction rates observed in this study this further analysis was not performed.

3.4.3 Inhibition of NANAS with ManNAc analogues

3.4.3.1 Inhibition of *Nme*NANAS with rManNAc

The inhibition of *Nme*NANAS with rManNAc gave a K_i value of 320 ± 30 µM, and therefore appears to be a relatively weak inhibitor of *Nme*NANAS (**Figure 3.8**). The obtained K_i value for rManNAc is approximately four times smaller than the measured K_M of ManNAc which indicates that rManNAc is a relatively strong inhibitor of *Nme*NANAS, with respect to the natural substrate.
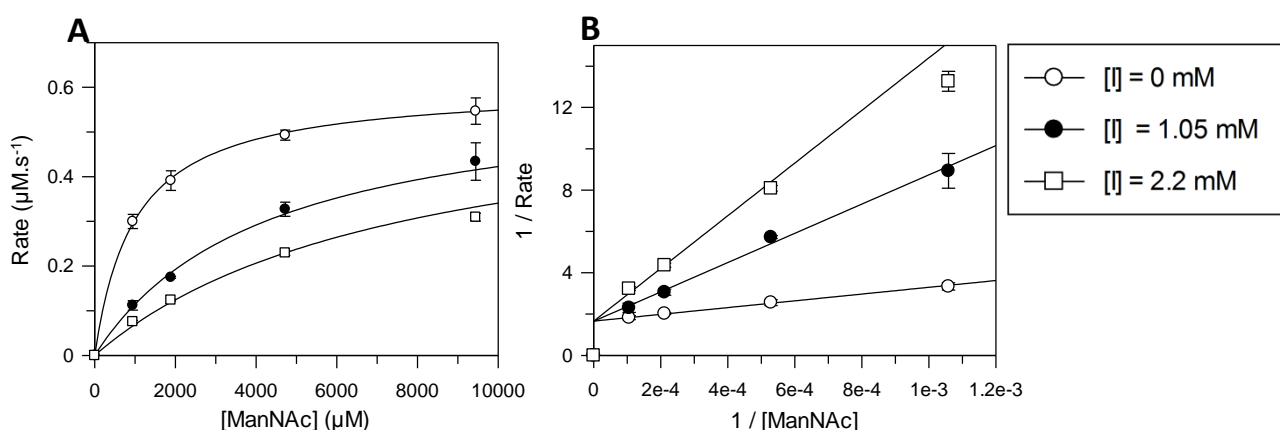
Figure 3.8 (A) Raw data and (B) Lineweaver-Burke plots of *Nme*NANAS Inhibition with rManNAc. Kinetic assays were performed using variable concentrations of ManNAc, a constant concentration of 0.22 mM PEP and were initiated with approximately 15 µg of the enzyme. The kinetic assay was repeated with the additional presence of 1.05 mM and 2.2 mM rManNAc. The assay was completed at 25 °C in BTP buffer (50 mM) at pH 8.

3.4.3.2 Inhibition of *Cje*NANAS with rManNAc

The inhibition analysis of *Cje*NANAS with rManNAc produced at K_i value of 9 ± 2 µM and appears to exhibit uncompetitive inhibition (**Figure 3.9**). The obtained K_i value of rManNAc is approximately 96 times lower than the measured K_M of ManNAc for *Cje*NANAS which indicates that rManNAc is a relatively strong inhibitor of *Cje*NANAS. The uncertainty for this K_i value is approximately 22% which is a large margin of error to be concerned. The plots on the double reciprocal graph indicate that the mode of inhibition for *Cje*NANAS with rManNAc is likely to be uncompetitive rather than competitive inhibition.
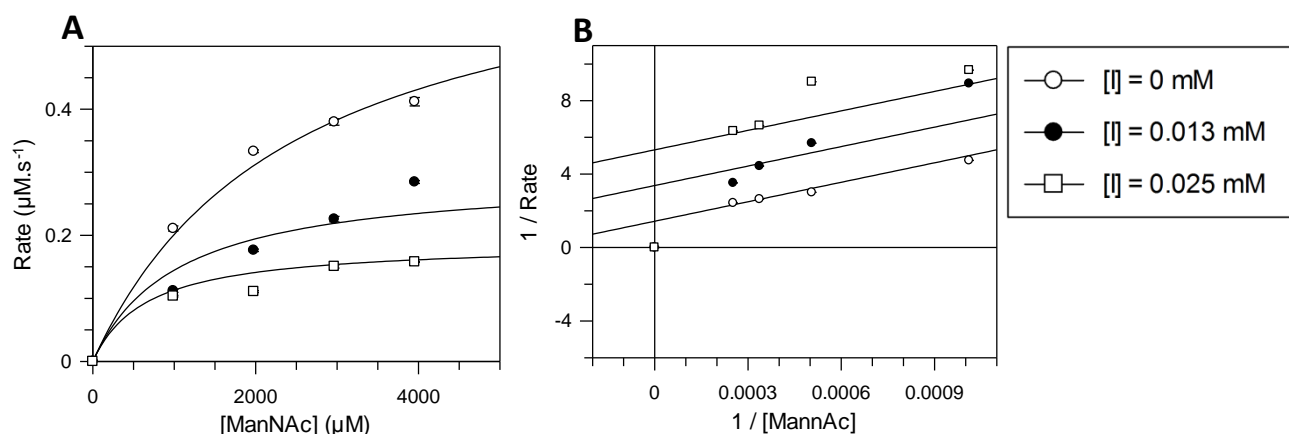
Figure 3.9 (A) Raw data and (B) Lineweaver-Burke plots of *Cje*NANAS Inhibition with rManNAc. Kinetic assays were performed using varied concentrations of ManNAc, a constant concentration of 0.29 mM PEP and were initiated with approximately 15 µg of the enzyme. The kinetic assay was repeated with the additional presence of 0.013 mM and 0.025 mM rManNAc. The assay was completed at 25 °C in BTP buffer (50 mM) at pH 8.

3.4.3.3 Kinetic assays of NANAS with other ManNAc analogues

*Nme*NANAS and *Cje*NANAS were tested with the ManNAc analogues, GluNAc, GalNAc, ManCl, and 2DG to probe whether these analogues exhibit inhibition. It was expected that GluNAc and GalNAc would show some inhibition of the enzyme because both analogues contain the important *N*-acetyl functionality. The *N*-acetyl group is recognised by the key conserved amino acid residue, Arg-314.[30] The remaining two analogues, ManCl and 2DG were expected to show weak or no inhibition of the enzyme because their *N*-acetyl group is altered (in ManCl) or abscent (in 2DG).

The kinetic assay was initiated with approximately 10 µg of either *Nme*NANAS or *Cje*NANAS at 25 °C. Fixed concentration of PEP and ManNAc were used to determine the control rate of loss of PEP over time at 232 nm. The assay was repeated in the presence of various ManNAc analogues and the rates of loss of absorbance over time were compared to the control rate (**Figure 3.10** and **Figure 3.11**).

All ManNAc analogues were present in greater concentration (10 mM) than the concentration of ManNAc (0.16 mM and 0.49 mM for testing against *Nme*NANAS and *Cje*NANAS respectively) in the reaction mixture, to ensure that any inhibition by these analogues could be observed.
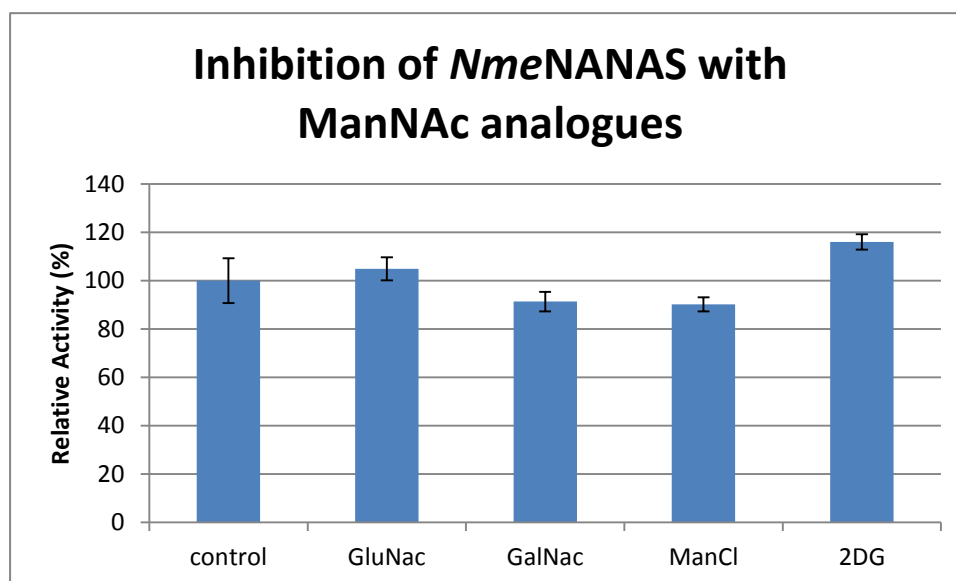
Figure 3.10 Relative activity measurements of *Cje*NANAS with ManNAc analogues. Kinetic assays were performed at a constant concentration of ManNAc (0.16 mM) and a constant concentration of PEP (1.91 mM) and were initiated with approximately 10 µg of the enzyme to determine the control rate of loss PEP (control). The kinetic assay was then repeated in the above conditions with the additional presence of ManNAc analogues (10 mM). The assay was completed at 25 °C in BTP buffer (50 mM) at pH 8.
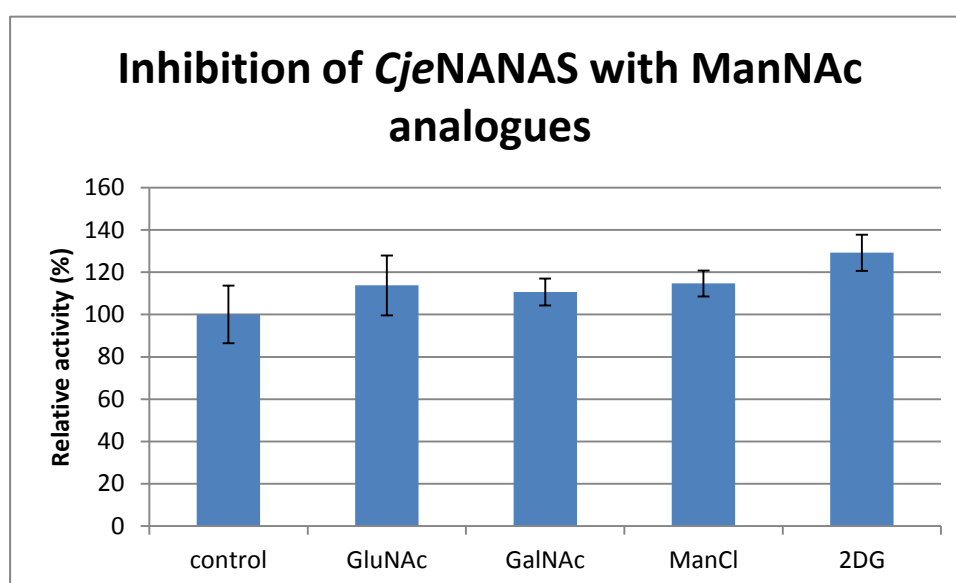
Figure 3.11 Relative activity measurements of *Cje*NANAS with ManNAc analogues. Kinetic assays were performed at a constant concentration of ManNAc (0.49 mM) and a constant concentration of PEP (0.29 mM) and were initiated with approximately 15 µg of the enzyme to determine the control rate of loss PEP (control). The kinetic assay was then repeated in above conditions with each additional presence ManNAc analogues (10 mM). The assay was completed at 25 °C in BTP buffer (50 mM) at pH 8.

The ManNAc analogues tested showd little evidence of inhibition. GluNAc and GalNAc, which were expected to show some degree of inhibition, were unable to significantly retard the rate of consumption of PEP. As stated, all ManNAc analogue concentrations were present at high concentrations (at least 10 mM in the cuvette) while the ManNAc concentration was relatively low, so the ManNAc analogues had the best possible opportunity to inhibit competitively.

Due to the insignificant differences in the enzyme activity between the control reaction and the reactions in the presence of ManNAc analogues the inhibition constants for the ManNAc analogues were not determined for either *Nme*NANAS or *Cje*NANAS.

There was a measured increase in rate of loss of absorbance at 232 nm in the presence of 2DG. Throughout kinetic testing, the amount of PEP is measured continuously by the use of UV spectrophotometry. The reason for the increased rate of PEP loss in the presence of 2DG is not clear. It is conceivable that 2DG encourages the loss of PEP *via* activation of the enzyme, or may be acting as a slow alternative substrate of the enzyme.

3.5 Product analogue

3.5.1 NANA the natural product

NANA is the natural product synthesised by the enzyme NANAS. As explained in the introduction chapter, NANA is a monosaccharide with a nine carbon backbone which has an *N*-acetyl functional group at the C5 position. The enzyme, NANAS synthesises and releases the product in its open ring form (**Figure 3.13**). Similarly to ManNAc, the released NANA is in equilibrium between an open ring and the closed ring structure (**Figure 3.14**). The equilibrium lies to the cyclic form.
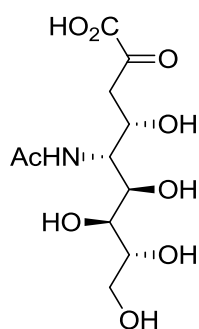
Figure 3.12 NANA, open ring form.
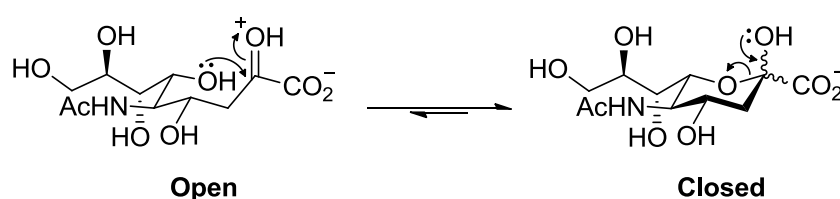
Figure 3.13 Cyclisation of NANA.

3.5.2 NANA analogue

Only one product analogue was tested on NANAS, this being the reduced form of NANA (rNANA). Another simple analogue, the difference between rNANA and NANA is that the carbonyl group is reduced to a hydroxyl group, which prevents cyclisation (**Figure 3.14**). rNANA used in this study was synthesised and provided by Andrew Watson using a method outlined in a previous study.[66] rNANA used in the kinetic study is in a racemic mixture containing two stereoisomers in a 50:50 ratio.
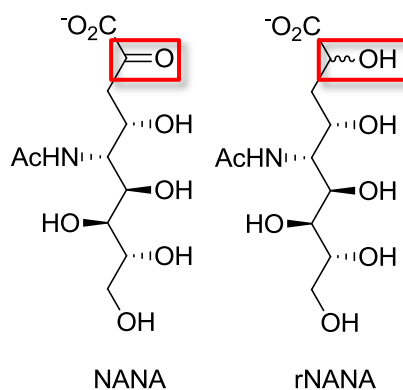
Figure 3.14 NANA analogue, rNANA

This analogue was expected to inhibit the enzyme by mimicking the structure of NANA, binding to the active site of the enzyme and preventing binding of PEP and ManNAc. The analogue rNANA was first tested against NmeNANAS to determine whether rNANA could inhibit the catalytic activity of the enzyme.

3.5.3 Kinetic results

Kinetic assays were performed using NmeNANAS and CjeNANAS as described in the materials and methods section in detail. Since rNANA is a structural mimic of the product and not the substrates, both PEP and ManNAc were tested against the inhibitor by testing the inhibitor in the presence of variable concentrations of PEP, with constant concentrations of ManNAc and *vice versa*. The K_i value for the inhibitor were determined for both NmeNANAS and CjeNANAS.

3.5.3.1 Inhibition of NmeNANAS with rNANA

Inhibition with respect to PEP

The inhibition assay of NmeNANAS with rNANA was used to obtain a K_i value of 0.5 ± 0.1 mM, exhibiting a competitive inhibition profile with respect to PEP (**Figure 3.15**). This value is 25 times greater than the measured K_M of PEP for NmeNANAS, and thus a poor inhibitor in respect to PEP.
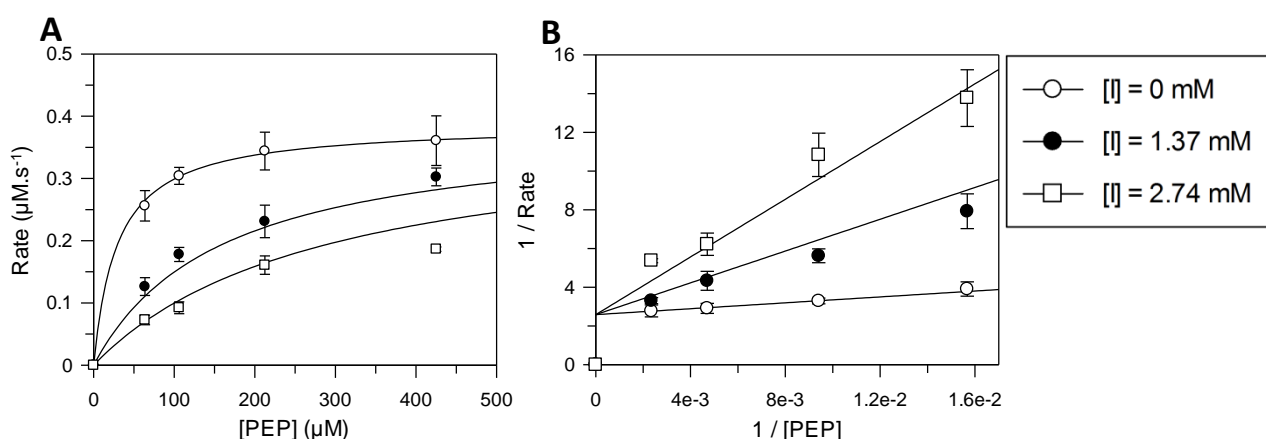
Figure 3.15 (A) Raw data and (B) Lineweaver-Burke plot of NmeNANAS Inhibition with rNANA against PEP. Kinetic assays were performed using varied concentrations of PEP, a constant concentration of 2.58 mM ManNAc and were initiated with approximately 15 µg of the enzyme. The kinetic assay was repeated with the additional presence of 1.37 mM and 2.74 mM rNANA. The assay was completed at 25 °C in BTP buffer (50 mM) at pH 8.

Inhibition with respect to ManNAc

The second K_i value for rNANA, as an inhibitor of *Nme*NANAS, was obtained by testing the analogue against an increasing concentration of ManNAc instead of PEP.

The K_i value for rNANA with respect to ManNAc was 3.0 ± 0.3 mM, and exhibited an uncompetitive inhibition profile with respect to a limiting concentration of ManNAc (**Figure 3.16**). The exhibition of uncompetitive inhibition may be justified as the enzyme is known to bind to PEP first in its ordered sequential mechanism.[48] The obtained K_i of rNANA with respect to ManNAc was approximately two times greater than the measured K_M value for ManNAc.
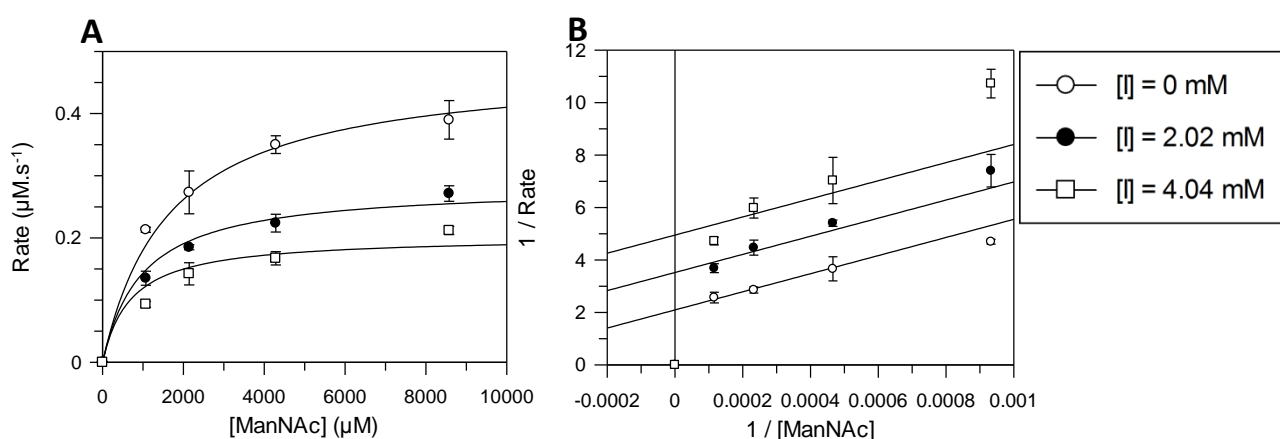
Figure 3.16 (A) Raw data and (B) Lineweaver-Burke plot of *Nme*NANAS Inhibition with rNANA against ManNAc. Kinetic assays were performed using varied concentrations of ManNAc, a constant concentration of 0.214 mM PEP and were initiated with approximately 15 µg of the enzyme. The kinetic assay was repeated with the additional presence of 2.02 mM and 4.04 mM rNANA. The assay was completed at 25 °C in BTP buffer (50 mM) at pH 8.

3.5.3.2 Inhibition of *Cje*NANAS with rNANA

Inhibition with respect to PEP

The inhibition assay of *Cje*NANAS with rNANA was used to obtain a K_i of 470 ± 60 µM, exhibiting competitive inhibition with respect to PEP (**Figure 3.17**). This value is approximately seven times greater than the measured K_M of PEP for *Cje*NANAS.
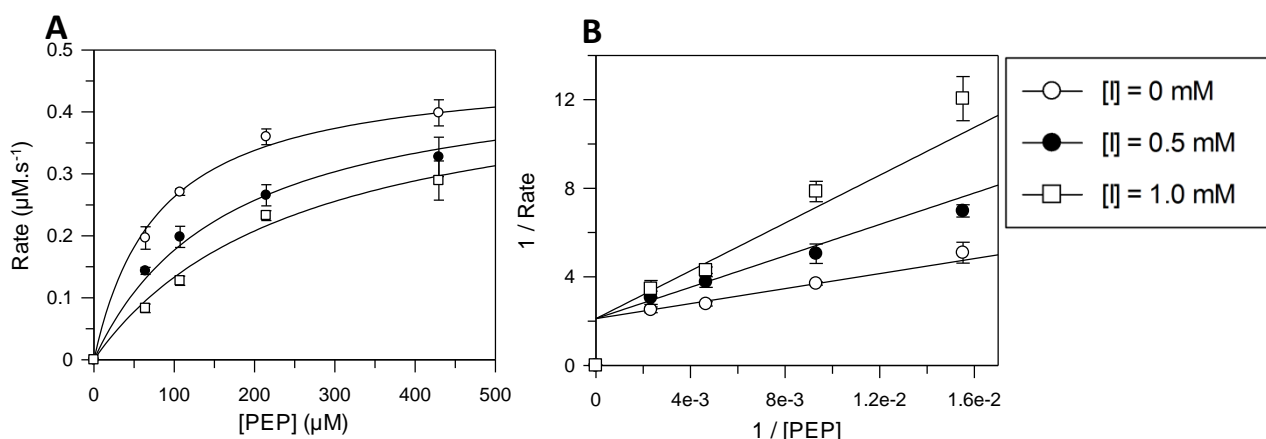
Figure 3.17 (A) Raw data and (B) Lineweaver-Burke plot of *Cje*NANAS Inhibition with rNANA against PEP. Kinetic assays were performed using varied concentrations of PEP, a constant concentration of 10.70 mM ManNAc and were initiated with approximately 15 µg of the enzyme. The kinetic assay was repeated with the additional presence of 0.5 mM and 1.0 mM rNANA. The assay was completed at 25 °C in BTP buffer (50 mM) at pH 8.

Inhibition with respect to ManNAc

The second K_i for rNANA, as an inhibitor of *Cje*NANAS, was obtained by testing the analogue against increasing concentrations of ManNAc instead of PEP.

The K_i value for rNANA with respect to ManNAc was 3.0 ± 0.4 mM, with this inhibitor exhibiting an uncompetitive inhibition profile with respect to ManNAc (**Figure 3.18**). The obtained K_i of rNANA with respect to ManNAc was approximately three times larger than the measured K_M of ManNAc for *Cje*NANAS.
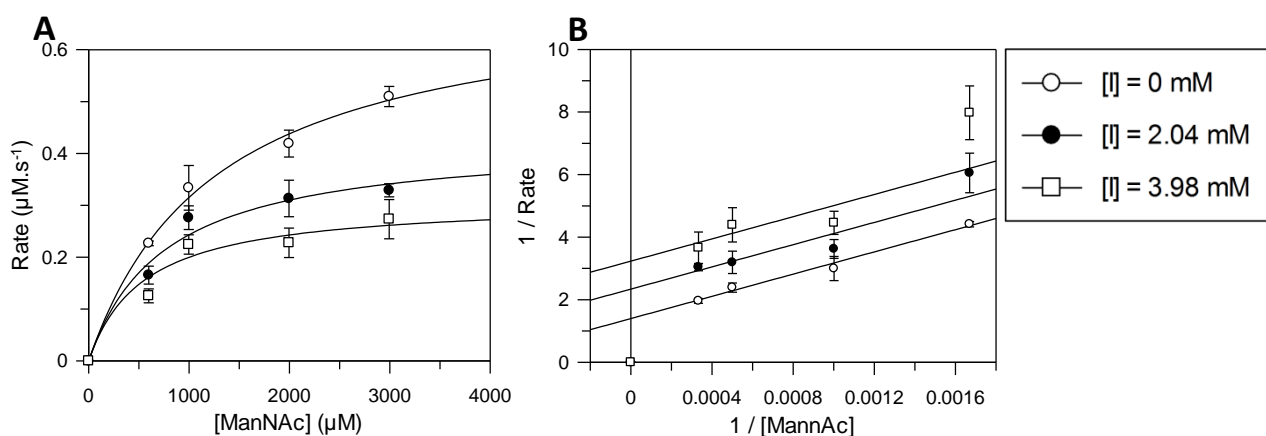
Figure 3.18 (A) Raw data and (B) Lineweaver-Burke plot of *Cje*NANAS Inhibition with rNANA against ManNAc. Kinetic assays were performed using varied concentrations of ManNAc, a constant concentration of 0.214 mM PEP and were initiated with approximately 15 µg of the enzyme. The kinetic assay was repeated with the additional presence of 2.04 mM and 3.98 mM rNANA. The assay was completed at 25 °C in BTP buffer (50 mM) at pH 8.

3.6 Summary of ManNAc and NANA analogue inhibition

The kinetic constants that were determined for NmeNANAS and CjeNANAS for each of the ManNAc analogues and the NANA analogue discussed in this chapter are summarised in **Table 3.3** and **Table 3.4** respectively.

None of the ManNAc analogues demonstrated any evidence of acting as alternative substrates for either NmeNANAS or CjeNANAS. This may indicate the importance of the specific stereochemistry of ManNAc for recognition and utilisation by NANAS.

The only ManNAc analogue that displayed any evidence to suggest it might be an alternative substrate for NmeNANAS and CjeNANAS was 2DG. However, the rate of loss of PEP over time was extremely low and thus it is not possible to conclude that 2DG is an alternative substrate for the NANAS enzyme. Confirmation would require the full characterisation of the alternative product formed between 2DG and NANAS. Obtaining sufficient quantities of this product will be a challenge, given the extremely low reaction rates.

rManNAc was the only ManNAc analogue that inhibited both NANAS enzymes with relative potency. The K_i values for rManNAc (against ManNAc) with NmeNANAS and CjeNANAS were 0.32 ± 0.02 mM and 9 ± 2 µM respectively. These values are approximately four times smaller than the measured K_M of ManNAc for NmeNANAS and 96 times smaller than the measured K_M of ManNAc for CjeNANAS respectively. rManNAc exhibited competitive inhibition with respect to ManNAc for both NANAS enzymes. The observation that rManNAc inhibits NANAS while the other ManNAc analogues were poor inhibitors may be explained by rManNAc lacking the ability to form a cyclic structure. It is particularly noteworthy that the enzyme is predicted to use an acyclic form of the substrate and may indeed catalyse the opening of the cyclic ManNAc substrate. This may account for the level of inhibition seen with rManNAc.

K_i values were determined for the product analogue, rNANA against PEP and ManNAc for both NmeNANAS and CjeNANAS. The K_i values of rNANA against PEP for NmeNANAS and CjeNANAS were 0.5 ± 0.1 mM and 470 ± 60 µM respectively. The inhibition of both NANAS enzyme with rNANA with respect to PEP exhibited a competitive inhibition. The K_i values of rNANA against ManNAc for NmeNANAS and CjeNANAS were 3.0 ± 0.3 mM and 3.0 ± 0.4 mM respectively. The inhibition of both NANAS enzymes by rNANA with respect to ManNAc

exhibited an uncompetitive inhibition profile. This observation can be explained by the binding order of substrates in the NANAS mechanism. PEP is known to bind to NANAS first which subsequently promotes the binding of ManNAc to the active site.[30]

Table 3.3 Summary of NANAS inhibition with ManNAc analogues**.** The displayed ManNAc analogues which are capable of cyclisation are depicted as pyranose forms.

Name	structure	*Nme*NANAS K_i	*Cje*NANAS K_i	Alternative substrate for *Nme*NANAS	Alternative substrate for *Cje*NANAS
rManNAc		0.32 ± 0.02 mM	9 ± 2 µM	NA	NA
GluNAc		NA	NA	No	No
GalNAc		NA	NA	No	No
ManCl		NA	NA	No	No
2DG		NA	NA	Maybe	Maybe

Table 3.4 Summary of NANAS inhibition with rNANA

Name	structure	*Nme*NANAS K_i with respect to PEP	*Nme*NANAS K_i with respect to ManNAc	*Cje*NANAS K_i with respect to PEP	*Cje*NANAS K_i with respect to ManNAc
rNANA		0.5 ± 0.1 mM	3.0 ± 0.3 mM	0.47 ± 0.06 mM	3.0 ± 0.4 mM

Chapter 4
Summary of thesis, discussions and future directions

4.1 Summary of results

The goal of this research was to investigate and compare the inhibition properties of the wild-type NANAS enzymes from the pathogenic organisms *N. meningitidis* and *C. jejuni* with various substrate and product analogues. Enzymes from these organisms were chosen due to their role in allowing the bacteria in which they are expressed to evade the host immune system *via* molecular mimicry.[23] Inhibition of these enzymes may aid the development of alternative antibiotics against these pathogenic bacteria.

In order to achieve this goal both wild-type *Nme*NANAS and *Cje*NANAS were prepared by protein expression and purification techniques. The obtained enzymes were tested against a range of substrate analogues to investigate whether substrate analogues were able to act as alternative substrates or inhibitors for the enzymes and kinetic parameters were determined.

Both PEP and ManNAc substrate analogues were used in this research. In addition, a product analogue was tested.

4.2 The large steric size of the 3-substituted PEP analogues may affect the inhibition of NANAS

K_i values were determined for the PEP analogues against both NANAS enzymes except for SEP and the allylic phosphonate, which were found to be non-inhibitory.

Me-PEP exhibited the poorest inhibition against *Nme*NANAS, whereas the strongest inhibition was shown by Br-PEP followed by Cl-PEP then F-PEP. Me-PEP and F-PEP were the poorest inhibitors against *Cje*NANAS while the strongest inhibitors were Cl-PEP and Br-PEP.

Inhibition for both types of NANAS by the 3-substituted halo-PEP (3-halo-PEP) analogues showed that the relatively larger substituents on the double bond (Br-PEP and Cl-PEP) were associated with stronger inhibition. This finding was unexpected since it is reasonable to

assume that the larger substituents of the PEP analogue would bind less well to NANAS due to steric hindrance with the residues within the active site. Thus the analogues bearing the smallest substituents would have been expected to bind to the active site more readily, competitively inhibiting NANAS with respect to PEP. All 3-halo-PEP used in this study are predominantly in the (*Z*)-configuration, so the amino acid residues located within the region of this substituent in this position would be expected to unfavourably sterically clash with the substituent on C3 of these analogues.

For *Nme*NANAS for which the structure is known, the residues that may clash can be predicted (**Figure 4.1**). Residues within 4 – 5 Å of C3 of PEP were examined.
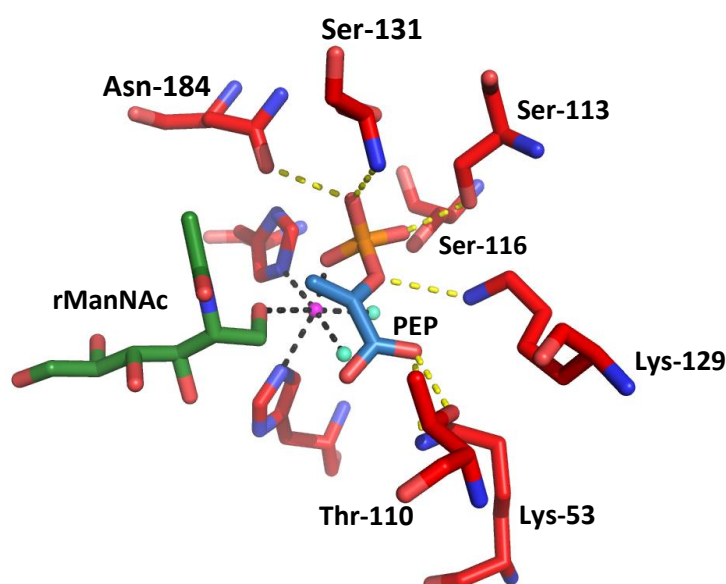
Figure 4.1 The PEP binding site of *Nme*NANAS. Residues interacting with PEP are labelled. Mn^{2+} as a pink sphere, PEP as blue with phosphate group shown as orange, and *N*-acetylmannosaminitol as green (rManNAc). The residues coloured red represent the amino acid residues from the TIM barrel fold and the cyan spheres represent water molecules (PDB code 1XUZ).

From an inspection of the PEP bound structure, it is likely that the backbone amino group of Ser-131 (which is found 4.1 Å from C3 of PEP), and the side-chain, amide group of Asn-184 (which is 4.7 Å from C3 of PEP) may clash with the C3-substituent of PEP analogue if the

substituent is large in size. All other surrounding residues are at least 6 Å away and therefore less likely to clash.

The observation in these studies was, however, that the 3-halo-PEP with the larger substituents exhibited stronger inhibition. This may suggest that the analogues are alternatively positioned within the PEP binding site of active site to natural PEP. This may relate to the poor ability of these compounds to act as alternative substrates for these enzymes.

Conversely the fluorine substituent of F-PEP is small, and may mean that this compound is likely to occupy the same binding position as that the natural substrate. The observation that F-PEP can react with ManNAc, albeit slowly, -supports this analogue binding in a similar mode to PEP in the active site.

However, clashes of the fluoro-substituent against surrounding residues are still possible. The size of the substituents may not be the only factor in determining whether an analogue can be accommodated as electronic factors may come into play. The fluoro substituent is highly electronegative in comparison to the hydrogen it replaces. This is especially noteworthy as the proposed mechanism for NANAS involves the nucleophilic attack by C3 of PEP on ManNAc. The nucleophilicity of the C3 will be reduced by the presence of fluorine on C3.

4.3 The structural conformation of ManNAc may be important for binding to the NANAS active site

Various ManNAc analogues were tested on both *Nme*NANAS and *Cje*NANAS, however rManNAc was the only analogue which was found to be an inhibitor of these enzymes. All other ManNAc analogues were neither alternative substrates nor effective inhibitors. This may indicate the importance of the specific stereochemistry of ManNAc for binding and utilisation by NANAS.

The ManNAc binding site of *Nme*NANAS was observed in the crystal structure 1XUZ (**Figure 4.2**). rManNAc was bound with the active site along with PEP, revealing the likely binding site of the acyclic aldehyde form of ManNAc. The hydroxyl groups and amino acetyl functionality of ManNAc interact with surrounding residues in the binding site. The C3

hydroxyl group interacts with both Asp-246 and Gln-55, the C5 hydroxyl group interacts with both Asp-246 and Asn-74, and the C6 hydroxyl group interacts with Asn-74. Arg'-314 (extending into the active site from the other chain of the protein) interacts with the acetyl functionality of the *N*-acetyl group of ManNAc, while the amino functionality of *N*-acetyl group interacts with Tyr-186.
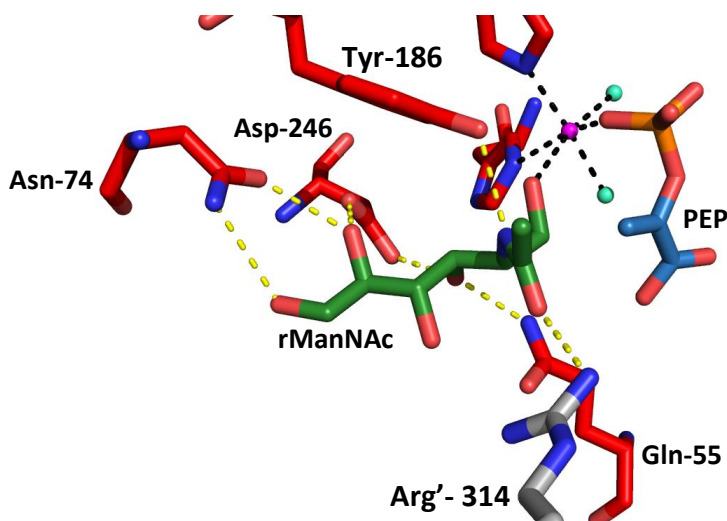
Figure 4.2 The ManNAc binding site of *Nme*NANAS. Residues interacting with rManNAc are labelled. Mn^{2+} as a pink sphere, PEP as blue with phosphate group shown as orange, and *N*-acetylmannosaminitol as green (rManNAc). The residues coloured red represent the amino acid residues from the TIM barrel fold, Arg-314' contributed by the other monomer is coloured as grey and the cyan spheres represent water molecules (PDB code 1XUZ).

Arg'-314 assists in the binding of ManNAc and its positioning within the active site so that the reactive aldehyde of ManNAc is close to the C3 of PEP to support nucleophilic attack in the first step of the reaction.[30] Arg-314 has been shown to be of importance by mutagenesis.[30] Tyr-186 may also aid in this process, interacting with the amino group at the C2 position of ManNAc *via* a hydrogen bond.

The interaction between Tyr-186 and the amino functionality of the *N*-acetyl group may suggest that this residue is also important for ManNAc binding and catalytic reaction with PEP. This may relate to the poor inhibition of the ManNAc analogues and their inability to act as alternative substrates, as these compounds all have the *N*-acetyl group altered in some way.

The different configuration of the hydroxyl group at C4 for GalNAc may have little significance in interrupting the binding to NANAS as there appears to be no significant interactions between this hydroxyl group and the protein. It is therefore surprising that this compound is not observed to be an inhibitor or substrate.

4.4 Cyclisation of ManNAc analogues and may interrupt the binding of the NANAS active site

The relatively strong inhibition by rManNAc may be explained by the inability of rManNAc to form a cyclic structure due to the lack of an aldehyde group. NANAS is predicted to utilise an acyclic form of the substrate ManNAc, in order to react with PEP to form NANA. Given only a small proportion of the ManNAc found in solution will be in the acyclic form, rManNAc will compete with relative advantage to the other analogues tested in these studies.

The same reasoning can also be applied to the product analogue rNANA inhibition against *Nme*NANAS and *Cje*NANAS. rNANA (analogue of the product NANA) will be present as an acyclic structure, although lactonisation of this compound is possible.

The large K_M of ManNAc for NANAS enzyme could also be explained by the cyclisation of ManNAc. The enzyme NANAS may catalyse the opening of the cyclic ManNAc substrate.

4.5 Future directions

4.5.1 Is 2DG really an alternative substrate for NANAS?

2DG demonstrated evidence suggesting that may be an alternative substrate for *Nme*NANAS and *Cje*NANAS, however the rate of loss of PEP over time was extremely low and thus it is not possible to conclude that 2DG is an alternative substrate for the NANAS enzyme from these studies. In order to confirm this full characterisation of the alternative product formed between 2DG and NANAS is required. Obtaining sufficient quantities of this will be a challenge, given the extremely low reaction rates.

4.5.2 Why does Me-PEP exhibit poor inhibition relative to Br-PEP?

The inhibition with the 3-substituted PEP analogues suggest that those that bear a large substituent may be bound in an alternative position to natural substrate PEP. Crystal

structures of these inhibitors in complex with the enzymes may help to ascertain how they are achieving their inhibition and rationalise their relative potency.

Me-PEP exhibited poorer inhibition in comparison to the 3-halo-PEP analogues which have an electronegative substituent at the C3 position. The electronegative substituents may allow stronger binding to the PEP binding site due to the formation of hydrogen bonding interactions to the neighbouring amino acid residue. Structures of these compounds in complex with these inhibitors may assist in understanding their potency.

4.5.3 Mutagenic study of residues within the active site of NANAS

Potential site directed mutagenesis of amino acid residues, which interact with PEP and ManNAc, needs to be performed.

The importance of amino acid residues within the active site, which interact with ManNAc could be investigated by mutating the residues. The mutated NANAS will then be characterised with the substrates to observe any significant changes in substrate binding. For example Tyr-186 could be mutated to Phe-186 to probe the importance of *N*-acetyl group–Tyr-186 interaction. The importance of other residues which interact with the hydroxyl groups of ManNAc could be investigated by mutating Gln-55, Asp-246 and Asn-74 into Met-55, Leu-246 and Leu-74 respectively.

Steric clashes with the substituents of 3-halo-PEP could be further investigated by mutating residues which are suspected to clash into a residue with smaller side-chain. Asn-184 could be mutated into Gly-184 however substrate and inhibitor acceptability could be significantly affected by this change. The mutation of Ser-131 may not be mutated since the amino group of the back bone of Ser-131 is likely to clash with 3-halo-PEP.

4.6 Concluding remarks

In conclusion, using substrate mimicry is a first step in probing the inhibition of an enzyme. These inhibitory studies of *Nme*NANAS and *Cje*NANAS have provided further understanding of how the enzyme accommodates its substrate and this is potentially a useful step in developing inhibitors as leads for alternative antibiotics for theses pathogens.

Chapter 5
Materials and methods

5.1 Figures and graphs

5.1.1 Protein 3-dimensional structures
Figures of protein structures were created using PyMOL version 1.5, Schrödinger LLC.

5.1.2 Graphing Kinetic Data
Kinetic constants of enzymes and inhibitors were determined and the data were shown as Michaelis Menten constant graphs and double reciprocal graphs (Lineweaver-Burk plot graphs) using GRAFIT7 software.

5.2 General procedures

5.2.1 Water
All water used throughout the study was treated with Millipore Milli-Q system for all buffers, and solutions.

5.2.2 pH measurements
All measurements were made using a Denver Instruments UB-10 Ultra-Basic pH meter, or using a Mettler Toledo Seven Compact pH meter with a standard or microprobe. The pH meter were calibrated when necessary with the use of standard pH buffer solutions; pH = 4, 7, and 10. Any solution which required being more acidic, the addition of 1 M HCl or 10 M HCl was added to the solution. If the solution required being more basic, the addition of 1 M or 10 M NaOH were added to the solution.

5.2.3 Incubation
All cell cultures were incubated using Ecotron shaking incubator (Infors HT), shaking at 180 rpm, incubating at the temperatures of 27 or 37 °C.

5.2.4 Bacterial cell culture
Bacterial cells were cultured in a growth media, lysogeny-broth (LB) solution. The LB solutions were prepared by the dissolving 20 grams of LB powder into 1 L of Milli-Q water in order to prepare LB solution at the concentration of The dissolved LB solution were then sterilised by the use of autoclaving and then cooled. The sterilised LB solutions were used as

soon as possible to prevent miscellaneous microbes growing significantly into large amounts. Antibiotics were added prior to use.

5.2.5 Bacterial cell preculture

Preculture of bacterial cells were also prepared into 20 gL^{-1} LB solution. The growth media for bacterial preculture were prepared from dissolving 2 g of LB powder into 100 mL of Milli-Q water. The prepared solution were sterilised by autoclaving then cooled before used. Antibiotics were added prior to use.

5.3 Cell growth

5.3.1 Preparation of bacterial preculture

The transformed *E. coli* carrying the vector bearing the gene of NANAS were grown in a cell growth medium for preculture. Antibiotics were added to the sterilised LB solution so that there was 0.1 mg/mL spectinomycin, 0.1 mg/mL ampicillin, and 0.025 mg/mL chloramphenicol as the final concentration in the culture. After inoculation with *Nme*NANAS, the LB solution was incubated at 37 °C in an incubator overnight.

5.3.2 Full scale growth of bacterial cell and IPTG-induced expression

2 L of 20 gL^{-1} LB solution were prepared and sterilised by autoclaving. Antibiotics, ampicillin and chloramphenicol, were added so that there is 0.1 mg/mL of ampicillin and 0.025 mg/mL chloramphenicol as the final concentration. To each of these LB solutions, 50 mL of the prepared preculture is added resulting in the inoculation of the 1 L LB solution. The OD_{600} of the cultures were monitored until reaching the OD of about 0.5-0.6 AU which generally takes about 3-4 hours. The cultures were induced by adding IPTG at this point causing the final concentration of IPTG to be approximately 0.1 mM. After induction, the LB solution was transferred to another shaking another incubator, at the temperature of 27 °C and then incubated overnight. The grown cells are harvested by the use of ultra-centrifugation in the following day, preferably in the morning in order to prevent the cells from over populating and dying.

5.3.3 Cell harvesting

The methods involving the harvest of cells from cultures vary depending on the availability of the rotor and centrifuge, but typically large cultures of LB solutions with cells cultured overnight were centrifuged down into pellets in 1 L bottles at 14,000 g for 30 minutes at the

temperature of 4 °C. The cell pellets were re-suspended in buffer used for immobilised metal affinity chromatography (IMAC) and then lysed for protein purification. If the cells were not being lysed immediately, the cell pellets were stored as -80 °C until required.

5.4 Protein purification

5.4.1 Cell lysis

Cells were lysed by the use of sonication with an Omni-Ruptor 4000 Ultrasonic Homogenizer (Omni International). After re-suspension of cell pellet in a buffer solution of 50 mL, the cell solution was lysed in a 50 mL beaker chilled by surrounding packed ice. The sonication protocol used 70% power burst for 5.5 minutes with 30 seconds of pauses between each bursts. Sonication were performed until the lysis had been completed by eye, as the whole lysed cell solution exhibit a more thinner and watery consistency. This usually takes about 4-5 cycles of sonication protocol. All cellular debris was removed by centrifugation at 21,000 g for 30 min at 4 °C and collecting the supernatant sample.

5.4.2 Chromatography systems

Chromatographic systems were used in order to isolate and purify the protein of interest. All chromatography was performed on a Bio-Rad Biologic Duo Flow system. Series of column chromatography were used in steps to obtain the purified protein of interest for experimentation. IMAC, desalt and size exclusion chromatography (SEC) were used for the process of purification. All buffers were filtered through 0.2 μm pore under vacuum and degassed prior to use. All samples to be purified were syringe filtered through 0.2 μm pore before loaded into a 10 mL or 50 mL Superloop™ (GE Healthcare). All chromatography was conducted at 4 °C for protocols taking approximately 1 hour or overnight.

The eluate from columns was fractionated in 2 mL fractions collected in 96-well plates. Elution from the columns was principally monitored at the wavelength 280 nm which is the wavelength absorbed by proteins. The wavelength of 260 nm, which is the absorbance of DNA, and conductivity were also monitored. Fractions were analysed by gel electrophoresis (SDS-PAGE). Fractions containing the enzyme of interest were then pooled and concentrated for the next step of purification (or storage) using 10,000 Da molecular weight cut-off (MWCO) devices (Vivaspin 2 [GE Healthcare], Vivaspin 500 and Vivaspin 20 [Sartorius Stedim Biotech]).

5.4.2.1 Immobilised metal affinity chromatography (IMAC)

The proteins purified contained polyhistidine tags (His-tag) with high affinity for Co^{2+} ions. IMAC were performed in order to isolate proteins with histidine tags from the supernatant, using a 5 mL cobalt affinity Talon® column (Clontech). The column was washed with at least five column volumes (25 mL) of binding buffer solution for equilibration. The sample was then injected, and the column washed with a further five column volumes (25 mL) of elution buffer to remove any unbound proteins.

Binding buffer: 500 mM NaCl and 50 mM K_2HPO_4 (pH 8).

Elution buffer: 500 mM NaCl, 200 mM imidazole, and 50 mM KH_2PO_4 (pH 8).

5.4.2.2 Desalting

Desalting was performed using a 50 mL Bio-Scale Mini Bio-Gel P-6 Desalting Cartridge (Bio-Rad). The column was used on a Duoflow system with a maximum injection volume of 30 mL. The column was equilibrated with two column volumes of buffer (100 mL), after which the protein was injected and then eluted with the same buffer. The buffer used for desalting, was the same buffer as the binding buffer for IMAC.

Buffer: 500 mM NaCl and 50 mM K_2HPO_4 (pH 8).

5.4.2.3 Size-exclusion chromatography (SEC)

The protein of interest was purified by SEC as a final stage of purification using a Superdex 200 26/60 column (GE Healthcare). The column was equilibrated with one column volume (1 L) of the appropriate SEC buffer before the protein was injected, and eluted with one column volume (1 L) of the same buffer. A flow rate of 1 ml/min was used overnight.

SEC buffer: 30 mM triethanolamine (pH 8).

5.4.3 Cleavage using TEV protease

The His-tag attached to the proteins were removed by the use of tobacco etch virus (TEV) protease. The protein of interest has a cleavage site which the TEV proteases recognise. The cleavage site sequence used was ENLYFQG, with the protease cleaving between the glutamine and glycine residues. Generally, cleavage was performed after an IMAC column, after excess imidazole was removed by desalting. TEV protease was used at a ratio of 1:100

to the substrate protein (by mass, as determined by absorbance). The TEV reaction was performed at 4 °C overnight.

5.5 Purification of TEV protease

Recombinant TEV protease was similarly purified as the first steps of the purification of NANAS. *E. coli* BL21 (DE3) cells containing the plasmids pRIL (for rare codon production) and pRK793 (encoding TEV protease) were grown in LB containing ampicillin and chloramphenicol and induced using IPTG as detailed above. Cells were lysed by sonication.

The protein was purified using a single IMAC step with Profinity cartridges, using the buffers detailed below. After purification, the TEV protease in the column bound fractions was concentrated to 1 mg/mL, buffer exchanged into storage buffer, and frozen in 1 mL aliquots.

TEV protease lysis buffer: 10% (v/v) glycerol, 50 mM potassium phosphate (pH 8), 300 mM KCl, 25 mM imidazole.

TEV protease elution buffer: 10% (v/v) glycerol, 50 mM potassium phosphate (pH 8), 300 mM KCl, 250 mM imidazole.

5.6 Gel electrophoresis

SDS-PAGE was performed using either NuPAGE® 10% Bis-Tris 12-well pre-cast gels (Invitrogen) or Bolt® 12% Bis-Tris 12-well gels. NuPAGE® gels were run in NuPAGE® MES SDS running buffer (Invitrogen). Bolt® gels were run in Bolt® MES SDS running buffer. Samples were mixed with protein loading buffer and heated with boiling water prior to analysis with gel electrophoresis. Electrophoresis was performed using a XCell SureLock™ Electrophoresis Cell (Invitrogen), also at 200 V for 50 min.

Protein loading buffer (4x) consisted of 41.5 mM Tris-HCl pH 6.8, 40% (v/v) glycerol, 8% (w/v) sodium dodecyl sulfate (SDS), 10 mM EDTA, sufficient bromophenol blue to be visible and 10 μL of 0.5 M DTT.

All SDS-PAGE gels were stained in square petri dishes using coomassie brilliant blue R-250, for about 15 min before being destained to remove excess dye. Staining and destaining times were reduced by heating gel and solution in a microwave oven until almost boiling. The molecular weight standard used was Novex® Sharp Pre-Stained Protein Standards

(Invitrogen). Photographs of gels were taken using a white light transilluminator in a Molecular Imager® Gel Doc™ XR (Bio-Rad).

Stain: 0.1% (w/v) coomassie brilliant blue R-250, 10% (v/v) acetic acid and 40% (v/v) methanol

Destain: 10% (v/v) acetic acid and 40% (v/v) methanol

5.7 Protein concentrations

Nanodrop ND-1000 spectrophotometer were used to measure the concentration of the purified protein. The spectrophotometer measured the absorption at 280 nm. Protein concentration was then calculated using the Beer-Lambert Law. The extinction coefficient for the protein used for the Beer-Lambert Law calculation was determined from Protparam (http://web.expasy.org/protparam/).

5.8 Enzyme storage

Purified protein was divided into aliquots in either thin-walled PCR or 0.6 mL micro-centrifuge tubes in 20 μL to 250 μL aliquots, flash-frozen in liquid nitrogen, and stored at −80 °C. All protein samples were rapidly thawed immediately before use and kept on ice.

5.9 Kinetic characterisations

5.9.1 Equipment

All kinetic assays were carried with a Varian Cary 100 UV-visible spectrophotometer, using stoppered quartz cuvettes with a pathlength of 1 cm or 0.2 cm.

The temperature was continuously controlled at 298 K by the use of jacketed multicell holder, connected to an external Varian Peltier temperature controller.

Rates of reaction were measured by calculating a line of least-squares fit of initial rate data in the Cary WinUV Kinetic Application (Version 3, Varian).

5.9.2 Enzyme kinetic assays

In general, all enzyme kinetics was conducted at 25 °C, in 50 mM BTP buffer at pH of 8, initiated with approximately 10 to 15 μg of enzyme.

Initial velocity data were obtained by the Enzyme activity which were monitored by UV-Visible spectrophotometry to continuously detect the loss of PEP at 232 nm

84

(ε = 2.8 x 10^3 M^{-1}cm^{-1}) overtime. The rate (initial velocity) was measured by a least-square fit. The continuous decrease in absorbance overtime is due to the enol alkene of PEP consumed by the catalytic reaction of NANAS.

Absorbance was measured through total volumes of 1 mL or 500 µL of sample with the path length of 1 cm or 0.2 cm respectively. Depending on the reaction, samples contained a range of PEP, ManNAc, and analogue concentrations in quartz cell cuvette. The concentrations are specified in the appropriate subsection of this chapter in detail.

5.9.3 Substrate concentration determination

The concentrations of the solutions of substrates such as PEP were determined using direct kinetic assay at 232 nm. The other substrate ManNAc was determined as the same way since the stoichiometry of the NANAS reaction between PEP and ManNAc is 1:1.

Limiting amounts of substrate to be measured were added to the stoppered quartz cuvette while the other substrate was held at excess concentration. The initial absorbance at the start of the initiation was subtracted to the final absorbance at the end of the enzymatic reaction to get the change of absorbance (ΔAbs). ΔAbs were measured in triplicate. A sample containing no substrates was used to measure the change in absorbance due to the increase in enzyme (ΔAbs$_E$). The corrected change in absorbance was then calculated as ΔAbs - ΔAbs$_E$. The corrected absorbance was then converted to the concentration of the limiting substrate using the Beer-Lambert Law with an extinction coefficient of 2.8 x 10^3 M^{-1}cm^{-1}.

5.9.4 Modelling of Kinetic data

K_M and k_{cat} values were determined by holding the concentration of one substrate constant and varying the concentration of the other. The exact substrate concentrations used differ in each assay and stated in the appropriate subsection of this chapter. The values were then non-linearly fitted to the Michaelis-Menten equation using Grafit5 (Erathicus Software). The double reciprocal plots shown in the figures were not used to fit the data and are provided simply for illustration.

K_i values were obtained by performing experimental inhibition assays at different concentrations of the substrates and inhibitor. Each substrate were at limiting concentrations depending on the inhibitor, whether it is a PEP analogue or ManNAc

analogue. The exact substrate and inhibitor concentrations used differ in each assay and stated in the appropriate subsection of this chapter. The data were modelled using Grafit5 fitting into a competitive model or a mixed inhibition model.

5.9.5 Kinetic conditions in chapter 2

5.9.5.1 Michaelis-Menten conditions for the determination of PEP K$_M$ values

5.9.5.1.1 *Nme*NANAS

The PEP K_M values were determined for *Nme*NANAS under the following conditions: constant concentrations of 1.2 mM ManNAc, and varying concentrations of PEP (0.0036 mM, 0.0073 mM, 0.015 mM, 0.022 mM, 0.029 mM, 0.0729 mM, 0.11 mM, and 0.15 mM) initiated with approximately 10 µg of *Nme*NANAS.

5.9.5.1.2 *Cje*NANAS

The PEP K_M values were determined for *Cje*NANAS under the following conditions: constant concentrations of 11.3 mM ManNAc, and increasing concentrations of PEP (0.011 mM, 0.021 mM, 0.032 mM, 0.053 mM, 0.074 mM, 0.11 mM, 0.13 mM, 0.16 mM, 0.21 mM, 0.27 mM, 0.32 mM, and 0.37 mM) initiated with approximately 15 µg of *Cje*NANAS.

5.9.5.2 Inhibition assay conditions

5.9.5.2.1 Enzyme kinetics for *Nme*NANAS with SEP

The kinetic assay was initiated with approximately 10 µg of *Nme*NANAS under the following conditions: constant concentration of 1.1 mM ManNAc and constant concentrations of 0.11 mM PEP to determine the control rate. The kinetic assay was repeated with the conditions above with the additional presence of 1.03 mM SEP. The enzyme with the presence of SEP showed no significant loss of activity than the control.

5.9.5.2.2 Enzyme kinetics for *Cje*NANAS with SEP

The kinetic assay was initiated with approximately 15 µg of *Cje*NANAS under the following conditions: constant concentration of 111.55 mM ManNAc and constant concentrations of 0.07 mM PEP to obtain the control. The kinetic assay was repeated with the conditions above with the additional presence of 1.0 mM SEP. The enzyme with the presence of SEP showed no significant loss of activity than the control.

5.9.5.2.3 Enzyme kinetics for *Nme*NANAS with allylic phosphonate

The kinetic assay was initiated with approximately 10 μg of *Nme*NANAS under the following conditions: constant concentration of 2.12 mM ManNAc and constant concentrations of 0.11 mM PEP to determine the control. The kinetic assay was repeated with the conditions above with the additional presence of 0.8 mM allylic phosphonate. The enzyme with the presence of SEP showed no significant loss of activity than with the control, absence of allylic phosphonate.

5.9.5.2.4 Enzyme kinetics for *Cje*NANAS with allylic phosphonate

The kinetic assay was initiated with approximately 15 μg of *Cje*NANAS under the following conditions: constant concentration of 111.55 mM ManNAc and constant concentrations of 0.07 mM PEP to determine the control. The kinetic assay was repeated with the conditions above with the additional presence of 1.0 mM allylic phosphonate. The enzyme with the presence of SEP showed no significant loss of activity than with the control, absence of allylic phosphonate.

5.9.5.2.5 Enzyme kinetics for *Nme*NANAS with F-PEP

The K_i value for *Nme*NANAS with F-PEP were determined under the following conditions: constant concentrations of 10.82 mM ManNAc, and increasing concentrations of PEP (0.10 mM, 0.21 mM, 0.62 mM, and 1.04 mM) initiated with approximately 10 μg of *Nme*NANAS. The kinetic assay was repeated with the above conditions with the additional presence of 0.410 mM, and 0.822 mM F-PEP.

5.9.5.2.6 Enzyme kinetics for *Cje*NANAS with F-PEP

The Ki value for CjeNANAS with F-PEP were determined under the following conditions: constant concentrations of 10.05 mM ManNAc, and increasing concentrations of PEP (0.07 mM, 0.11 mM, 0.22 mM, and 0.44 mM) initiated with approximately 15 μg of *Nme*NANAS. The kinetic assay was repeated with the above conditions with the additional presence of 0.32 mM, and 0.065 mM F-PEP.

5.9.5.2.7 Enzyme kinetics for *Nme*NANAS with Cl-PEP

The K_i value for *Nme*NANAS with Cl-PEP were determined under the following conditions: constant concentrations of 10.9 mM ManNAc, and increasing concentrations of PEP (0.11 mM, 0.21 mM, 0.63 mM, and 1.06 mM) initiated with approximately 10 μg of *Nme*NANAS.

The kinetic assay was repeated with the above conditions with the additional presence of 0.21 mM, and 0.42 mM Cl-PEP.

5.9.5.2.8 Enzyme kinetics for *Cje*NANAS with Cl-PEP

The Ki value for CjeNANAS with Cl-PEP were determined under the following conditions: constant concentrations of 11.15 mM ManNAc, and increasing concentrations of PEP (0.11 mM, 0.21 mM, 0.43 mM, and 0.64 mM) initiated with approximately 15 µg of *Cje*NANAS. The kinetic assay was repeated with the above conditions with the additional presence of 0.01 mM, and 0.03 mM Cl-PEP.

5.9.5.2.9 Enzyme kinetics for *Nme*NANAS with Br-PEP

The K_i value for *Nme*NANAS with Br-PEP were determined under the following conditions: constant concentrations of 20.2 mM ManNAc, and increasing concentrations of PEP (0.07 mM, 0.11 mM, 0.33 mM, and 0.44 mM) initiated with approximately 10 µg of *Nme*NANAS. The kinetic assay was repeated with the above conditions with the additional presence of 0.39 mM, and 0.75 mM Br-PEP.

5.9.5.2.10 Enzyme kinetics for *Cje*NANAS with Br-PEP

The K_i value for *Cje*NANAS with Br-PEP were determined under the following conditions: constant concentrations of 11.16 mM ManNAc, and increasing concentrations of PEP (0.11 mM, 0.21 mM, 0.43 mM, and 0.64 mM) initiated with approximately 15 µg of *Cje*NANAS. The kinetic assay was repeated with the above conditions with the additional presence of 0.01 mM, and 0.03 mM Br-PEP.

5.9.5.2.11 Enzyme kinetics for *Nme*NANAS with Me-PEP

The K_i value for *Nme*NANAS with Me-PEP were determined under the following conditions: constant concentrations of 10.9 mM ManNAc, and increasing concentrations of PEP (0.09 mM, 0.18 mM, 0.54 mM, and 0.89 mM) initiated with approximately 10 µg of *Nme*NANAS. The kinetic assay was repeated with the above conditions with the additional presence of 0.68 mM, and 1.35 mM Me-PEP.

5.9.5.2.12 Enzyme kinetics for *Cje*NANAS with Me-PEP

The K_i value for *Cje*NANAS with Me-PEP were determined under the following conditions: constant concentrations of 10.05 mM ManNAc, and increasing concentrations of PEP (0.07 mM, 0.11 mM, 0.22 mM, and 0.44 mM) initiated with approximately 15 µg of *Cje*NANAS.

The kinetic assay was repeated with the above conditions with the additional presence of 0.04 mM, and 0.08 mM Me-PEP.

5.9.6 Kinetic conditions in chapter 3

5.9.6.1 Michaelis-Menten conditions for the determination of ManNAc K_M values

5.9.6.1.1 *Nme*NANAS

The ManNAc K_M values were determined for *Nme*NANAS under the following conditions: constant concentrations of 0.19 mM PEP, and varying concentrations of ManNAc (0.29 mM, 0.43 mM, 0.72 mM, 1.44 mM, 2.88 mM, 5.76 mM, 7.20 mM, 8.64 mM, 10.08 mM, and 13.97 mM) initiated with approximately 10 µg of *Nme*NANAS.

5.9.6.1.2 *Cje*NANAS

The ManNAc K_M values were determined for *Cje*NANAS under the following conditions: constant concentrations of 0.32 mM PEP, and varying concentrations of ManNAc (0.11 mM, 0.17 mM, 0.23 mM, 0.34 mM, 0.45 mM, 0.56 mM, 0.68 mM, 1.13 mM, 2.26 mM, 3.38 mM, 4.51 mM, 5.64 mM, 6.77 mM, 7.90 mM, 9.03 mM, 10.15 mM, and 11.28 mM) initiated with approximately 15 µg of *Cje*NANAS.

5.9.6.2 Inhibition assay conditions

5.9.6.2.1 Enzyme kinetics for *Nme*NANAS with rManNAc

The K_i value for *Nme*NANAS with rManNAc were determined under the following conditions: constant concentrations of 0.22 mM PEP, and increasing concentrations of ManNAc (0.94 mM, 1.89 mM, 4.7 mM, and 9.4 mM) initiated with approximately 10 µg of *Nme*NANAS. The kinetic assay was repeated with the above conditions with the additional presence of 1.05 mM, and 2.2 mM rManNAc.

5.9.6.2.2 Enzyme kinetics for *Cje*NANAS with rManNAc

The K_i value for *Cje*NANAS with rManNAc were determined under the following conditions: constant concentrations of 0.29 mM PEP, and increasing concentrations of ManNAc (0.99 mM, 1.98 mM, 2.97 mM, and 3.96 mM) initiated with approximately 15 µg of *Cje*NANAS. The kinetic assay was repeated with the above conditions with the additional presence of 0.013 mM, and 0.025 mM rManNAc.

5.9.6.2.3 Enzyme kinetics for *Nme*NANAS and *Cje*NANAS with other ManNAc analogues

The rest of the ManNAc analogues GluNAc, GalNAc, ManCl, and 2DG were tested with *Nme*NANAS and *Cje*NANAS.

All ManNAc analogues, used in this study (with the exception of rManNAc), were purchased from Sigma-Aldrich®. The analogue rManNAc was prepared by the reduction of ManNAc with sodium borohydride, as described in the experimental chapter.[9]

The kinetic assay was initiated with approximately 10 to 15 µg of *Nme*NANAS and *Cje*NANAS respectively under the following conditions: constant concentration of 0.2 mM and 0.28 mM PEP respectively and constant concentration of 0.5 mM ManNAc (for both enzymes) to determine the control reaction rate. The assay was repeated with additional presence of various 10 mM ManNAc analogues in excess. The enzyme with the presence of other ManNAc analogues showed no significant loss of activity than the control.

5.10 Preparation of rManNAc

Reduced ManNAc (rManNAc) was synthesised using the method outlined in Gunawan et al.[9] 0.21 g of ManNAc (1 mM) was dissolved in 10 mL of water and 0.08 g of sodium borohydride (2 mM) added to the solution. The mixture was subsequently stirred at room temperature for 2 hours. The resulting solution was neutralised using Dowex® 50WX8 hydrogen form, 100-200 mesh (Sigma-Aldrich). The solution was then filtered and lyophilised, producing a white solid. The product was subsequently refluxed in 50 mL of methanol for 30 min and concentrated under reduced pressure. The resultant oily film was re-dissolved in water and lyophilised to produce a white solid (0.15 – 0.16 g). Purity of rManNAc was determined through ^{1}HNMR to be above 99 %.

Bibliography

(1)   Schauer, R. Sialic acids: Fascinating sugars in higher animals and man. *Zoology.* **2004**, *107*, 49.

(2)   Tanner, M. E. The enzymes of sialic acid biosynthesis. *Bioorganic Chemistry.* **2005**, *33*, 216.

(3)   Liu, F.; Lee, H. J.; Strynadka, N. C. J.; Tanner, M. E. Inhibition of *Neisseria meningitidis* sialic acid synthase by a tetrahedral intermediate analogue. *Biochemistry.* **2009**, *48*, 9194.

(4)   Neu, H. C. The crisis in antibiotic-resistance. *Science.* **1992**, *257*, 1064.

(5)   Schoenhofen, I. C.; Vinogradov, E.; Whitfield, D. M.; Brisson, J. R.; Logan, S. M. The CMP-legionaminic acid pathway in *Campylobacter*: Biosynthesis involving novel GDP-linked precursors. *Glycobiology.* **2009**, *19*, 715.

(6)   Chou, W. K.; Dick, S.; Wakarchuk, W. W.; Tanner, M. E. Identification and characterization of *NeuB3* from *Campylobacter jejuni* as a pseudaminic acid synthase. *Journal of Biological Chemistry.* **2005**, *280*, 35922.

(7)   Angata, T.; Varki, A. Chemical diversity in the sialic acids and related alpha-keto acids: An evolutionary perspective. *Chemical Reviews.* **2002**, *102*, 439.

(8)   Traving, C.; Schauer, R. Structure, function and metabolism of sialic acids. *Cellular and Molecular Life Sciences.* **1998**, *54*, 1330.

(9)   Gunawan, J.; Simard, D.; Gilbert, M.; Lovering, A. L.; Wakarchuk, W. W.; Tanner, M. E.; Strynadka, N. C. J. Structural and mechanistic analysis of sialic acid synthase *NeuB* from *Neisseria meningitidis* in complex with Mn^{2+} phosphoenolpyruvate, and *N*-acetylmannosaminitol. *Journal of Biological Chemistry.* **2005**, *280*, 3555.

(10)   Varki, A. In *Yearbook of Physical Anthropology, Vol 44*; Ruff, C., Ed. 2001; Vol. 44, p 54.

(11)   Campanero-Rhodes, M. A.; Solis, D.; Carrera, E.; de la Cruz, M. J.; Diaz-Maurino, T. Rat liver contains age-regulated cytosolic 3-deoxy-D-glycero-D-galacto-non-2-ulopyranosonic acid (Kdn). *Glycobiology.* **1999**, *9*, 527.

(12)   Varki, A. Sialic acids as ligands in recognition phenomena. *Faseb Journal.* **1997**, *11*, 248.

(13)   Muhlenhoff, M.; Eckhardt, M.; Gerardy-Schahn, R. Polysialic acid: Three-dimensional structure, biosynthesis and function. *Current Opinion in Structural Biology.* **1998**, *8*, 558.

(14)   Varki, A. Sialic acids in human health and disease. *Trends in Molecular Medicine.* **2008**, *14*, 351.

(15)   Varki, N. M.; Varki, A. Diversity in cell surface sialic acid presentations: Implications for biology and disease. *Laboratory Investigation.* **2007**, *87*, 851.

(16)   Muehlenhoff, M.; Rollenhagen, M.; Werneburg, S.; Gerardy-Schahn, R.; Hildebrandt, H. Polysialic acid: Versatile modification of NCAM, SynCAM 1 and Neuropilin-2. *Neurochemical Research.* **2013**, *38*, 1134.

(17)   Rutishauser, U. Polysialic acid at the cell surface: Biophysics in service of cell interactions and tissue plasticity. *Journal of Cellular Biochemistry.* **1998**, *70*, 304.

(18)   Fuster, M. M.; Esko, J. D. The sweet and sour of cancer: Glycans as novel therapeutic targets. *Nature Reviews Cancer.* **2005**, *5*, 526.

(19)   Fukuda, M. Possible roles of tumor-associated carbohydrate antigens. *Cancer Research.* **1996**, *56*, 2237.

(20)   Seidenfaden, R.; Krauter, A.; Schertzinger, F.; Gerardy-Schahn, R.; Hildebrandt, H. Polysialic acid directs tumor cell growth by controlling heterophilic neural cell adhesion molecule interactions. *Molecular and Cellular Biology.* **2003**, *23*, 5908.

(21)   Galeano, B.; Klootwijk, R.; Manoli, I.; Sun, M.; Ciccone, C.; Darvish, D.; Starost, M. F.; Zerfas, P. M.; Hoffmann, V. J.; Hoogstraten-Miller, S.; Krasnewich, D. M.; Gahl, W. A.; Huizing, M. Mutation in the key enzyme of sialic acid biosynthesis causes severe glomerular proteinuria and is rescued by N-acetylmannosamine. *Journal of Clinical Investigation.* **2007**, *117*, 1585.

(22)   Du, J.; Meledeo, M. A.; Wang, Z. Y.; Khanna, H. S.; Paruchuri, V. D. P.; Yarema, K. J. Metabolic glycoengineering: Sialic acid and beyond. *Glycobiology.* **2009**, *19*, 1382.

(23)   Severi, E.; Hood, D. W.; Thomas, G. H. Sialic acid utilization by bacterial pathogens. *Microbiology-Sgm.* **2007**, *153*, 2817.

(24)   Olson, M. E.; King, J. M.; Yahr, T. L.; Horswill, A. R.   Sialic acid catabolism in staphylococcus aureus. *Journal of Bacteriology.* **2013**, *195*, 1779.

(25)   Preston, A.; Mandrell, R. E.; Gibson, B. W.; Apicella, M. A. The lipooligosaccharides of pathogenic gram-negative bacteria. *Critical Reviews in Microbiology.* **1996**, *22*, 139.

(26)   Nudelman, Y.; Tunkel, A. R.   Bacterial meningitis epidemiology, pathogenesis and management update. *Drugs.* **2009**, *69*, 2577.

(27)   Coureuil, M.; Join-Lambert, O.; Lecuyer, H.; Bourdoulous, S.; Marullo, S.; Nassif, X. Pathogenesis of meningococcemia. *Cold Spring Harbor perspectives in medicine.* **2013**, *3*.

(28)   Altekruse, S. F.; Stern, N. J.; Fields, P. I.; Swerdlow, D. L., 1999.

(29)   Sundaram, A. K.; Pitts, L.; Muhammad, K.; Wu, J.; Betenbaugh, M.; Woodard, R. W.; Vann, W. F. Characterization of *N*-acetylneuraminic acid synthase isoenzyme 1 from *Campylobacter jejuni*. *Biochemical Journal.* **2004**, *383*, 83.

(30)   Joseph, D. D. A.; Jiao, W. T.; Parker, E. J. Arg314 is essential for catalysis by *N*-acetyl neuraminic acid synthase from *Neisseria meningitidis*. *Biochemistry.* **2013**, *52*, 2609.

(31)   Vimr, E. R.; Troy, F. A. Identification of an inducible catabolic system for sialic acids (NAN) in *Escherichia-coli*. *Journal of Bacteriology.* **1985**, *164*, 845.

(32)   Hao, J. J.; Balagurumoorthy, P.; Suryakala, S.; Sundaramoorthy, M.   Cloning, expression, and characterization of sialic acid synthases. *Biochemical and Biophysical Research Communications.* **2005**, *338*, 1507.

(33)   Shumilin, I. A.; Bauerle, R.; Wu, J.; Woodard, R. W.; Kretsinger, R. H.   Crystal structure of the reaction complex of 3-deoxy-D-*arabino*-heptulosonate-7-phosphate synthase from *Thermotoga maritima* refines the catalytic mechanism and indicates a new mechanism of allosteric regulation. *Journal of Molecular Biology.* **2004**, *341*, 455.

(34)   Hedstrom, L.; Abeles, R.   3-Deoxy-D-*manno*-octulosonate-8-phosphate synthase catalyzes the C-O bond-cleavage of Phosphoenolpyruvate. *Biochemical and Biophysical Research Communications.* **1988**, *157*, 816.

(35)   Reichau, S.; Jiao, W. T.; Walker, S. R.; Hutton, R. D.; Baker, E. N.; Parker, E. J. Potent Inhibitors of a Shikimate Pathway Enzyme from Mycobacterium tuberculosis combining mechanism-And modeling-based design. *Journal of Biological Chemistry.* **2011**, *286*.

(36)   Schofield, L. R.; Anderson, B. F.; Patchett, M. L.; Norris, G. E.; Jameson, G. B.; Parker, E. J.   Substrate ambiguity and crystal structure of *Pyrococcus furiosus* 3-Deoxy-D-*arabino*-heptulosonate-7-phosphate synthase: An ancestral 3-Deoxyald-2-ulosonate-phosphate synthase?, *Biochemistry.* **2005**, *44*, 11950.

(37)   Walker, S. R.; Parker, E. J. Synthesis and evaluation of a mechanism-based inhibitor of a 3-deoxy-D-*arabino* heptulosonate 7-phosphate synthase. *Bioorganic & Medicinal Chemistry Letters.* **2006**, *16*, 2951.

(38)   Bravo, I. G.; Garcia-Vallve, S.; Romeu, A.; Reglero, A.   Prokaryotic origin of cytidylyltransferases and alpha-ketoacid synthases. *Trends in Microbiology.* **2004**, *12*, 120.

(39)   Bentley, R. The shikimate pathway - A metabolic tree with many branches. *Critical Reviews in Biochemistry and Molecular Biology.* **1990**, *25*, 307.

(40)   Srinivasan, P. R.; Sprinson, D. B. 2-Keto-3-deoxy-d-*arabo*-heptonic acid 7-phosphate synthetase. *Journal of Biological Chemistry.* **1959**, *234*, 716.

(41)   Zhou, L.; Wu, J.; Janakiraman, V.; Shumilin, I. A.; Bauerle, R.; Kretsinger, R. H.; Woodard, R. W.   Structure and characterization of the 3-deoxy-D-*arabino*-heptulosonate 7-phosphate synthase from Aeropyrum pernix. *Bioorganic Chemistry.* **2012**, *40*, 79.

(42)   Walker, S. R.; Cumming, H.; Parker, E. J. Substrate and reaction intermediate mimics as inhibitors of 3-deoxy-D-*arabino*-heptulosonate 7-phosphate synthase. *Organic & Biomolecular Chemistry.* **2009**, *7*, 3031.

(43)   Deleo, A. B.; Sprinson, D. B.   Mechanism of 3-deoxy-D-*arabino*-heptulosonate 7-phosphate (DAHP) synthetase. *Biochemical and Biophysical Research Communications.* **1968**, *32*, 873.

(44)   Floss, H. G.; Carroll, M.; Onderka, D. K.   Stereochemistry of 3-deoxy-D-*arabino*-heptulosonate 7-phosphate synthetase reaction and chorismate synthetase reaction. *Journal of Biological Chemistry.* **1972**, *247*, 736.

(45)   Levin, D. H.; Racker, E. Condensation of arabinose 5-phosphate and phosphorylenol pyruvate by 2-keto-3-deoxy-8-phosphooctonic acid synthetase. *Journal of Biological Chemistry.* **1959**, *234*, 2532.

(46)   Raetz, C. R. H.; Whitfield, C.   Lipopolysaccharide endotoxins. *Annual Review of Biochemistry.* **2002**, *71*, 635.

(47)   Dotson, G. D.; Nanjappan, P.; Reily, M. D.; Woodard, R. W.   Stereochemistry of 3-deoxyoctulosonate 8-phosphate synthase. *Biochemistry.* **1993**, *32*, 12392.

(48)   Joseph, D. D. A., University of Canterbury, 2014.

(49)   Walsh, C. T.; Benson, T. E.; Kim, D. H.; Lees, W. J.   The versatility of phosphoenolpyruvate and its vinyl ether products in biosynthesis. *Chemistry & Biology.* **1996**, *3*, 83.

(50)   Wang, W. N.; Hellinga, H. W.; Beese, L. S. Structural evidence for the rare tautomer hypothesis of spontaneous mutagenesis. *Proceedings of the National Academy of Sciences of the United States of America.* **2011**, *108*, 17644.

(51)   Cumming, H. A., University of Canterbury, 2007.

(52)   Garcia-Alles, L. F.; Erni, B. Synthesis of phosphoenolpyruvate (PEP) analogues and evaluation as inhibitors of PEP-utilizing enzymes. *European Journal of Biochemistry.* **2002**, *269*, 3226.

(53)   Wagner, T.; Shumilin, I. A.; Bauerle, R.; Kretsinger, R. H.   Structure of 3-deoxy-D-*arabino*-heptulosonate-7-phosphate synthase from *Escherichia coli*: Comparison of the Mn2+*2-phosphoglycolate and the Pb2+*2-phosphoenolpyruvate complexes and implications for catalysis. *Journal of Molecular Biology.* **2000**, *301*, 389.

(54)   Webby, C. J.; Baker, H. M.; Lott, J. S.; Baker, E. N.; Parker, E. J. The structure of 3-deoxy-d-*arabino*-heptulosonate 7-phosphate synthase from Mycobacterium tuberculosis reveals a common catalytic scaffold and ancestry for type I and type II enzymes. *Journal of Molecular Biology.* **2005**, *354*, 927.

(55)   Jakeman, D. L.; Evans, J. N. S. Overexpression, purification, and use of phosphoenol pyruvate synthetase in the synthesis of PEP analogues. *Bioorganic Chemistry.* **1998**, *26*, 245.

(56)   Chollet, R.; Vidal, J.; Oleary, M. H. Phosphoenolpyruvate carboxylase: A ubiquitous, highly regulated enzyme in plants. *Annual Review of Plant Physiology and Plant Molecular Biology.* **1996**, *47*, 273.

(57)   Peliska, J. A.; Oleary, M. H.   Sulfuryl transfer catalyzed by pyruvate-kinase. *Biochemistry.* **1989**, *28*, 1604.

(58)   Catte, M.; Dussap, C. G.; Gros, J. B.   A PHYSICAL-CHEMICAL UNIFAC MODEL FOR AQUEOUS-SOLUTIONS OF SUGARS. *Fluid Phase Equilibria.* **1995**, *105*, 1.

(59)   Deijl, C. M.; Vliegenthart, J. F. G. CONFIGURATION OF SUBSTRATE AND PRODUCTS OF N-ACETYLNEURAMINATE PYRUVATE-LYASE FROM CLOSTRIDIUM-PERFRINGENS. *Biochemical and Biophysical Research Communications.* **1983**, *111*, 668.

(60)   Kikusui, T.; Shimozawa, A.; Kitagawa, A.; Nagasawa, M.; Mogi, K.; Yagi, S.; Shiota, K. *N*-Acetylmannosamine improves object recognition and hippocampal cell proliferation in middle-aged mice. *Bioscience Biotechnology and Biochemistry.* **2012**, *76*, 2249.

(61)   Voermans, N. C.; Guillard, M.; Doedee, R.; Lammens, M.; Huizing, M.; Padberg, G. W.; Wevers, R. A.; van Engelen, B. G.; Lefeber, D. J. Clinical features, lectin staining, and a novel GNE frameshift mutation in hereditary inclusion body myopathy. *Clinical Neuropathology.* **2010**, *29*, 71.

(62)   Plumbridge, J.; Vimr, E. Convergent pathways for utilization of the amino sugars *N*-acetylglucosamine, *N*-acetylmannosamine, and *N*-acetylneuraminic acid by Escherichia coli. *Journal of Bacteriology.* **1999**, *181*, 47.

(63)   Suryanti, V.; Nelson, A.; Berry, A. Cloning, over-expression, purification, and characterisation of N-acetylneuraminate synthase from Streptococcus agalactiae. *Protein Expression and Purification.* **2003**, *27*, 346.

(64)   Kayser, H.; Zeitler, R.; Kannicht, C.; Grunow, D.; Nuck, R.; Reutter, W. BIOSYNTHESIS OF A NONPHYSIOLOGICAL SIALIC-ACID IN DIFFERENT RAT ORGANS, USING N-PROPANOYL-D-HEXOSAMINES AS PRECURSORS. *Journal of Biological Chemistry.* **1992**, *267*, 16934.

(65)   Collins, B. E.; Fralich, T. J.; Itonori, S.; Ichikawa, Y.; Schnaar, R. L. Conversion of cellular sialic acid expression from N-acetyl- to N-glycolylneuraminic acid using a synthetic precursor, N-glycolylmannosamine pentaacetate: inhibition of myelin-associated glycoprotein binding to neural cells. *Glycobiology.* **2000**, *10*, 11.

(66)   Ooi, H. C.; Marcuccio, S. M.; Jackson, W. R. A new preparation of the diastereoisomeric N-acetylneuraminic alditols. *Australian Journal of Chemistry.* **2000**, *53*, 171.